Pêches et Océans Canada Sciences
Fisheries and Oceans Canada Science

2006 No. 5

Atlantic Zone Monitoring Program

AZMP Bulletin PMZA

Programme de Monitorage de la Zone Atlantique

http://www.meds-sdmm.dfo-mpo.gc.ca/zmp/main_zmp_e.html

Contents / *Table des matières*

Edited by / Édité par
Jean-Claude Therriault[1], Brian Petrie[2] & Laure Devine[1]
[1]Institut Maurice-Lamontagne
850, route de la Mer, Mont-Joli, QC, G5H 3Z4
[2]Bedford Institute of Oceanography
Box 1006, Dartmouth, NS, B2Y 4A2

therriaultjcsci@dfo-mpo.gc.ca

Le Bulletin du PMZA

Le Bulletin annuel du PMZA publie des articles en anglais, français ou bilingues afin de fournir aux océanographes et aux chercheurs des pêches, aux gestionnaires de l'habitat et de l'environnement, ainsi qu'au public en général les plus récentes informations concernant le Programme de Monitorage de la Zone Atlantique (PMZA). Le bulletin présente une revue annuelle des conditions océanographiques générales pour la région nord-ouest de l'Atlantique, incluant le golfe du Saint-Laurent, ainsi que de l'information reliée au PMZA concernant des événements particuliers, des études ou des activités qui ont eu lieu au cours de l'année précédente.

The AZMP Bulletin

The AZMP annual Bulletin publishes English, French, and bilingual articles to provide oceanographers and fisheries scientists, habitat and environment managers, and the general public with the latest information concerning the Atlantic Zone Monitoring Program (AZMP). The Bulletin presents an annual review of the general oceanographic conditions in the Northwest Atlantic region, including the Gulf of St. Lawrence, as well as AZMP-related information concerning particular events, studies, or activities that took place during the previous year.

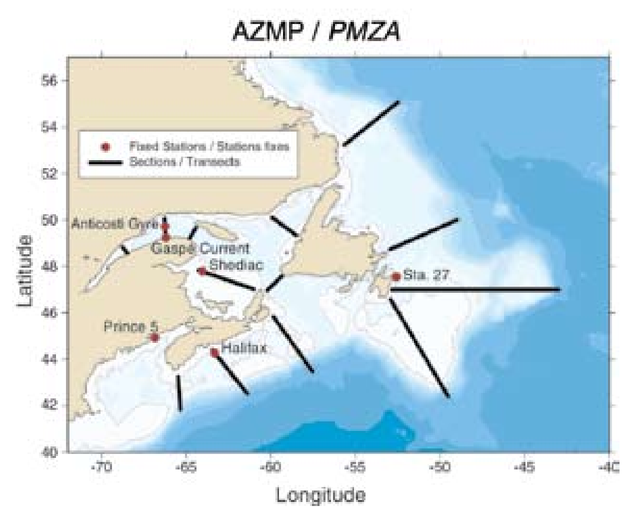

Fig. 1 Locations of sections and fixed stations.

Position des transects et des stations fixes.

The Atlantic Zone Monitoring Program

The AZMP was implemented in 1998 with the aim of collecting and analyzing the biological, chemical, and physical field data that are necessary to (1) characterize and understand the causes of oceanic variability at the seasonal, interannual, and decadal scales, (2) provide multidisciplinary data sets that can be used to establish relationships among the biological, chemical, and physical variables, and (3) provide adequate data to support the sound development of ocean activities. AZMP involves the Gulf, Québec, Maritimes, and Newfoundland regions of DFO. Its sampling strategy is based on (1) seasonal and opportunistic sampling along "sections" to quantify the oceanographic variability in the Canadian NW Atlantic shelf region, (2) higher-frequency temporal sampling at more accessible "fixed sites" to monitor the shorter time scale dynamics in representative areas, (3) fish survey and remote sensing data to provide broader spatial coverage and a context to interpret other data, and (4) data from other existing monitoring programs such as CPR (Continuous Plankton Recorder) lines, Sea Level Network, nearshore Long-Term Temperature Monitoring, Toxic Algae monitoring, or from other external organizations (e.g., winds and air temperatures from Environment Canada) to complement AZMP data.

The key element of the AZMP sampling strategy is the oceanographic sampling at fixed stations and along sections. The fixed stations are occupied about every two weeks, conditions permitting, and the sections are sampled from one to three times during the year. The location of the regular sections and the fixed stations are shown in Figure 1. Temperature, salinity, fluorescence, oxygen, chl *a*, nitrates, silicates, and phosphates are measured, and phytoplankton and zooplankton samples are collected. These measurements are carried out following well-established common protocols.

AZMP Personnel

A large number of scientists and technicians participate in the AZMP, either collecting, editing, processing, analyzing, or presenting the data. The following people have each played a significant role in the activities of the program; however, the list does not include all of the personnel who have contributed. For those not mentioned in the list, but who have helped during the past years, the AZMP is truly appreciative.

Gulf Region / Région du Golfe

Joël Chassé[1], Doug Swain[6]

Marine Environmental Data Service / Service des données sur le milieu marin

Bob Keeley[3], Mathieu Ouellet[3,7,8], Don Spear[3]

Maritimes Region / Région des Maritimes

Doug Gregory[3], Glen Harrison[2], Erica Head[2], Ross Hendry[1], Mary Kennedy[3], Bill Li[2], Heidi Maass[4], Michel Mitchell[1], Kevin Pauley[5,6], Tim Perry[5,6], Brian Petrie[1], Liam Petrie[8], Roger Pettipas[8], Doug Sameoto[2], Victor Soukhovtsef[8], Jeff Spry[5,6]

Le Programme de Monitorage de la Zone Atlantique

Le PMZA a été mis en œuvre en 1998 et vise à collecter et analyser l'information biologique, chimique et physique recueillie sur le terrain afin de (1) caractériser et comprendre les causes de la variabilité océanique aux échelles saisonnières, inter-annuelles et décadales, (2) fournir les ensembles de données pluridisciplinaires qui sont nécessaires pour établir des relations entre les variables biologiques, chimiques et physiques et (3) fournir les données pour le développement durable des activités océaniques. Le PMZA implique les régions du Golfe, du Québec, des Maritimes et de Terre-Neuve du MPO. Sa stratégie d'échantillonnage est fondée sur (1) l'échantillonnage saisonnier et opportuniste le long de «transects» afin de quantifier la variabilité biologique, chimique et physique de l'environnement, (2) l'échantillonnage à plus haute fréquence à des «stations fixes» plus accessibles pour monitorer la dynamique à plus fine échelle de temps dans des régions représentatives, (3) l'utilisation des données provenant des missions d'évaluation de stocks et de la télédétection pour fournir une couverture spatiale plus vaste et le contexte pour l'interprétation des autres données et (4) l'utilisation de données provenant d'autres programmes de monitorage comme les transects CPR (*Continuous Plankton Recorder*), les réseaux côtiers de niveau d'eau et de température, le monitorage des algues toxiques, ou provenant d'autres organismes externes (ex. vents et température de l'air de Environnement Canada) pour complémenter les données du PMZA.

L'élément clé de la stratégie d'échantillonnage est la collecte de mesures océanographiques des stations fixes et le long de transects. Les stations fixes sont occupées à toutes les deux semaines, dépendant des conditions, et les sections sont échantillonnées de 1 à 3 fois durant l'année. La localisation des transects et des stations fixes est illustrée à la Figure 1. L'échantillonnage régulier comprend des mesures de température, salinité, fluorescence, oxygène, chl *a*, nitrates, silicates et phosphates, ainsi que la collecte d'échantillons de phytoplancton et de zooplancton. Ces mesures sont effectuées suivant des protocoles communs bien établis.

Personnel du PMZA

Un grand nombre de scientifiques et de techniciens participent au PMZA, soit à la collecte, l'édition, la réalisation, l'analyse ou la présentation des données. Les personnes suivantes ont joué un rôle significatif dans les activités du programme, mais la liste n'inclue pas tout le personnel qui a contribué. Pour ceux qui ne sont pas mentionnés dans la liste, nous aimerions leur exprimer notre gratitude pour l'aide précieuse qu'ils ont fournie au PMZA au cours des dernières années.

Newfoundland Region / Région de Terre-Neuve

Wade Bailey[1], Eugene Colbourne[1], Joe Craig[1], Charles Fitzpatrick[1], Sandy Fraser[2], Daniel Lane[1], Gary Maillet[2], Pierre Pepin[2], Dave Senciall[3], Tim Shears[2], Paul Stead[1]

Québec Region / Région du Québec

Marie-France Beaulieu[5], Laure Devine[3], Marie-Lyne Dubé[5], Alain Gagné[5], Yves Gagnon[5], Peter Galbraith[1], Denis Gilbert[1], Sandrine Guittard[2], Michel Harvey[2], Pierre Joly[5], Caroline Lafleur[1,3], Pierre Larouche[4], Bernard Pelchat[3], Bernard Pettigrew[5], Stéphane Plourde[2], Liliane St-Amand[2,5], Jean-François St. Pierre[2], Michel Starr[2], Jean-Claude Therriault[2]

[1]Physical Oceanography / Océanographie physique; [2]Biological Oceanography / Océanographie biologique; [3]Data Management / Gestion des données; [4]Remote Sensing /Télédétection; [5]Sampling & laboratory analyses / Échantillonnage & analyses en laboratoire; [6]Fish Surveys / Missions d'évaluation de poissons; [7]Webmaster / Webmestre; [8]Graphic & Data Analyst / Graphiste et analyste de données.

Physical and Biological Status of the Environment

État de l'environnement physique et biologique

AZMP Monitoring Group
Northwest Atlantic Fisheries Centre, Box 5667, St. John's, NL, A1C 5X1
Institut Maurice-Lamontagne, B.P. 1000, Mont-Joli, QC, G5H 3Z4
Bedford Institute of Oceanography, Box 1006, Dartmouth, NS, B2Y 4A2
Marine Environmental Data Service, 200 Kent St., Ottawa, ON, K1A 0E6
PepinP@dfo-mpo.gc.ca (AZMP Chairman)

Physical Environment

A satellite image from early spring 2004 shows a vast area of cold surface water over the Labrador and northeast Newfoundland shelves, Gulf of St. Lawrence and the inshore half of the Scotian Shelf (Fig. 1). The offshore branch of the Labrador Current, which is the dominant flow on the Canadian east coast, is partly visible on the edge of the Grand Banks as sporadic patches of cold water; the inshore branch is seen in Avalon Channel. The cold-water outflow from the Gulf of St. Lawrence marks the Nova Scotia Current from Cabot Strait to Cape Sable. However, relative to the long-term means, the 2004 winter and spring sea-surface temperatures were generally above normal over the Newfoundland Shelf and in the Gulf of St. Lawrence.

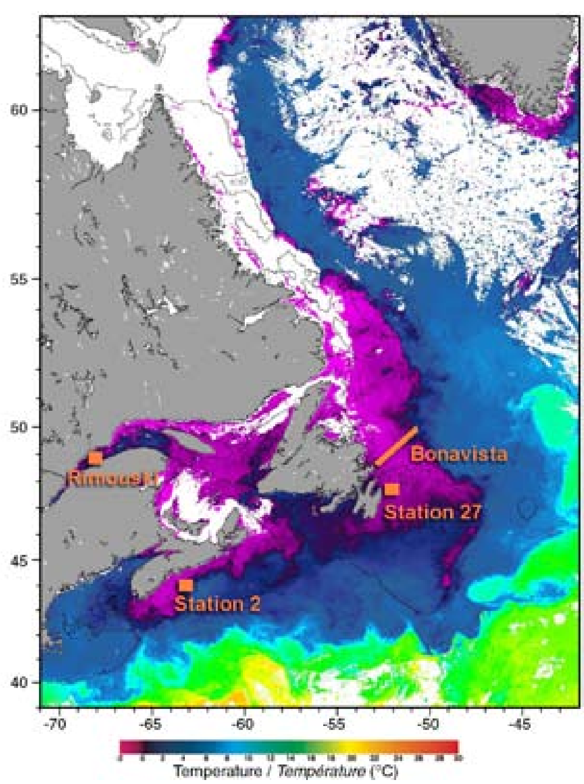

Fig. 1 Sea-surface temperature in the AZMP region during spring 2004. The locations of fixed stations (squares) and the Bonavista section (line) discussed in the article are shown. White areas indicate sea-ice or clouds.

Température de surface de la mer dans la région couverte par le PMZA au printemps 2004. Les positions des stations fixes (carrés) et du transect de Bonavista (ligne) qui sont discutées dans cet article sont indiquées. Les régions blanches représentent de la glace à la surface de la mer ou des nuages.

Environnement physique

Une image satellitaire de début du printemps 2004 montre une vaste région d'eau de surface froide couvrant les plateaux du Labrador et de Terre-Neuve, le golfe du Saint-Laurent ainsi que la moitié plus côtière du plateau Néo-Écossais (Fig. 1). La branche plus au large du courant du Labrador qui représente le flux dominant sur la côte est canadienne est partiellement visible sur le périmètre des Grands Bancs en tant que bulles sporadiques d'eaux froides, la branche plus côtière de ce courant passe au dessus du chenal Avalon. La sortie d'eaux froides du golfe du Saint-Laurent démarque le courant de la Nouvelle-Écosse à partir du Cap Breton jusqu'à Cape Sable. Cependant, par comparaison avec les moyennes à long terme, les températures de surface au cours de l'hiver et du printemps 2004 étaient généralement au-dessus de la normale sur le plateau de Terre-Neuve et dans le golfe du Saint-Laurent. Sur le plateau Néo-Écossais et dans le golfe du Maine, des températures sous la normale prévalaient. Des températures au dessus de la normale ainsi qu'une une étendue de glace et une surface occupée par la couche intermédiaire froide sous la normale étaient les caractéristiques océanographiques marquantes pour le plateau de Terre-Neuve en 2004.

Les températures de l'air sont une indication de la quantité de chaleur qui peut être transférée de l'atmosphère vers l'océan. Au cours de 2004, les températures au dessus de toute la région pour l'année ont été de 0.6 à 2 °C plus chaudes que la normale pour Terre-Neuve, le Labrador et le golfe du Saint-Laurent et de 0.2 à 0.7 °C sous la normale pour le plateau Néo-Écossais et le golfe du Maine (Fig. 2).

La Station 27, la Station Rimouski et la Station 2 de Halifax sont au cœur de notre discussion présente sur la variabilité océanique biologique et physique. Les données pour les autres stations fixes sont présentées dans les documents de recherche et les rapports sur l'état de l'environnement qui sont accessibles sur le site web du SCCS (http://www.dfo-mpo.gc.ca/csas/).

La température de l'eau dans toute la colonne d'eau à la Station 27 de St. John's s'est refroidie jusqu'à des valeurs atteignant 0.35 °C vers la mi-mars, i.e., ~0.9 °C au dessus de la normale (Fig. 3). Une couche peu profonde d'eau chaude s'est développée durant le printemps et l'été et a atteint une valeur maximale de près de 17 °C à la surface en août. Les températures moyennes annuelles intégrées sur la profondeur à la Station 27 ont été les plus élevées depuis que la collection systématique de données a débutée en 1946, et étaient ~1.1 °C plus chaude qu'en 1991, l'année la plus froide.

Over the Scotian Shelf and in the Gulf of Maine, below-normal sea-surface temperatures prevailed. Above-normal water temperatures and below-normal ice extent and cold intermediate layer area on the Newfoundland Shelf were the notable oceanographic features of 2004 for the entire region.

Air temperatures are an indication of the amount of heat that can be transferred from the atmosphere into the ocean. During 2004, they varied systematically over the region, typically 0.6-2°C warmer than normal for the year for the Labrador–Newfoundland region and the Gulf of St. Lawrence and from 0.2-0.7°C below normal for the Scotian Shelf and Gulf of Maine (Fig. 2).

Station 27, Rimouski Station and Halifax Station 2 are the focus of our discussion of the physical and biological oceanic variability. Data from other fixed stations are presented in the research documents and environmental status reports available on the CSAS website (http://www.dfo-mpo.gc.ca/csas/).

Water temperatures at Station 27 off St. John's cooled during the winter to -0.35°C at all depths by mid-March, i.e., ~0.9°C above normal (Fig. 3). A shallow warm layer developed during spring and summer and reached a maximum value of nearly 17°C at the surface in August. The annual, depth-averaged ocean temperatures at Station 27 were the highest since systematic data collection began in 1946 and were ~1.1°C warmer than in 1991, the coldest year.

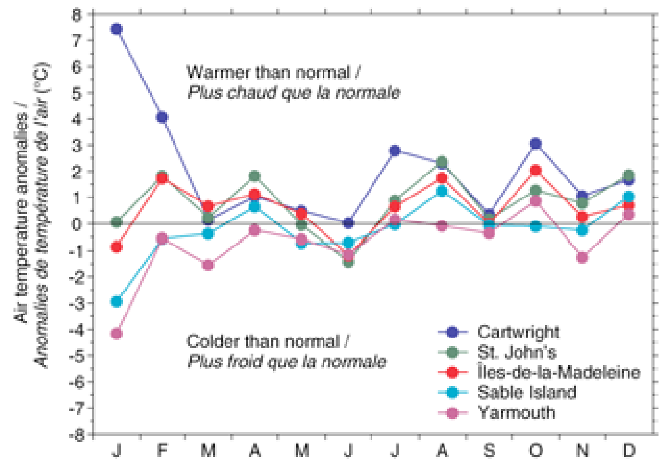

Fig. 2 Monthly air temperature anomalies in 2004 based on the 1971-2000 average values for Cartwright, Labrador; St. John's, Newfoundland; Îles-de-la-Madeleine, Québec; and Sable Island and Yarmouth, Nova Scotia.

Anomalies mensuelles de la température de l'air en 2004 comparées aux valeurs moyennes 1971-2000 pour Cartwright au Labrador, St. John's Terre-Neuve, Îles-de-le-Madeleine au Québec, et Sable Island et Yarmouth en Nouvelle-Écosse.

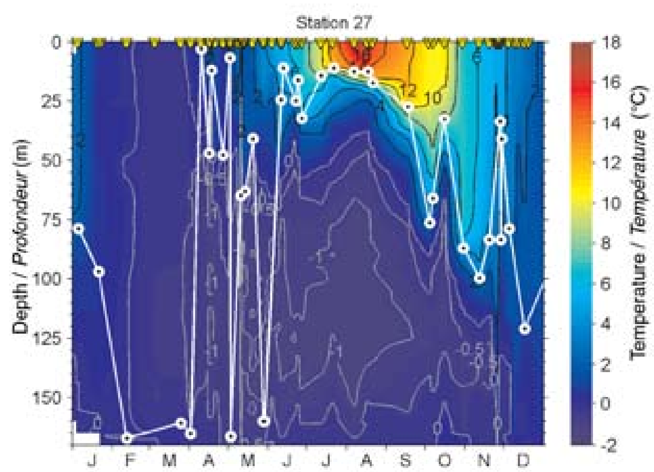

Fig. 3 Temporal evolution of the vertical temperature profiles (yellow triangles) in 2004 for Station 27 off St. John's, Newfoundland. The thick white line shows the depth of the mixed layer, derived from the density profiles.

Évolution temporelle des profils verticaux de température (triangles jaunes) en 2004 pour la Station 27 au large de St. John's Terre-Neuve. La ligne blanche épaisse indique la profondeur de la couche de mélange, dérivée des profils de densité.

In 2004, the Gaspé Current station was sampled only 5 times. Since it is likely that this station will be sparsely sampled in the future, the data from the Rimouski station are featured. Temperatures were slightly (maximum ~0.3°C) below normal from 0 to 100 m for the June–August period (Fig. 4). The maximum surface temperature reached 13.6°C in late July. The surface mixed layer was only ~10 m deep due to low

En 2004, la station du Courant de Gaspé a été échantillonnée seulement 5 fois. Parce qu'il est probable que cette station ne soit toujours que partiellement échantillonnée dans le futur, nous avons décidé d'utiliser ici les données de la station de Rimouski. Les températures étaient légèrement sous la normale (maximum ~0.3 °C) dans la couche 0-100 m pour la période de juin à août 2004 (Fig. 4). La température de surface a atteint un maximum de 13.6 °C vers la fin juillet. La couche de mélange de surface avait seulement ~10 m de profondeur en raison des faibles salinités en eaux peu profondes durant l'été, en dépit des débits d'eau douce sous la normale.

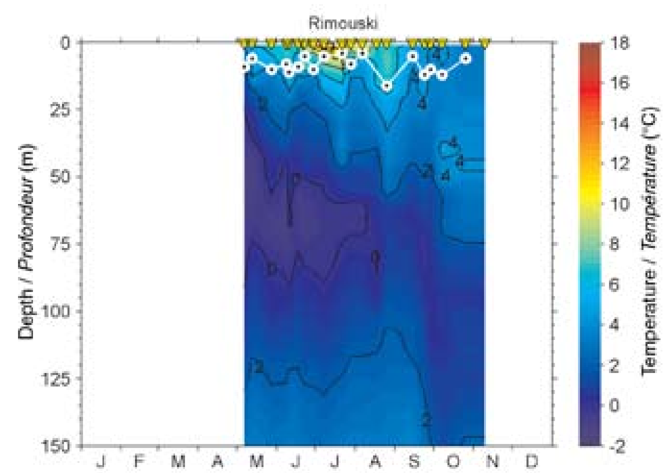

Fig. 4 Temporal evolution of the vertical temperature profiles (yellow triangles) in 2004 for the Rimouski fixed station in the Lower St. Lawrence Estuary. The thick white line shows the depth of the mixed layer, derived from the density profiles. White areas are data gaps.

Évolution temporelle des profils verticaux de température (triangles jaunes) en 2004 pour la station de Rimouski dans l'estuaire maritime du Saint-Laurent. La ligne blanche épaisse indique la profondeur de la couche de mélange, dérivée des profils de densité. Les zones blanches indiquent une absence de données.

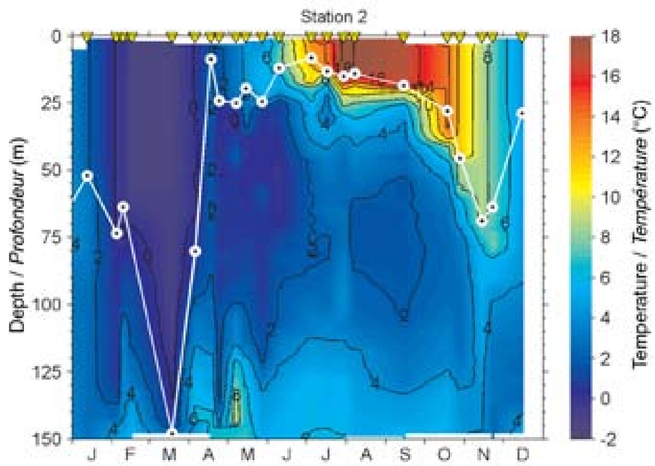

Fig. 5 Temporal evolution of the vertical temperature profiles (yellow triangles) in 2004 at Halifax Station 2. The thick white line shows the depth of the mixed layer, derived from the density profiles.

Évolution temporelle des profils verticaux de température en 2004 pour la Station 2 de Halifax. La ligne blanche épaisse indique la profondeur de la couche de mélange, dérivée des profils de densité.

salinities at shallow depths during summer despite below-normal freshwater inflow.

Temperatures were predominantly below normal by about 1°C for most of the year at all depths at Halifax Station 2 (Fig. 5). This represents a warming of ~1°C from the very cold temperatures of the previous year. The mixed layer depth—the layer extending from the surface with nearly uniform properties—was deeper than normal throughout most of 2004, particularly in winter and fall.

Time series of the cold intermediate layer (CIL, temperature ≤ 0°C) area from the Bonavista section, Newfoundland, as well as the volume of the CIL in the Gulf of St. Lawrence and of shelf water (water mass analysis) on the Scotian Shelf can vary substantially from year to year (Fig. 6). In 2004, the area of the CIL on the Bonavista section was below normal for the tenth consecutive year and the lowest since 1965. This indicates warmer-than-normal conditions and agrees with the observations at Station 27. The CIL volume in the Gulf of St. Lawrence was also less than the long-term mean, indicating a warmer-than-normal year. Its volume was the 5th lowest in the 20-year time series and 20% lower than normal. On the other hand, the 30-100 and 100-200 m temperature layers for the entire Gulf were slightly lower than normal, giving a mixed picture of overall environmental conditions. On the Scotian Shelf, the water volume of the CIL increased to its all-time high in 2004, with an average temperature the third coldest in 30 years.

Chemical and Biological Environment

At Station 27, surface nutrient concentrations in 2004 were higher overall than observed in previous years. The onset and duration of the spring phytoplankton bloom (Fig. 7A) were similar to the long-term means; however, the magnitude of the bloom was lower than in previous years, despite higher-than-normal nutrient concentrations. No fall bloom was observed in 2004. The abundances of most major phytoplankton groups were lower than in previous years, following a trend beginning in 2000.

Les températures étaient d'environ 1 °C sous la normale à toutes les profondeurs pendant presque toute l'année à la Station 2 de Halifax (Fig. 5). Ceci représente un réchauffement ~1 °C par rapport aux températures très froides de l'année précédente. La couche de mélange – la couche de surface avec des propriétés presque uniformes – était plus profonde que la normale durant presque toute l'année 2004, particulièrement en hiver et à l'automne.

La série temporelle de l'aire couverte par la couche intermédiaire froide (CIF, avec des températures ≤ 0 °C) le long du transect de Bonavista à Terre-Neuve, aussi bien que le volume de la CIF dans le golfe du Saint-Laurent et celui de la masse d'eau (selon une analyse statistique) du plateau Néo-Écossais peuvent montrer des variations interannuelles significatives (Fig. 6). En 2004, l'aire couverte par la CIF sur le transect de Bonavista était sous la moyenne à long terme pour la 10ième année consécutive et la plus petite depuis 1965. D'un autre côté, le volume de la CIF dans le golfe du Saint-Laurent était lui aussi plus faible que la moyenne à long terme, indiquant une année plus chaude que la normale. Ce volume était le 5ième plus faible au cours des 20 ans de la série d'observations, soit 20 % de moins que la normale. Par ailleurs, les températures des couches 30-100 et 100-200 m étaient légèrement plus basses que la normale pour l'ensemble du Golfe, fournissant ainsi une image mixte des conditions environnementales. Sur le plateau Néo-Écossais, le volume d'eau de la CIF était à son plus haut en 2004, avec une moyenne de température la 3ième plus froide en 30 ans.

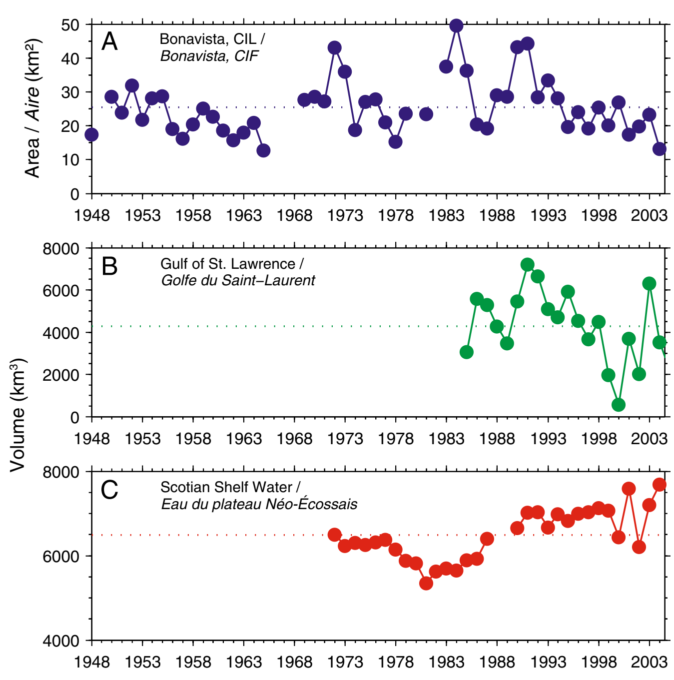

Fig. 6 Time series of (A) the CIL area on the Bonavista Section, (B) CIL volume in the Gulf of St. Lawrence and (C) shelf water volume on the Scotian Shelf. Horizontal lines are the means of all points in each plot.

Séries temporelles (A) de l'aire occupée par la CIF le long du transect de Bonavista, (B) du volume de la CIF dans le golfe du Saint-Laurent et (C) du volume d'eau du plateau Néo-Écossais. Les lignes horizontales représentent la moyenne de tous les points pour chaque graphique.

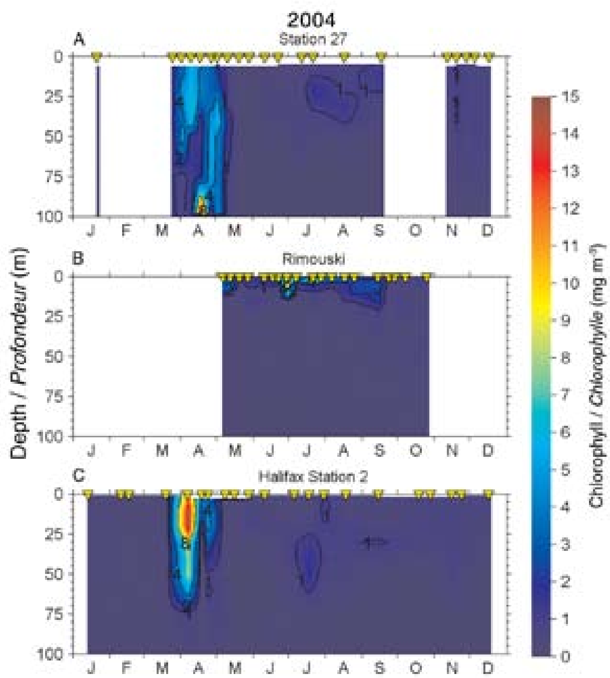

Fig. 7 Temporal evolution of the vertical phytoplankton chlorophyll concentration for the fixed stations: (A) Station 27, (B) Rimouski Station and (C) Halifax Station 2. The yellow triangles indicate sampling points.

Évolution temporelle des concentrations en chlorophylle du phytoplancton pour les stations fixes : (A) Station 27, (B) station de Rimouski et (C) Station 2 de Halifax. Les triangles jaunes indiquent les moments d'échantillonnage.

In 2004, surface nutrient concentrations were relatively high (non-limiting for phytoplankton growth) throughout the year at Rimouski Station in contrast to previous years. For the first time since observations began, there was no spring-summer phytoplankton bloom observed (Fig. 7B). In addition, the annual mean phytoplankton biomass and primary productivity were the lowest seen in over a decade. Typically, the bloom follows the spring-summer runoff peak in this region and its absence in 2004 may have resulted from the above-normal freshwater runoff during the early summer. For the fourth consecutive year, the analysis of the phytoplankton community composition in 2004 revealed the presence of the diatom *Neodenticula seminae*, probably originating from the Pacific Ocean.

Surface nutrient concentrations in 2004 off Halifax were the highest observed in winter and lowest in summer since systematic observations began in 1999. A pronounced spring bloom was seen, comparable in magnitude to the record bloom in 2003 (Fig. 7C); the timing and duration of the bloom in 2004 was similar to the long-term mean. High bloom levels were likely linked to high winter nutrient inventories. In contrast to observations made in previous years, flagellates were an important component of the phytoplankton community in winter and spring off Halifax when diatoms typically dominate.

Large calanoid copepods continue to make up the bulk of the mesozooplankton biomass at the three fixed stations, but smaller species (*Pseudocalanus* sp. and *Oithona* spp.) represent ~20% of the biomass at Station 27 and off Halifax; their contribution to the total biomass in the lower

Environnement biologique et chimique

À la Station 27, les concentrations en sels nutritifs en 2004 étaient en général plus élevées que celles observées au cours des années précédentes. L'initiation et la durée de la floraison printanière de phytoplancton (Fig. 7A) étaient similaires à la moyenne à long terme. Cependant, l'amplitude de cette floraison était plus faible que pour les années précédentes, malgré des concentrations en sels nutritifs plus élevées que la normale. Aucune floraison automnale n'a été observée en 2004. L'abondance de la plupart des groupes majeurs de phytoplancton était plus faible qu'au cours des années précédentes, perpétuant ainsi le patron qui a débuté en 2000.

En contraste avec les années précédentes, les concentrations de sels nutritifs en surface en 2004 étaient relativement élevées (non limitant pour la croissance du phytoplancton) durant toute l'année à la station de Rimouski. Pour la première fois depuis le début des observations, il n'y a pas eu de floraison printanière de phytoplancton et la production primaire a été la plus faible observée depuis une décade (Fig. 7B). Habituellement, la floraison de phytoplancton suit le pic de débit d'eau douce du printemps–début d'été dans cette région. L'absence de floraison en 2004 est donc peut être reliée à la présence de débits d'eau douce au dessus de la normale en cette période de début d'été. Pour la quatrième année consécutive, l'analyse de la composition de la communauté phytoplanctonique en 2004 a révélé la présence de la diatomée *Neodenticula seminae*, une algue qui origine probablement de l'océan Pacifique.

Les concentrations en éléments nutritifs à la Station 2 de Halifax en 2004 étaient les plus fortes observées en hiver et les plus basses en été depuis qu'ont débuté les observations systématiques en 1999. Une floraison printanière élevée de phytoplancton a été observée qui était comparable en amplitude à la floraison record de 2003 (Fig. 7C); le moment de l'initiation et la durée de cette floraison en 2004 étaient cependant similaires à la moyenne à long terme. Ces niveaux élevés de la floraison étaient probablement liés au fort pool de sels nutritifs. En contraste avec les observations effectuées les années précédentes, les flagellés étaient une composante importante de la communauté phytoplanctonique en hiver et au printemps au large de Halifax, à un moment où les diatomées dominent normalement.

Les gros copépodes de type calanoides forment la majeure partie de la biomasse aux trois stations fixes, mais les plus petites espèces comme *Pseudocalanus* sp. and *Oithona* spp. représentent ~20 % de la biomasse à la Station 27; leur contribution à la biomasse totale dans l'estuaire maritime du Saint-Laurent est négligeable (Fig. 8). Les espèces d'eaux froides et profondes (*Calanus glacialis* and *Calanus hyperboreus*) représentent aussi une partie significative de la biomasse totale à toutes les stations fixes et expliquent en grande partie le pic saisonnier. À toutes les stations, *Calanus finmarchicus* est une espèce clé représentant presque la moitié de la biomasse totale au cours de l'année.

La biomasse du mésozooplancton au large de St. John's était plus faible pour 8 des 12 espèces dominantes en 2004 en comparaison avec la moyenne à long terme. L'augmentation graduelle de l'abondance et la présence d'espèces de copépodes

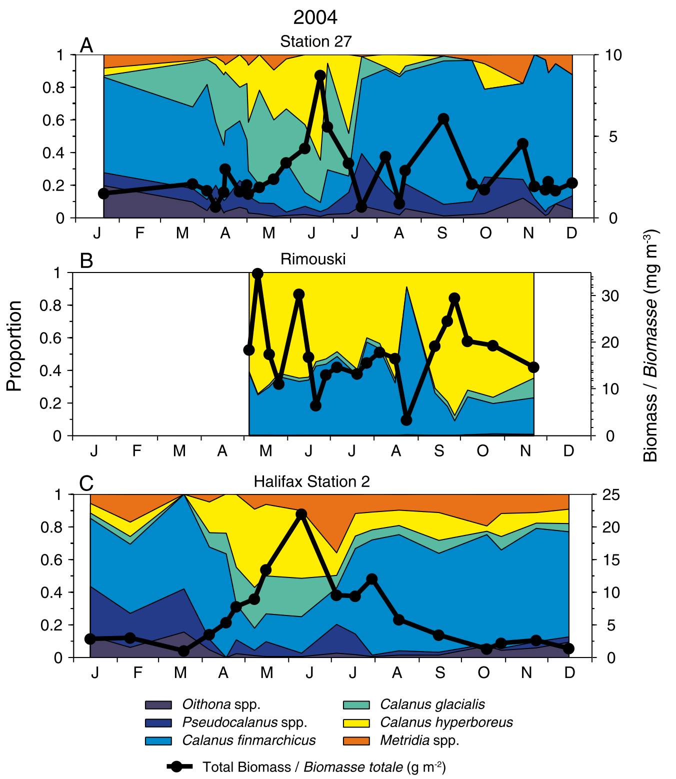

Fig. 8 Relative importance of the dominant copepod species for the fixed stations: (A) Station 27, (B) Rimouski Station and (C) Halifax Station 2. The solid line shows the estimated integrated biomass of copepods (surface–bottom).

Importance relative de quelques espèces dominantes de copépodes pour les stations fixes : (A) Station 27, (B) station de Rimouski et (C) Station 2 de Halifax. La ligne noire épaisse indique la biomasse intégrée de copépodes (surface-fond).

St Lawrence Estuary is negligible (Fig. 8). Deep, cold-water species (*Calanus glacialis* and *Calanus hyperboreus*) are a significant part of the total biomass at all of the fixed stations as well and largely account for the seasonal biomass peaks. At all sites, *Calanus finmarchicus* is a key species, representing almost half of the biomass over the year.

Mesozooplankton biomass off St. John's was lower for 8 of the 12 dominant species in 2004 relative to the long-term mean. The gradual increase of abundance and occurrence of copepod species normally associated with cold water (*C. glacialis* and *C. hyperboreus*) that had occurred at Station 27 since 1999 shifted back toward warm-water species in 2003; this trend continued in 2004.

The mesozooplankton community structure at the Rimouski station was similar to that observed in previous years; however, changes in developmental stage structure suggested that reproductive success was lower in 2004. Macrozooplankton biomass was higher than observed previously, although euphausiid biomass was the lowest seen in a decade. Hyperiid amphipod biomass was higher than euphausiid biomass for the first time, and the biomass of chaetognaths and jellies was the highest on record.

Mesozooplankton biomass and the abundance of the dominant copepod, *Calanus finmarchicus*, off Halifax were similar

normalement associées avec des eaux froides (*C. glacialis, C. hyperboreus*) qui ont été observées à la Station 27 depuis 1999 s'est renversée vers les espèces d'eaux plus chaudes en 2003; ce patron se perpétue en 2004.

La structure de communauté du mésozooplancton à la station Rimouski était similaire à celle observée au cours des années précédentes; cependant, des changements dans la structure des stades de développement suggèrent que le succès de reproduction a été plus faible en 2004. La biomasse du macrozooplancton était plus élevée que celle observée auparavant quoique la biomasse des euphausides était la plus basse observée depuis une décade. La biomasse des amphipodes hypérides était plus élevée que la biomasse des euphausides pour la première fois et la biomasse des chaetognates et des méduses étaient les plus hautes déjà enregistrées.

La biomasse du mésozooplancton et l'abondance du copépode dominant *Calanus finmarchicus* au large de Halifax étaient similaires à celle observée en 2003, mais considérablement plus faible que les niveaux observés au cours des trois années précédentes. En se basant sur l'apparence des jeunes stades de développement, le moment de l'initiation de la reproduction de *C. finmarchicus* a débuté plus tôt qu'au cours des quatre dernières années.

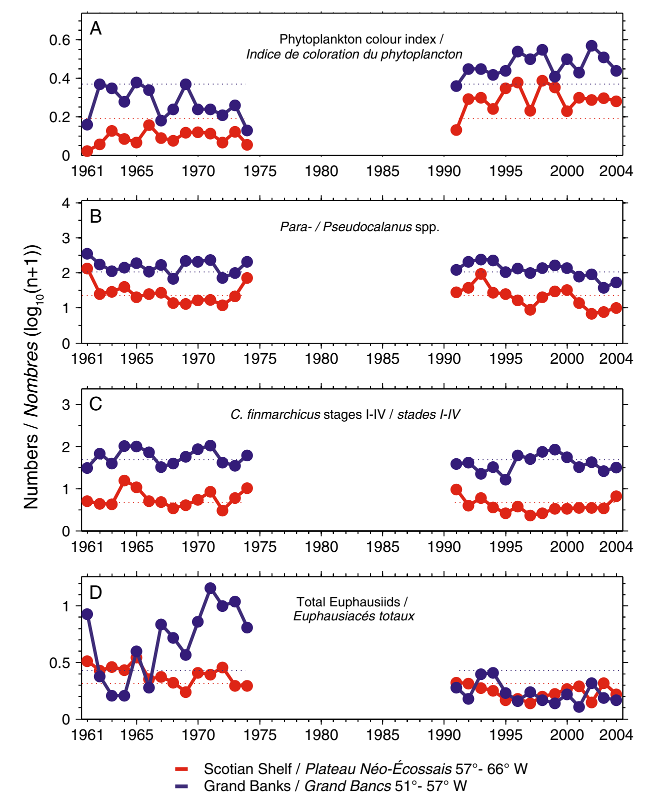

Fig. 9 Data from the Continuous Plankton Recorder (CPR): annual phytoplankton colour index (A) and annual average abundances of dominant zooplankton taxa (B, C, D) from the Scotian Shelf (red) and Grand Banks (blue) regions.

Données CPR (Continuous Plankton Recorder) *: (A) l'indice annuel de coloration du phytoplancton et les abondances annuelles moyennes de certains taxons dominants du zooplancton (B, C, D) pour les régions du plateau Néo-Écossais (rouge) et des Grands Bancs (bleu).*

to those seen in 2003 and considerably lower than levels observed in the previous three years. The timing of *C. finmarchicus* reproduction was earlier than in the previous four years based on the appearance of young development stages.

Time series from the Continuous Plankton Recorder showed that phytoplankton abundance, as estimated by the phytoplankton colour index, was well above levels observed in the 1960s and 1970s on both the Grand Banks and the Scotian Shelf (Fig. 9A). On the other hand, zooplankton (*Para- / Pseudocalanus* spp., *C. finmarchicus*, total euphasiids), particularly the larger species (*C. finmarchicus* and euphasiids) which make up the bulk of the biomass, were generally less abundant during the 1990s and early 2000s relative to the early part of the time series in both regions (Fig. 9B, C, D).

Highlights 2004

The outstanding feature of the physical environment in 2004 was the persistence of warm conditions on the Newfoundland Shelf. The warmest annual, depth-averaged temperatures in the 59 year time series were observed at Station 27. Depth-averaged temperature increased by nearly 0.5°C from 2003. In addition, the area of the CIL, an indicator of the quantity of cold water on the eastern Newfoundland and Labrador Shelf, was the lowest since 1965. The CIL area decreased by about 40% from a nearly normal value in 2003. These observations are part of a larger scale trend extending from Newfoundland to the waters of Greenland, the Labrador Sea, Iceland and the Barents Sea.

While local air temperatures and winds play the major role in the annual cycle of water temperatures throughout the region, Canadian east coast waters are also strongly influenced by flow from the arctic. Currents from the north bring not only cold water but also northern species of plankton. For example, we continue to observe high abundances of cold-water copepods such as *C. glacialis* and *C. hyperboreus* in all regions. In addition, the abundance of the arctic hyperiid amphipod *Themisto libellula* has continued to be a dominant component of the macrozooplankton of the Gulf of St. Lawrence. The latter has been attributed to a significant increased inflow of cold Labrador Shelf water to the Gulf of St. Lawrence via the Strait of Belle Isle.

Les séries temporelles de données CPR (*Continuous Plankton Recorder*) montrent que l'abondance du phytoplancton, déterminée par un indice de coloration, était bien au dessus des niveaux observés durant les années 1960 et 1970 autant sur les Grands Bancs que sur le plateau Néo-Écossais (Fig. 9A). D'un autre côté, le zooplancton (*Para- / Pseudocalanus* spp., *C. finmarchicus* et les euphausides totaux) et particulièrement les grosses espèces (*C. finmarchicus* et les euphausides) qui forment la majeure partie de la biomasse, étaient généralement moins abondants durant les années 1990 et le début des années 2000 en comparaison avec la première partie de la série temporelle dans ces deux régions (Fig. 9B, C, D).

Faits saillants en 2004

La principale caractéristique de l'environnement physique en 2004 était la persistance de conditions chaudes sur le plateau de Terre-Neuve. Les plus chaudes températures annuelles intégrées sur la profondeur ont alors été observées à la Station 27 au cours de la série de 59 ans. La température moyenne dans la colonne d'eau a augmenté de près de 0.5 °C depuis 2003. De plus, la surface de la CIF, un indicateur de la quantité d'eaux froides sur la partie est des plateaux de Terre-Neuve et du Labrador, était la plus faible observée depuis 1965. La surface de la CIF a diminuée d'environ 40 % à partir d'une valeur presque normale en 2003. Ces observations font partie d'un patron de variation à plus grande échelle comprenant les eaux de Terre-Neuve, de la mer du Labrador, de l'Islande et de la mer de Barents.

Quoique les températures de l'air et le vent jouent un rôle majeur dans le cycle annuel de la température de l'eau dans toute la région, les eaux de la côte est canadienne sont aussi fortement influencées par les influx d'eaux de l'arctique. Les courants provenant du nord amènent non seulement des eaux froides mais aussi des espèces nordiques de plancton. Par exemple, on a continué à observer une forte abondance de copépodes d'eaux froides tels que *C. glacialis* and *C. hyperboreus* dans toutes les régions. De plus, l'amphipode arctique *Themisto libellula* a continué à être une composante dominante du macrozooplancton du golfe du Saint-Laurent. Sa plus grande abondance a été attribuée à une augmentation significative des influx d'eaux du plateau Labrador entrant dans le Golfe via le détroit de Belle Isle.

Publications

Primary Publications / Publications primaires

Choi, J.S., K.T. Frank, B. Petrie and W.C. Leggett. 2005. Integrated assessment of a large marine ecosystem: a case study of the devolution of the Eastern Scotian Shelf, Canada. Oceanogr. Mar. Biol. Annu. Rev. 43: 47-67.

Descroix, A., M. Harvey, S. Roy and P.S. Galbraith. 2005. Macrozooplankton community patterns driven by water circulation in the St. Lawrence marine system, Canada. Mar. Ecol. Prog. Ser. 302: 103-119.

Frank, K.T., B. Petrie, J.S. Choi and W.C. Leggett. 2005. Trophic cascades in a formerly cod-dominated ecosystem. Science 308: 1621-1623.

Gilbert, D., B. Sundby, C. Gobeil, A. Mucci and G.H. Tremblay. 2005. A seventy-two-year record of diminishing deep-water oxygen in the St. Lawrence estuary: The northwest Atlantic connection. Limnol. Oceanogr. 50(5): 1654-1666.

Head, E.J.H., D. Brickman and L.R. Harris. 2005. An exceptional haddock year-class and unusual environmental conditions on the Scotian Shelf in 1999. J. Plankton Res. 27: 597-602.

Herman, A.W., and M. Harvey. 2006. The application of normalized biomass size spectra to LOPC-net intercomparisons. J. Geophys. Res. (in press).

Le Fouest, V., B. Zakardjian, F. Saucier and M. Starr. 2005. Seasonal versus synoptic variability in planktonic production in a high-latitude marginal sea: the Gulf of St. Lawrence (Canada). J. Geophys. Res. 110, C09012, doi 10.1029/2004JC002423: 1-21.

Li, W.K.W., W.G. Harrison and E.J.H. Head. 2006. Coherent assembly of phytoplankton communities in diverse temperate ocean ecosystems. Proc. R. Soc. B, 273 doi:10.1098/rspb.2006.3529.

Li, W.K.W., W.G. Harrison and E.J.H. Head. 2006. Coherent sign switching in multiyear trends of microbial plankton. Science 311: 1157-1160.

Maillet, G.L., P. Pepin, J. D. C. Craig, S. Fraser and D. Lane. 2005. Overview of biological and chemical conditions on the Flemish Cap with comparisons of the Grand Banks shelf and slope waters during 1996-2003. e-J. Northw. Atl. Fish. Sci. 37, article no. 3.

Technical Publications / Publications techniques

DFO Technical Reports/ Rapports techniques du MPO

Pepin, P., B. Petrie, J.-C. Therriault, S. Narayanan, W.G. Harrison, K.T. Frank, J. Chassé, E.B. Colbourne, D. Gilbert, D. Gregory, M. Harvey, G.L. Maillet, M. Mitchell and M. Starr. 2005. The Atlantic Zone Monitoring Program (AZMP): Review of 1998-2003. Can. Tech. Rep. Hydrogr. Ocean Sci. 242, v+87 pp.

NAFO Research Document Series / Séries de Documents de recherche OPANO

Colbourne, E.B. 2005. Oceanographic conditions on the Flemish Cap in NAFO Division 3M during the summer 2005. NAFO SCR Doc. 05/87, Serial No. N5192, 14 pp.

Colbourne, E.B., and D.C. Orr. 2005. The distribution and abundance of northern shrimp (*Pandalus borealis*) in relation to bottom temperatures in NAFO Divisions 3LNO based on multi-species surveys from 1995-2005. NAFO SCR Doc. 05/91, Serial No. N5196, 24 pp.

Colbourne, E.B., C. Fitzpatrick, D. Senciall, P. Stead, J. Craig and W. Bailey. 2005. An assessment of the physical oceanographic environment on the Newfoundland and Labrador Shelf in NAFO Subareas 2 and 3 during 2004. NAFO SCR Doc. 05/23, Serial No. N5107, 31 pp.

Hendry, R.M. 2005. Environmental conditions in the Labrador Sea in 2004. NAFO SCR Doc. 05/7, Serial No. N5082, 15 pp.

Maillet, G.L., and P. Pepin. 2005. Timing of plankton cycles on the Newfoundland Grand Banks: potential influence of climate change. NAFO SCR Doc. 05/12, Serial No. N5091, 12 pp.

Maillet, G.L., P. Pepin, S. Fraser and D. Lane. 2005. Biological oceanographic conditions in NAFO Subareas 2 and 3 on the Newfoundland and Labrador Shelf during 2004. NAFO SCR Doc. 05/22, Serial No. N5106, 17 pp.

Petrie, B., R.G. Pettipas and W.M. Petrie. 2005. An overview of meteorological, sea ice and sea-surface temperature conditions off eastern Canada during 2004. NAFO SCR Doc. 05/5, Serial No. N5080, 32 pp.

Petrie, B., R.G. Pettipas, W.M. Petrie and V. Soukhovtsev. 2005. Physical oceanographic conditions on the Scotian Shelf and in the Gulf of Maine during 2004. NAFO SCR Doc. 05/6, Serial No. N5081, 29 pp.

Canadian Science Advisory Secretariat (CSAS) / Secrétariat canadien de consultation scientifique (SCCS)

Research Documents / Documents de recherche

Colbourne, E.B., and E.F. Murphy. 2005. Physical oceanographic conditions in NAFO Division 3P during 2005 - possible influences on the distribution and abundance of Atlantic cod (*Gadus morhua*). 2005. DFO CSAS Res. Doc. 2005/065.

Colbourne, E., C. Fitzpatrick, D. Senciall, P. Stead, J. Craig and W. Bailey. 2005. An assessment of the physical oceanographic environment on the Newfoundland and Labrador Shelf during 2004. DFO CSAS Res. Doc. 2005/014, 36 pp.

Facey, A., and B. Petrie. 2005. Temperature conditions in lobster fishing area 34 on the Scotian Shelf and eastern Gulf of Maine: 1999-2004. DFO CSAS Res. Doc. 2005/27, 28 pp.

Harrison, G., D. Sameoto, J. Spry, K. Pauley, H. Maass, M. Kennedy and V. Soukhovtsev. 2005. Optical, chemical and biological oceanographic conditions in the Maritimes/Gulf regions in 2004. DFO CSAS Res. Doc. 2005/054, 51 pp.

Harvey, M., J.F. St-Pierre, L. Devine, A. Gagné, Y. Gagnon and M.F. Beaulieu. 2005. Oceanographic conditions in the Estuary and the Gulf of St. Lawrence during 2004: zooplankton. DFO CSAS Res. Doc. 2005/043, 25 pp.

Pepin, P., G.L. Maillet, S. Fraser and D. Lane. 2005. Biological and chemical oceanographic conditions on the Newfoundland Shelf during 2004. CSAS Res. Doc. 2005/015, 66 pp.

Petrie, B., R.G. Pettipas and W.M. Petrie. 2005. An overview of meteorological, sea ice and sea-surface temperature conditions off eastern Canada during 2004. DFO CSAS Res. Doc. 2005/20, 44 pp.

Petrie, B., R.G. Pettipas, W.M. Petrie and V. Soukhovtsev. 2005. Physical oceanographic conditions on the Scotian Shelf and in the Gulf of Maine during 2004. DFO CSAS Res. Doc. 2005/21, 41 pp.

Starr, M., L. St-Amand, L. Devine, L. Bérard-Therriault and P. Galbraith. 2005. State of phytoplankton in the Estuary and Gulf of St. Lawrence during 2004. CSAS Res. Doc 2005/XXX (in press), 31 pp.

Science Advisory Reports / Rapports d'avis scientifiques

(All advisory reports are available in English and French / Tous les rapports d'avis sont disponibles en français et en anglais)

DFO (Colbourne, E.B.). 2004 state of the ocean: physical oceanographic conditions in the Newfoundland and Labrador Region. DFO CSAS Sci. Advis. Rep. 2005/018, 9 pp.

DFO (Pepin, P.). 2005. 2004 state of the ocean: chemical and biological oceanographic conditions in the Newfoundland Region. DFO CSAS Sci. Advis. Rep. 2005/029, 7 pp.

DFO (Harrison, G.). 2005. 2004 state of the ocean: chemical and biological oceanographic conditions in the Gulf of Maine - Bay of Fundy, Scotian Shelf and the southern Gulf of St. Lawrence. DFO CSAS Sci. Advis. Rep. 2005/046, 15 pp.

DFO (Harvey, M., and M. Starr). 2005. State of the ocean 2003: chemical and biological oceanographic conditions in the Estuary and Gulf of St. Lawrence. DFO CSAS Sci. Advis. Rep. 2005/053, 22 pp.

Upper-Ocean Variability in the Labrador Sea in Recent Years

Ross Hendry
Bedford Institute of Oceanography, Box 1006, Dartmouth, NS, B2Y 4A2
HendryR@mar.dfo-mpo.gc.ca

Sommaire
Le système climatique de l'Atlantique Nord montre de fortes variabilités interannuelles qui sont spatialement cohérentes et qui affectent toutes les eaux canadiennes de l'Atlantique. Au cours des dernières années, la mer du Labrador a été caractérisée par des conditions générales exceptionnellement chaudes. Les températures de l'air et des eaux de surface ont été plus hautes que la normale, et la perte de chaleur hivernale à l'interface air-mer a été plus basse que la normale. Nos échantillonnages annuels de la section hydrographique AR7W depuis 1990 ont permis de documenter le réchauffement des couches superficielles de la mer du Labrador.

Introduction

The Labrador Sea is an important part of the North Atlantic climate system and has a strong influence on oceanographic variability on the Atlantic Canadian shelf and slope. The hydrographic properties of the Labrador Sea change in reaction to the energetic interannual variability that characterizes this system. Recent warm winters have led to a trend to warmer conditions in the upper 2000 m of the central Labrador Sea and a weakening of the regional wintertime convection that produces well-mixed Labrador Sea Waters (LSW) (Lazier et al. 2002, Hendry et al. 2003, Yashayaev and Clarke 2006). The depth of convection in the Labrador Sea ranges from 200 m to over 2000 m, depending on the severity of winter cooling. The vertical mixing that gives rise to the formation of LSW provides an important mechanism for the transport of atmospheric gases, including carbon dioxide and transient tracers such as chlorofluorocarbons, to intermediate depths of the North Atlantic Ocean. The physical variability also influences the regional ecosystem dynamics. Associated changes in the properties of the Labrador Current give rise to major effects on the oceanography and ecosystems of the entire Atlantic Canadian coastal ocean.

Since 1990, the Ocean Sciences Division at the Bedford Institute of Oceanography has carried out annual occupations of a hydrographic section across the Labrador Sea (Fig. 1). It is designated AR7W (Atlantic Repeat Hydrography Line 7) in the World Ocean Circulation Experiment (WOCE); it continues as a contribution to the Climate Variability (CLIVAR) component of the World Climate Research Program (WCRP). DFO chemical and biological research programs associated with the AR7W surveys have contributed to a better understanding of the carbon cycle within the international Joint Global Ocean Flux (JGOFS) research program and the Canadian program on Enhancement of Greenhouse Gas Sinks (EGGS). Maritimes Region of DFO has designated the AR7W surveys as a core element of its regional ocean monitoring program. As such, they will continue to contribute both to a better scientific understanding of this region and its links to processes in eastern Canadian waters, and to the monitoring mandate of the international Global Climate Observing System.

The present article provides a review of meteorological and physical oceanographic time series data from the Labrador Sea that highlight the exceptionally warm period of the past few years. Future reports will be part of the general Environmental Review of the AZMP Bulletin and will include chemical and biological components as well.

The map of Labrador Sea in Figure 1 shows the locations of standard AR7W stations, selected meteorological stations discussed below, and the station Ocean Weather Station Bravo, which operated in the area from 1963 to 1974. Wintertime convection to depths as little as 200 m and as great as 1500 m have been observed in the OWS Bravo record (Lazier 1980). The circled area in the west-central Labrador Sea marks the region where convection to depths as great as 2000 m was observed during the cold period of the early 1990s (Lazier et al. 2002).

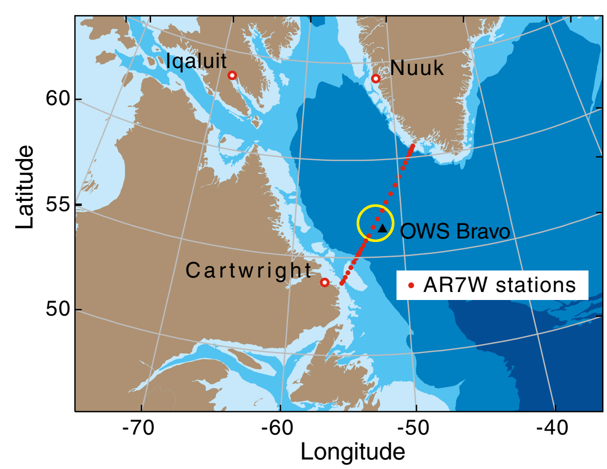

Fig. 1 Map of the Labrador Sea showing the locations of standard AR7W stations, selected meteorological stations, and OWS Bravo. The circled area is discussed in the text.

Carte de la mer du Labrador montrant la position des stations standard du transect AR7W, une sélection de quelques stations météorologiques, ainsi que la station OWS Bravo. L'aire encerclée est discutée dans le texte.

Air Temperature

Figure 2 shows time series of monthly mean air temperature anomalies for 2003-2005 for Cartwright, Iqaluit, and Nuuk. The normal seasonal cycle defined by the mean temperature for each month over the 30-year period 1971-2000 has been removed to show the interannual variability. Although the normal annual average air temperature at Iqaluit is more than 9˚C colder than at Cartwright and about 8˚C colder than at

Nuuk, the ranges and patterns of variability at these three stations bordering the Labrador Sea are remarkably similar. Over the past three years, the annual mean temperature at each site has been 1-2˚C warmer than normal. The greatest interannual variability occurs during winter months. Early winter 2005 (December 2004 and January 2005) was generally cooler than normal. Temperatures were notably above normal in January-February 2004 and February-March 2005.

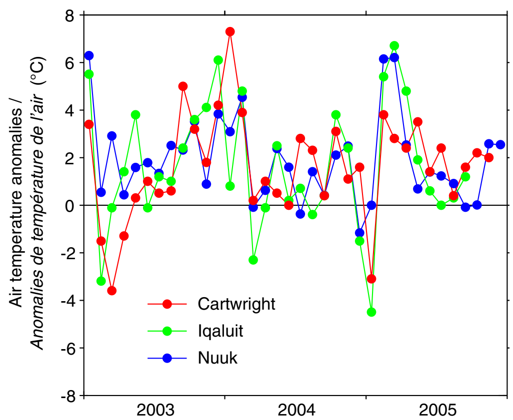

Fig. 2 Monthly mean air temperature anomalies for 2003-2005 relative to the 1971-2000 normal values for Cartwright (Labrador), Iqaluit (Nunavut), and Nuuk (Greenland).

Anomalies mensuelles moyennes de la température de l'air pour 2003-2005 par rapport aux valeurs normales 1971-2000 pour Cartwright (Labrador), Iqaluit (Nunavut) et Nuuk (Groenland).

Sea-Surface Temperature

Figure 3 shows a time series of monthly mean sea-surface temperature anomalies (defined in the same way as for the air temperature anomalies above) from the west-central Labrador Sea based on gridded global sea-surface temperature data compiled by the Hadley Centre at the U.K. Met Office. The anomalies are averaged over a 2 degree x 2 degree area centred at 56.5˚N, 52.5˚W within the circled region in Figure 1. The normal annual mean temperature is 4.2˚C. The normal monthly means have an annual range of about 6˚C. The 2003 and 2004 annual mean sea-surface temperatures were about 1˚C warmer than normal, setting record high values for the 1960-2004 period covered by the Hadley Centre data set. The first half of 2005 shows a continuation of these exceptionally warm conditions.

Sea–Air Heat Flux

On an annual average, the Labrador Sea loses heat to the overlying atmosphere. This heat loss is balanced by the heat supplied by ocean currents flowing from more southern latitudes. The rate of heat loss depends on the difference in temperature between the ocean and the overlying atmosphere and on the strength of the winds blowing over the surface of the ocean.

Figure 4 shows a time series of monthly mean heat flux anomalies (defined in the same way as for the air temperature and sea-surface temperature anomalies above) from the west-central Labrador Sea based on gridded U.S. National Centers for Environmental Prediction (NCEP) Reanalysis Data. The time series represents conditions in an approximately 2

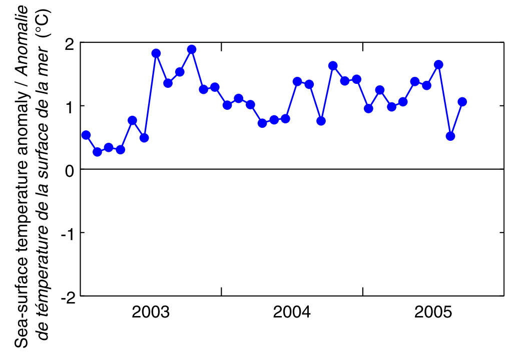

Fig. 3 Monthly mean sea-surface temperature anomalies for 2003-2005 relative to the 1971-2000 normal values for the west-central Labrador Sea based on gridded data from the Hadley Centre at the U.K. Met Office.

Moyennes mensuelles des anomalies de température de surface de la mer pour 2003-2005 par rapport aux valeurs normales 1971-2000 pour la partie centre-ouest de la mer du Labrador calculées à partir d'une grille de données fournie par le Centre de recherche Hadley du bureau météorologique du Royaume-Uni.

degree x 2 degree area centred at 56.2˚N, 52.5˚W within the circled region in Figure 1. The normal annual average heat flux is about 66 W m^{-2}. Positive anomalies correspond to greater-than-normal heat loss from the ocean. The largest heat fluxes occur in the winter months, when the air temperatures are low and the winds are strong. Wintertime variability is the dominant contributor to interannual variability of the annual mean heat flux. The 2004 annual mean heat flux was about 27 W m^{-2} lower than normal; this was the eighth consecutive year of lower-than-normal annual mean heat fluxes in the west-central Labrador Sea. The monthly mean heat flux for January 2005 was higher than normal, but a return to mild conditions and low heat fluxes in the succeeding months gives a mean 2005 heat flux about 26 W m^{-2} lower than normal for the nine months of data available to date.

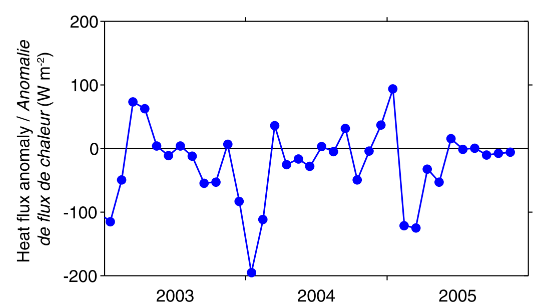

Fig. 4 Monthly mean ocean-to-atmosphere heat flux anomalies for 2003-2005 relative to the 1971-2000 normal values for the west-central Labrador Sea based on gridded data from the NCEP Reanalysis Project.

Moyennes mensuelles des anomalies de flux de chaleur océan-atmosphère pour 2003-2005 par rapport aux valeurs normales 1971-2000 pour la partie centre-ouest de la mer du Labrador calculées à partir d'une grille de données fournie par le projet de réanalyse NCEP.

Upper Layer Temperature from AR7W Occupations

Figure 5 shows the average 0-150 m potential temperature in the west-central Labrador Sea from stations within the circled area in Figure 1 for all AR7W occupations since 1990. A long-

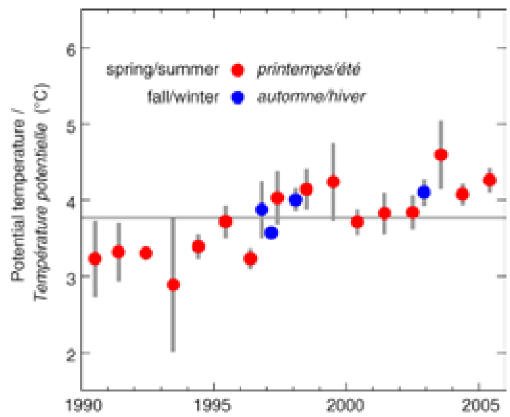

Fig. 5 De-seasoned averages of the 0-150 m potential temperature in the west-central Labrador Sea from AR7W occupations since 1990.

Moyennes désaisonnalisées du potentiel de température dans la couche 0-150 m dans la partie centre-ouest de la mer du Labrador à partir des données provenant de l'échantillonnage des stations du transect AR7W depuis 1990.

term seasonal cycle was used to remove seasonal effects. Most of the averages involve four stations; the error bars are the standard deviations of the 0-150 m mean values for the contributing stations for each case. The primary survey takes place in spring or early summer. The occasional fall and winter occupations included in Figure 5 are consistent with the other values. The average temperature over the past three years (2003-2005) is more than 1˚C warmer than the average during the cold period of 1990-1994 that ended with two years of intense deep convection.

The early 1990s were anomalously cool. The most recent decade shows a warming trend, with interannual variability on shorter time scales. OWS Bravo measurements from 1963 to 1974 showed a decade-long cooling trend of similar magnitude, leading to a resumption of deep convection in the two winters before the abandonment of the weather station (Lazier 1980). Continued monitoring of the AR7W section is one means of resolving whether the recent trend is related to natural decadal variability, global warming, or a combination of both.

Acknowledgements

Many staff and associates of Ocean Sciences Division (OSD) at BIO have contributed to the Labrador Sea programme. John Loder presently leads the associated OSD Ocean Circulation and Variability Programme. Allyn Clarke, Glen Harrison, and Igor Yashayaev have provided critical leadership to the surveys in recent years. These efforts, together with those of the officers and crew of CCGS *Hudson*, are gratefully acknowledged.

References

Hendry, R., Yashayaev, I., Clarke, A., and Lazier, J. 2003. Interannual changes in the hydrography of the Labrador Sea: 1990-2002. AZMP Bulletin PMZA 3: 33-37.

Lazier, J. 1980. Oceanographic conditions at Ocean Weather Ship Bravo, 1964-1974. Atmos.-Ocean 18: 227-238.

Lazier, J., Hendry, R., Clarke, A., Yashayaev, I., and Rhines, P. 2002. Convection and restratification in the Labrador Sea, 1990-2000. Deep-Sea Res. 49: 1819-1835.

Yashayaev, I., and Clarke, A. 2006. Recent warming of the Labrador Sea. AZMP Bulletin PMZA 5: 12-20.

Recent Warming of the Labrador Sea

Igor Yashayaev and Allyn Clarke
Bedford Institute of Oceanography, Box 1006, Dartmouth, NS, B2Y 4A2
Yashayaevl@mar.dfo-mpo.gc.ca

Sommaire

Au cours des dernières 45 années, des variables océanographiques comme la température et la salinité ont montré des variations significatives dans la mer du Labrador. Quoique la couche des 2000 m supérieurs de la mer du Labrador ont enregistré les conditions les plus froides et les moins salées en 1994, durant la dernière décade, cette couche supérieure est devenue plus chaude et plus saline et elle approche maintenant le record des conditions les plus chaudes et les plus salées qui ont été observées entre la fin des années 1960 et le début des années 1970. Ces changements ont des implications importantes pour le système climatique global et le climat régional, ainsi que pour les écosystèmes marins nordiques en général.

Introduction

The Labrador Sea has exhibited significant variations in its temperature and salinity over the past 45 years. These changes have important implications for both the global climate system and the regional climate and marine ecosystems. While the upper 2000 m of the Labrador Sea were the coldest and freshest on record in 1994, these waters have warmed and become more saline and are now approaching the conditions observed in the early 1960s—the warmest and saltiest period on record.

The Labrador Sea is an important part of the regional and global climate system for the following reasons:

- While the Labrador Sea is the coldest and freshest (least salty) basin of the subpolar North Atlantic, it is also the last recipient of the warm and salty waters of the North Atlantic Current system, now cooled and freshened during its passage around the subpolar gyre. In winter, cold Arctic outbreaks from Labrador result in intense atmosphere–ocean heat exchanges, transferring large amounts of heat from the sea to air;

- The extreme winter heat losses and the subpolar gyre circulation mean that the Labrador Sea creates the densest winter mixed layers in the North Atlantic excluding the Nordic Seas and Baffin Bay. Episodically this deep convective mixing modifies water properties to depths of over 2000 m and produces a characteristic water mass (Lazier 1980);

- The Labrador Sea is a principal compartment in the global ocean overturning circulation or conveyor belt, supplying the conveyor with newly formed or modified intermediate-depth water masses; in addition, the deeper water masses, originating from the deep Nordic Seas outflows, pass through the Labrador Sea;

- Local processes and current systems influence the dynamic strength of the global ocean conveyor belt;

- It is the source region of the Labrador Current, which exports the upper cold and fresh waters toward the south of the Labrador Sea and, therefore, strongly affects the hydrography and ecosystems of the shelf areas downstream;

- Large temperature and salinity anomalies develop intermittently at and near the surface of the Labrador Sea. Following their formation, these anomalies move out of the Labrador Sea, enter the subpolar circulation gyre and spread east-to-northeast across the North Atlantic and south-to-southwest along the western boundary of the North Atlantic (Yashayaev, in prep.). In some cases these anomalies cross the Subpolar Front and influence the Gulf Stream and the North Atlantic Current.

The two main freshwater inflows from the Arctic Ocean to the North Atlantic pass around the Labrador Sea margins (by way of the Canadian Arctic archipelago and the East Greenland shelf), forming boundary currents in the Labrador Sea. Distinct patches of warmer and saltier water are found within a short distance of the Greenland and Labrador continental slopes (inward from the Labrador Sea). These patches are associated with a flow, originating from a branch of the North Atlantic Current or its modified water mass, that is commonly known as the Subpolar Mode Water (McCartney and Talley 1982). The counterclockwise flow of warm and salty water around the rim of the Labrador Sea has several naming conventions, the most common of which is the Irminger Current. The Irminger Current and its derived eddies contribute to the overall heat, salt and freshwater budget of the basin and, by maintaining the flux of heat and salt toward the centre of the Labrador Sea, influence the development of winter convection.

Monitoring the Labrador Sea

Over the past 16 years (1990-2005), the Ocean Sciences Division of the Bedford Institute of Oceanography (BIO) has conducted annual occupations of a hydrographic section across the Labrador Sea known in World Ocean Circulation Experiment (WOCE) and Climate Variability and Predictability (CLIVAR) terminology as AR7W (Fig. 1). The observations from the occupations of these sections, when combined with

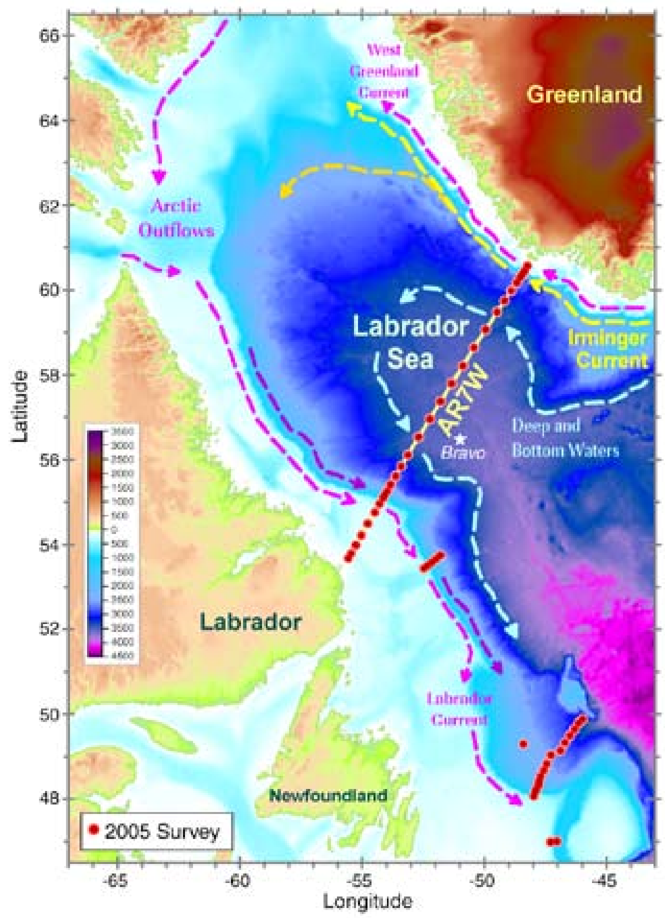

Fig. 1 Location of CTD stations occupied by the Bedford Institute of Oceanography in the Labrador Sea in the spring of 2005 (May 18 to June 4). AR7W is a standard section line.

Localisation des stations CTD occupées par l'Institut Océanographique de Bedford dans la mer du Labrador au printemps 2005 (18 mai au 4 juin). AR7W est un transect d'échantillonnage standard.

the U.S. Coast Guard's Ocean Weather Ship (OWS) Bravo time series (1950-1974) and other archived data, document prominent interannual and decadal changes through the entire depth in this key region (Fig. 2[1]).

The annual AR7W surveys measure the distribution of seawater temperature, salinity, density and other physical as well as chemical and biological parameters across the Labrador Sea. The primary goal of these annual hydrographic surveys is to observe the interannual changes in the properties of the intermediate and deep waters of the North Atlantic, particularly the changes in the properties and volumes of Labrador Sea Water (LSW).

The interannual changes in the properties of LSW can be captured by examining the average temperature and salinity of the upper 2000 m layer[2] over the central part of the Labrador Sea basin (Fig. 2). This is also a layer of complex dynamics, exhibiting considerable variability in water properties and

[1] Figure 2 only goes back to 1960; the preceding observations were generally coarser and had larger errors.

[2] To avoid influence of the unresolved seasonal variability, the upper 150 m measurements were not used in the computations of the 0-2000 m estimates.

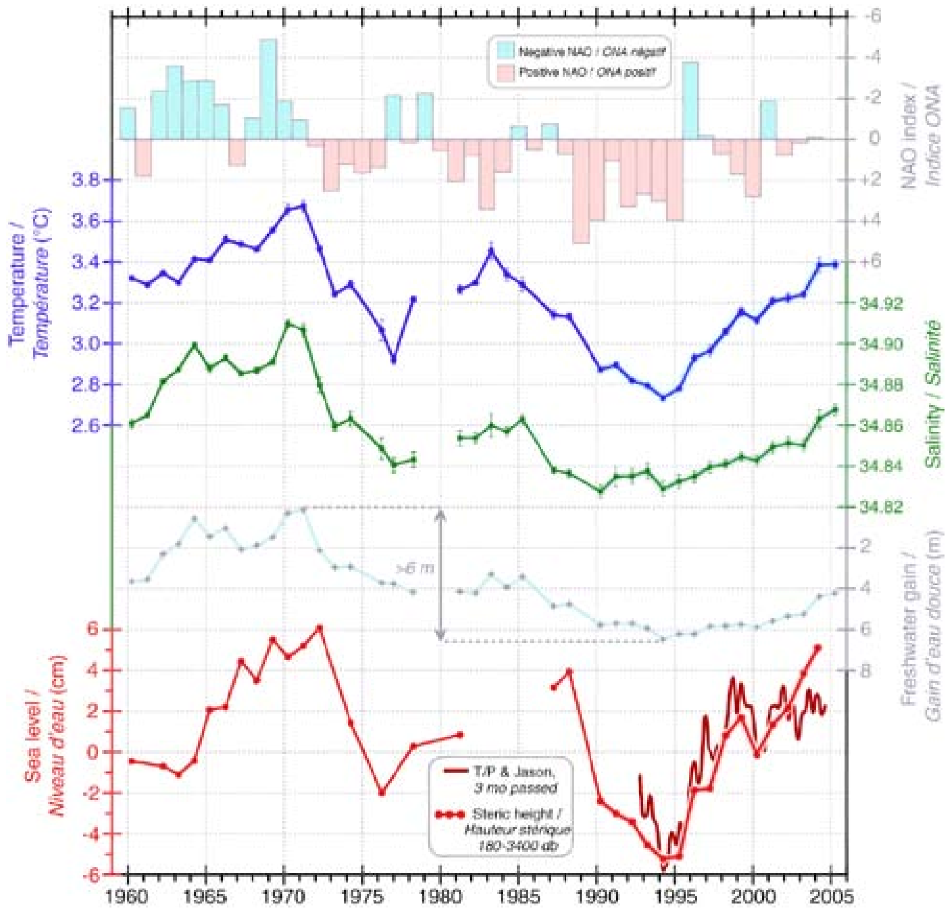

Fig. 2 A predominance of high values of the North Atlantic Oscillation index (NAO; note inverted axis) is reflected in periods of cooling and freshening of the Labrador Sea associated with sustained renewal of the intermediate waters reaching 2000 m and deeper. The temperature and salinity values are means from 150-2000 m in the central Labrador Sea confined by the 3250 m isobath. The freshwater gain (note inverted axis) was calculated over the full water depth. The steric height (lower plot, red line, 1960-2005) represents the water column thickness; it was derived from all available temperature and salinity measurements in the central Labrador Sea. The observed sea-level anomalies (brown line, 3-mo low-pass filtered anomalies relative to the record mean, 1992-2004) were calculated from satellite altimeter data acquired by the Topex/Poseidon and Jason missions.

Une prédominance des valeurs fortes de l'indice de l'oscillation Nord Atlantique (ONA; noter que l'axe inversé) est reflété par des périodes de refroidissement et de diminution de salinité de la mer du Labrador associées à un renouvellement soutenu des eaux intermédiaires atteignant 2000 m et plus. Les valeurs de température et de salinité représentent des moyennes entre 150 et 2000 m pour la partie centrale de la mer du Labrador qui est confinée par l'isobathe 3250 m. Le gain en eaux douces (noter l'axe inversé) a été calculé sur toute la profondeur. La hauteur stérique (graphique du bas, ligne rouge, 1960-2005) représente l'épaisseur de la colonne d'eau; il a été dérivé à partir de toutes les mesures de température et de salinité disponible pour la partie centrale de la mer du Labrador. Les anomalies de niveau d'eau observées (ligne brune, anomalies filtrées par un filtre passe-bas de 3 mois, 1992-2004) ont été calculées à partir des données altimétriques acquises par les satellites Topex/Poseidon et Jason.

stratification (Figs. 3, 4). The cooling and freshening of this layer over the 1980s and early 1990s led to a characteristic LSW in 1994 that was the coldest, freshest, densest, deepest and most voluminous since the 1960s and indeed in the entire historical record back to the 1930s. It is unfortunate that there were no regular sustained observations in the Labrador Sea between 1974 and 1990 to document how the Labrador Sea cooled and freshened from its warmest and saltiest state in 1971 to its coolest state in 1994.

The 45-year record does clearly show three periods of the Labrador Sea warming. The first and second periods lasted from 1960 to 1971 and from 1977 to 1983. At the end of the first warming period, the Labrador Sea reached the warmest and saltiest state ever observed. The last warming started in 1994 and was seen through 2005 (the year of the last AR7W occupation). The average temperature and salinity of the upper 2000 m layer have already returned to the levels observed in the mid 1960s and, if the tendencies of their change persist, they soon will be approaching the record highest levels. In the context of the longer-term changes (Fig. 2), this recent development can be seen as a part of some cyclical process typical for the Labrador Sea and the whole subpolar North Atlantic. These cyclical changes are associated with the production, evolution and dissipation of LSW on the one hand and the competing influence of other warmer and saltier North Atlantic intermediate waters on the other. We discuss below the LSW "life cycle."

The warm and salty conditions in the 1960s and the early 1970s and the fresh and cold conditions from the late 1980s to the late 1990s represent the extreme states of the LSW development over the entire period of reliable observations (since the 1930s).

AR7W Temperature and Salinity Distributions in 1994 and 2005

In 1994, the LSW filled the entire central part of the Labrador Sea basin within the depth range of 500-2400 m, with potential temperatures (θ) <2.8°C and salinities (S) <34.837 (Fig. 3). Within the same depth range, saltier water is found over both the Greenland and Labrador slopes. Shallower than 1500 m, this water is warmer than the LSW and originates from the warm salty inflow from the Irminger Sea. In fact, this is the flow that we name the Irminger Current. The signal associated with this flow is stronger on the Greenland side and weaker on the Labrador side. There are several reasons for this along-path weakening, cooling and freshening of the Irminger Current. The eddy production and Irminger Current recirculation lessen the net amount of warm and salty water passing around the Labrador Sea. On the other hand, the properties of the Irminger Current are strongly affected by the vertical and lateral mixing with the fresher and colder waters, especially in the northern regions of the Labrador Sea.

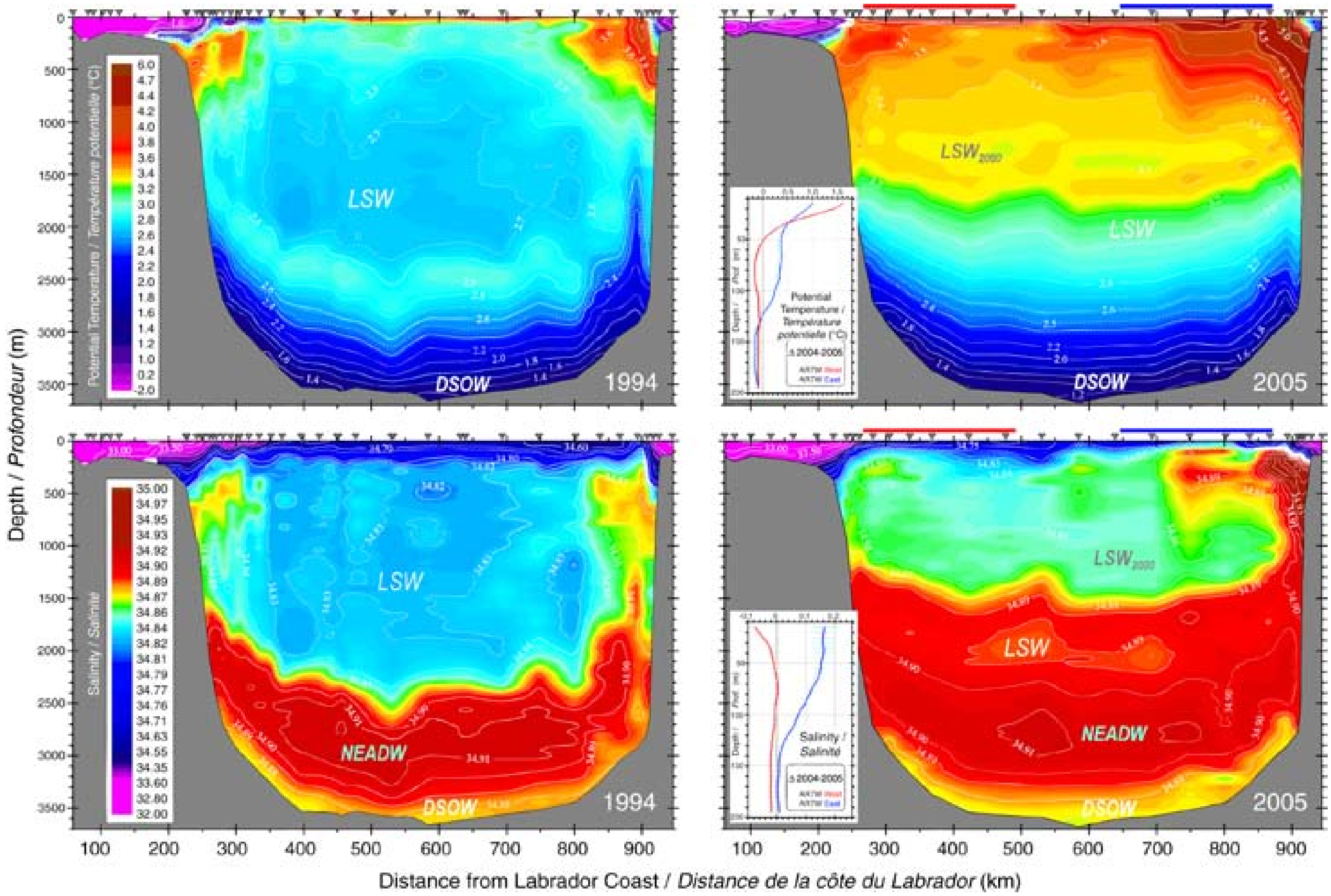

Fig. 3 Vertical section plots of potential temperature and salinity from the 1994 (left panels) and 2005 (right panels) occupations (grey triangles) of the AR7W section. The section extends from the Labrador coast (left) to the west coast of Greenland (right). The 1994 survey shows a pool of newly formed extremely cold and fresh Labrador Sea Water (LSW) extending to 2400 m. LSW is formed in the Labrador Sea through deep convection caused by high heat losses during severe winters (Lazier 1980, Lazier et al. 2002, Yashayaev et al. 2003). In the Labrador Sea, the core of this water mass can be identified by a temperature-salinity or density class occupying its largest volume (Yashayaev et al. 2003). The inset profiles in the right panels are discussed in the text.

Profils verticaux de la température potentielle et de la salinité au cours des occupations (indiquées par des triangles gris) de stations en 1994 (panneaux de gauche) et en 2005 (panneaux de droite) le long du transect AW7R. Le transect s'étend de la côte du Labrador (à gauche) jusqu'à la côte ouest du Groenland (à droite). Les données de 1994 montrent une masse d'eau de la mer du Labrador extrêmement froide et douce nouvellement formée et qui s'étend jusqu'à 2400 m. Cette masse d'eau s'est formée dans la mer du Labrador via le processus de convection profonde qui est causé par une forte perte de chaleur durant des hivers sévères (Lazier 1980, Lazier et al. 2002, Yashayev et al. 2003). Dans la mer du Labrador, le cœur de cette masse d'eau peut être identifié par une classe de température-salinité ou de densité occupant un plus grand volume (Yashayev et al. 2003). Les profils insérés dans les panneaux de droite font l'objet d'un examen dans le texte.

In 2005, the central basin was warmer, saltier and much more uniformly stratified in density, temperature and salinity over the upper 2000 m (Fig. 3; "uniformly stratified" means gradually or uniformly changing with depth). If one follows the evolution of the water masses and does a careful θ/S analysis, there are, in fact, two LSW masses in the 2005 sections. The shallower one with θ<3.4°C and S<34.86 is found in the depth range between 500 and 1500 m. This is a water mass that was first formed by winter convection in 2000 (Yashayaev et al. 2003) and has been subsequently modified through mixing and weak convection during some subsequent winters. The remnants of the 1994 LSW mass could still be detected in 2005. Its signature is the slight spreading of the isotherms between 2.8 and 3.0°C (Fig. 3) and the broad volume of water with salinities between 34.88 and 34.90 in the depth range between 1500 and 2400 m.

Changes in the Upper Layer

The question remains, what causes these interannual changes in winter convection in the Labrador Sea? There are certainly changes in the net air–sea heat flux over each annual cycle, some of which are discussed in a companion article included in this bulletin (Hendry 2006). Our spring occupations make it difficult to deal with changes in the upper 150 m since these changes are also subject to a rapid restratification, freshening and warming immediately after the end of the cooling cycle in early April. Since the seasonal variability is the strongest in the upper 150 m, the seasonal cycle must be removed from observations prior to detection of interannual changes. The OWS Bravo sampling had a fairly dense seasonal coverage; however, it lacked the broader spatial coverage of the more recent data. Close to the OWS Bravo location, an average seasonal cycle can be computed from the earlier data. However, it is likely that the seasonal cycle of the last decade and a half has changed from that of the 1950s and 1960s. The new observations from profiling floats (ARGO, PALACE) and other innovative systems (Seagliders, moored CTD profilers, etc.) do offer hope that new estimates of the seasonal cycle can be made, but that is beyond our present analysis.

Fortunately, the 2004 and 2005 AR7W occupations were both conducted at the end of May, which cancels a seasonal component in the differences between these datasets. Vertical profiles of the temperature and salinity differences between the 2004 and 2005 occupations were averaged over the western and eastern parts of the deep Labrador Sea basin. The vertical profiles of the average changes over these zones are shown in the inserts in the 2005 section plots[3] (Fig. 3). The 2005 occupation shows a significant basin-wide increase in the spring warming in the upper 50 m[4]. In the western zone, the warming increased by >1.5°C at 15 m. This 2005 increase in the spring warming diminished monotonically with depth and dropped to 0°C at 50 m. In the eastern zone, the near-surface (15 m) warming increased by ~1°C or ~1/3 less than in the western zone. At the same time, the increase in warming in the eastern zone had spread to a greater depth, remaining ~0.4°C between 50 and 90 m. The two zones show a notable contrast in the 2005-2004 salinity difference. The upper 150 m of the eastern zone became saltier in 2005 by as much as ~0.17 at 15 m and ~0.15 at 60 m. Between 60 and 150 m, this salinity increase was almost linearly dropping to 0. The upper 50 m in the western zone became fresher by ~0.1 near the sea surface.

Are the changes between two consecutive surveys indicative of some larger scale shifts in ocean dynamics and redistribution of heat, salt and freshwater, or are they simply due to natural noise in air–sea heat and freshwater exchange? The increased warming in 2005 in the upper 30 m is likely due to differences in the air–sea fluxes over the previous weeks. However, the deeper warming to 100 m on the eastern side coupled with the increased salinity in the same layer is suggestive of an increased advection of warm salty water from the Irminger Sea. This is consistent with what is seen in the upper 500 m on the eastern side. The change in the eastern part is most likely an imprint of the large-scale warming trend in the Irminger Current showing a high correlation between temperature and salinity increases. The trend in the Irminger Current, in its turn, is probably a result of a volumetric increase or warming of the original North Atlantic Current water delivered to the Labrador Sea by the Irminger Current. The Irminger Current can also become warmer because now it loses less heat along its entire path.

The western upper layer is more affected by the fresher and colder waters arriving from the Arctic along the Labrador Shelf. The observed increase in surface freshening may have been caused by an increase in precipitation, ice melt or transfer of shelf waters across the shelf-break front. The fresher upper layer increases vertical stability (especially if it is also warmer) and inhibits the exchange with the underlying layer, so all the heat to be received during the warm season will be mostly confined to the shallower layer.

[3] The zones used for spatial averaging are indicated by red and blue lines above the section plots.

[4] The rates of increase/decrease are based on the 2005-2004 differences.

The North Atlantic Oscillation and Subsurface Ventilation

The long-term cyclic changes in the stratification of the Labrador Sea and the properties of LSW have been linked to the North Atlantic Oscillation (NAO). The North Atlantic Oscillation is the primary mode of climate variability that involves the winter atmospheric circulation over the northern hemisphere and principally over the North Atlantic. The NAO index is the normalized Azores-to-Iceland sea level pressure difference[5]. A strong positive NAO means a strong pressure difference over the central North Atlantic and hence strong winter winds over the Labrador Sea. A predominance of negative NAO years from 1960 through to 1971 were reflected in little convective renewal of LSW (Fig. 2) and its becoming warmer and more saline. The convective renewal of LSW from 1972 to 1976 and from 1988 to 1994 can be associated with periods of strong positive NAO values. However, the agreement between convection and the NAO is not perfect for several reasons. First, the essentially high correlation between the NAO and the net air–sea heat flux over the Labrador Sea is largely a result of the shift in the atmospheric conditions between the 1960s and the early 1990s. The NAO and heat flux series with the interdecadal changes removed show a weaker correlation. Second, the ocean, because of its thermal inertia, creates a “memory” of past winters through its stratification; it might take several severe winters to erode away the stratification built up over several years of mild winters, meaning that on short time scales, the ocean can respond passively to a fairly strong forcing. On the other hand, intense convection in preceding years homogenizes the water column, making it easier to remix large volumes of water in subsequent years, thus letting a weaker forcing operate over the whole mixed layer. Finally, the interannual changes in the sources of saltier and fresher waters feeding the upper layers of the Labrador Sea can, to a certain degree, influence development of convection and determine the properties of its product, the LSW.

Formation, Evolution and Discharge of the Labrador Sea Water

The temporal evolution of each LSW generation can be effectively visualized by robustly averaging[6] all of the CTD profiles from the central basin of each annual occupation to form a single average profile (Fig. 4). This averaging is done within density layers, revealing the survey-typical conditions and reducing the high frequency variance that could be significant in a single profile. (The central basin was identified by the bottom depths greater than 3300 m within 150 km of AR7W).

The LSW and the entire central Labrador Sea became warmer and saltier over the 1960s into the early 1970s before becoming anomalously cold and fresh during the severe winters of 1974 and 1976 (Figs. 4 and 5 start in 1987, focussing on the recent changes in the Labrador Sea; the preceding developments of the LSW are reflected in Fig. 2). This cooling and

[5] Since the meteorological record at Lisbon is longer than at the Azores, Lisbon is often used instead.

[6] This technique (robust estimation) implies weighting all members from a certain group with respect to the closeness of these members to their typical (median) value. This assumes that the weights of individual outliers and their contribution to the results are negligibly small.

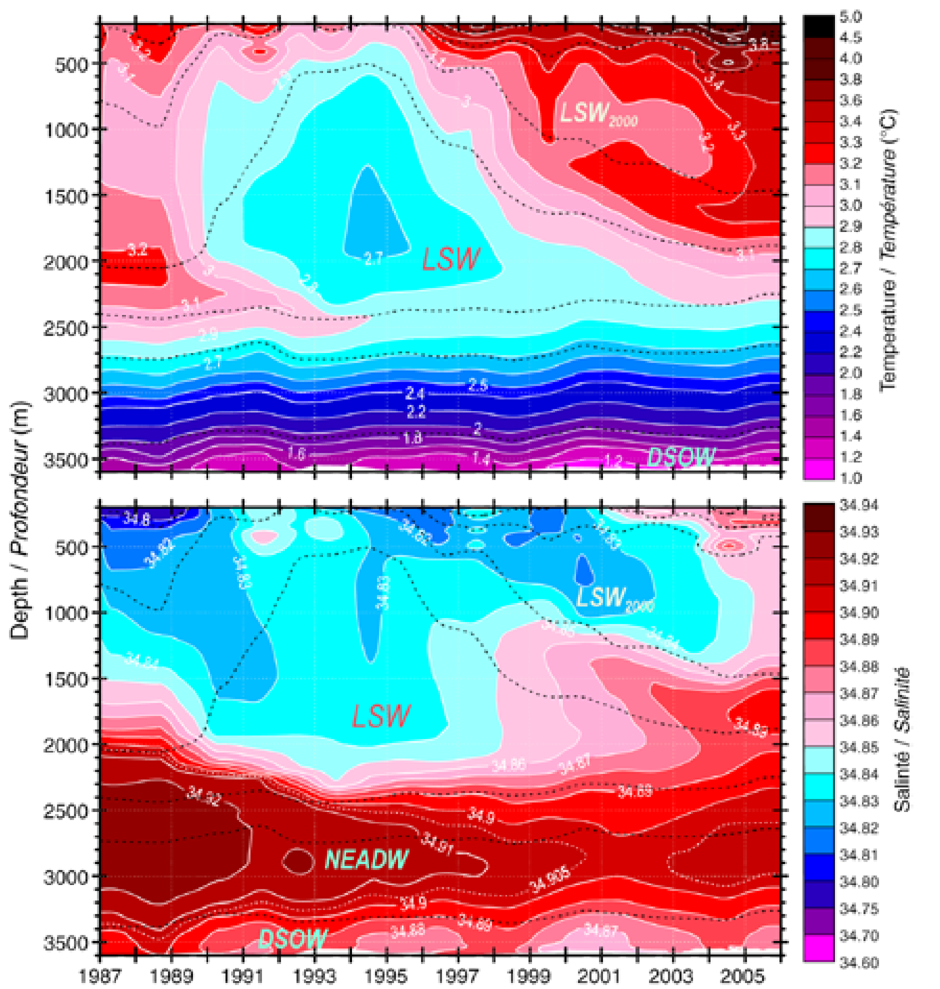

Fig. 4 Temperature and salinity in the central Labrador Sea (confined by the 3250 m isobath) between 1987 and 2005. Density contours (dashed lines) indicate that the Labrador Sea water produced between 1990 and 1994 was the densest in the record and that the upper Labrador Sea water classes formed in the early 2000s can also be defined as the layers of low vertical stability (weak density gradients).

Température et salinité dans la partie centrale de la mer du Labrador (confiné par l'isobathe de 3250 m) entre 1987 et 2005. Les contours de densité (lignes brisées) indiquent que la masse d'eau de la mer du Labrador entre 1990 et 1994 était la plus dense enregistrée dans les records et que les classes supérieures des eaux de la mer du Labrador qui se sont formées au début des années 2000 peuvent aussi être définies comme des couches de faible stabilité verticale (gradient de densité faible).

freshening was short-lived: between 1980 and 1985, the LSW was warmer and saltier than in the mid-1970s, but not as saline as it was between 1963 and 1971 (Fig. 2).

During the late 1980s, a freshwater anomaly appeared in the upper 500 m. Over subsequent years it was mixed down through winter convection (Fig. 4). A series of strong winter convection events from 1987-1988 to 1993-1994 produced a large homogeneous volume of exceptionally cold, fresh and dense LSW reaching ~2400 m (see LSW on Figs. 3, 4). This LSW was colder, fresher, denser and deeper than in any previous deep measurements in the Labrador Sea. From 1970 to 1994 (a 25-year period), the LSW became 0.08 fresher, 0.9°C colder and 0.08 kg m^{-3} denser, and its thickness more than doubled.

After the LSW mass achieved its greatest thickness and strength in 1994, it began to thin out and weaken. As time progressed, temperature and density stratification re-established above the thinning patch of LSW (Fig. 4). Such isolation of the deep and dense version of LSW was due to a substantial decrease in the net annual heat loss from the Labrador Sea to the atmosphere after 1994 (Lazier et al. 2002). This weakening in the atmospheric forcing (associated with the low NAO; Fig. 2) resulted in less intense convective mixing, mostly limited to the shallower depths of the LSW. This has meant that the LSW layer formed in 1994 has continued to become warmer, saltier and thinner (Lazier et al. 2002, Yashayaev et al. 2003).

The combination of lower heat loss to the atmosphere and continued mixing of heat and salt into the LSW layers (brought by warm and salty boundary flows and LSW recirculation) has resulted in the upper 2000 m of the Labrador Sea becoming warmer and saltier. However, this change was not the same at different depths (Fig. 4). The annual changes between 1800 and 2300 m are smaller but steadier than those occurring at shallower depths. Although we do not dismiss the possibility that there might have been occasional short convective events penetrating deeper than 1500 m and reaching into the deep and dense LSW classes after 1994, there is no evidence that such events made any significant change in the properties and volume of this deep LSW created in 1994 and earlier. The evenness in the annual changes of the deepest LSW over a decade (specifically, 1994-2005) implies that, although the whole body of the deep LSW loses its mass by draining or leaking out of the subpolar gyre[7], a significant part of it is still recirculating within the Labrador and Irminger seas and possibly elsewhere. Along its extensive outer boundary, this deep recirculation places LSW into contact with warmer and saltier waters of the same density, allowing their mixing and exchange, and, consequently, maintaining the steady transfer of heat and salt into the LSW core at the center of the Labrador Sea (which in turn results in the nearly constant changes of temperature and salinity observed in the deep LSW core between AR7W occupations).

The general increase in temperature and salinity of the upper 2000 meters since 1994 (Fig. 2) was disrupted by a cooling and freshening event that occurred in 2000, which was the most significant winter convection since 1994. A freshwater anomaly that appeared in the upper 500 m in the previous

[7] The upper classes of LSW are being replaced by warmer, saltier and lighter waters.

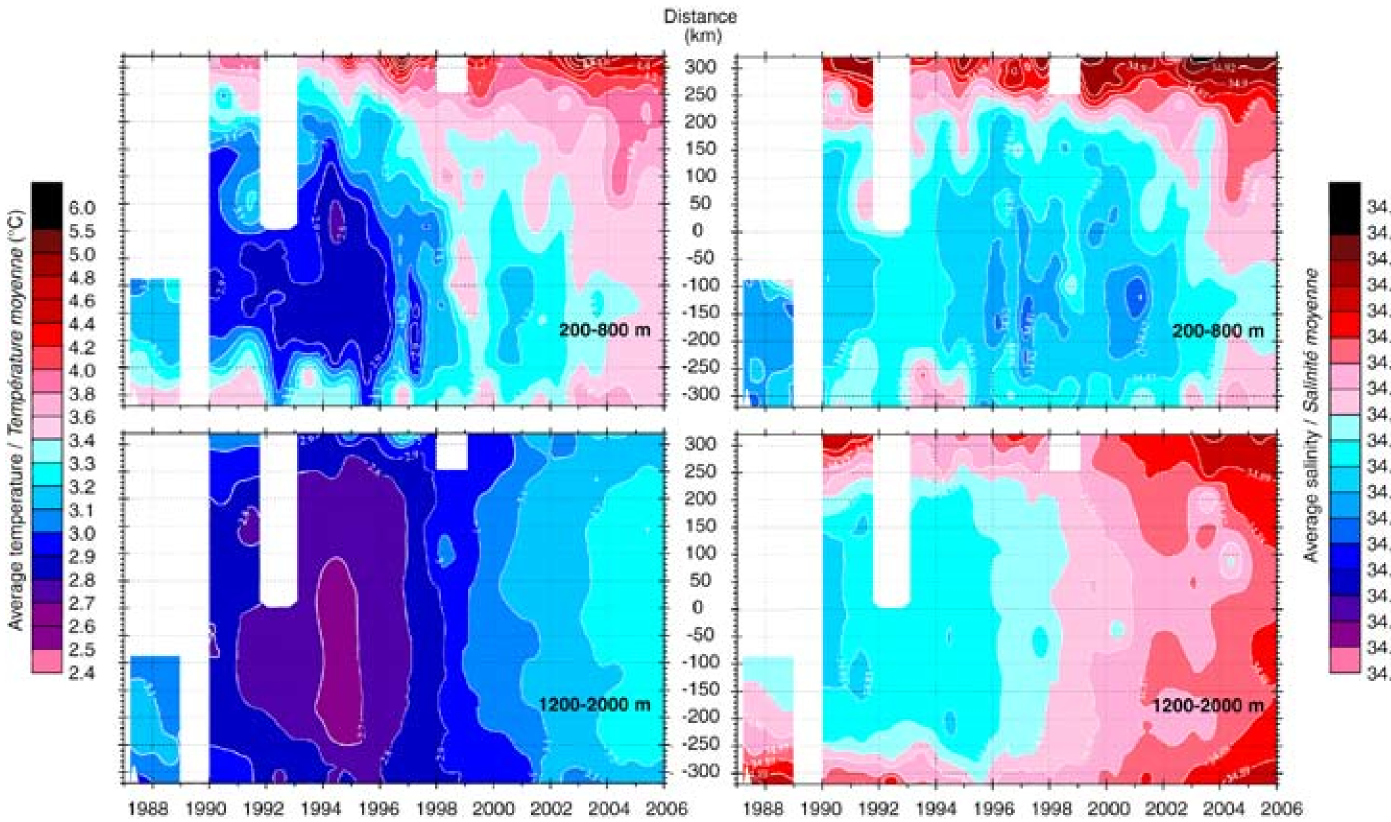

Fig. 5 Temperature and salinity averaged over the 200-800 m (upper panels) and 1200-2000 m (lower panels) layers along the Labrador Sea section AR7W (Fig. 1). The vertical axis between the two sets of panels is the distance to the central point of the section line, with its values increasing toward the Greenland coast (positive direction) and decreasing toward the Labrador coast (negative direction). OWS Bravo station is about -100 km from the central point.

Température et salinité moyennes pour les couches de 200 à 800 m (panneaux du haut) et 1200 et 2000 (panneaux du bas) le long de la section AR7W de la mer du Labrador (Fig. 1). L'axe vertical entre les deux sets de panneaux représente la distance au point central de la section avec ses valeurs augmentant vers la côte du Groenland (direction positive) et diminuant vers la côte du Labrador (direction négative). La station OWS Bravo se situe à environ -100 km.

years was carried down through winter convection in 2000 (salinities <34.82; Fig. 4, lower panel) and subsequent years (similar to the convectively driven redistribution of freshwater from the late 1980s to the early 1990s). The 2000 convection reached 1600 m and was extensive enough to produce a distinct LSW class that is still seen in the Labrador and Irminger seas (designated LSW_{2000} in Figs. 3, 4). The LSW_{2000} is on the warmer, fresher and lighter sides of the long-term ranges of LSW temperatures, salinities and densities. Even though this LSW is warmer, less dense and shallower than that formed in 1990-1994, these two LSW classes have much in common (e.g., rates of annual change, spreading pathways). Although the LSW_{2000} class could have been renewed in the years following its formation, winter convection from 2001 to 2005[8] failed to increase its density (its density, in fact, decreased); now, as has been discussed for the densest and deepest LSW_{1994}, the LSW_{2000} and the intermediate depths occupied by this water mass are also becoming warmer and saltier. It is likely that most of this change is due to mixing with warmer and saltier waters from outside the Labrador Sea. However, there are also indications that winter convection after 2000 has also brought warmer and saltier waters into the LSW_{2000} layer. In fact, in 2001-2003, it did appear to become thicker and show irregular year-to-year changes in salinity and oxygen, suggesting its renewal after 2000.

In spite of the increasing salinity in the upper 500 m in 2004 and 2005, the warming of the upper layer is increasing the density stratification of the Labrador Sea, making it more difficult for winter renewal of LSW to take place and leading to isolation of LSW_{2000}.

Changes in the Intermediate Layers Across the Labrador Sea

The annual occupations of the AR7W hydrographic section since the late 1980s allow us to examine how the various intermediate and deep water masses evolve across the Labrador Basin and to determine the pathways of the major signals influencing certain layers within the subpolar gyre. In particular, the role that the subpolar gyre circulation plays in the restratification of the Labrador Sea can be clearly seen in Figure 5, which shows how the average temperature and salinity of the upper (200-800 m) and lower (1200-2000 m) LSW layers vary across the AR7W section from 1987 to 2005. This figure is based on vertical averaging of profiles from individual stations over the corresponding layers (200-800 m for the upper LSW or upper intermediate layer and 1200-2000 m for the deep LSW or lower intermediate layer).

[8] In these years, deep convection could happen in the Labrador Sea, in the Irminger Sea, or in both.

The upper intermediate layer features two major LSW events since 1987, while the lower intermediate shows just one LSW development. Through the early 1990s, both layers had similar temperatures and salinities because the entire depth range was filled with the developing 1994 class of LSW (LSW_{1994}). After 1994, the upper intermediate layer (200-800 m; Fig. 5) showed continued freshening (except near the Greenland coast) as winter convection renewed the upper LSW layers, while the lower intermediate layer (1200-2000 m; Fig. 5) exhibited the decay of the LSW_{1994} through advection and mixing. Since 1994, the deep LSW and the whole lower intermediate layer have been steadily becoming warmer and saltier over the entire basin, whereas the asymmetric and irregular warming of the upper intermediate layer was interrupted by the cooling of 1999/2000. In 2000, the western part of the upper intermediate layer was the freshest in 15 years.

The May 2004 survey showed that the upper 1500 m of the Labrador Sea were the warmest since the beginning of annual occupations of the AR7W section line in 1990, which were conducted under the aegis of WOCE. The most rapid warming of this layer occurred between 2003 and 2004. This warming was not simply a consequence of the warming in the surface and LSW layers. In 2004, a large volume of warm and salty water appeared over the continental slopes on the Greenland and Labrador ends of the section. This water is thought to have come from the Irminger Sea, carried north and west by the Irminger Sea branch of the North Atlantic Current. The upper layer (Fig. 5) shows a rapid increase in temperature and salinity over the whole eastern part of the Labrador Sea between 2003 and 2004. This warm and salty water from the Irminger Sea, seen along the eastern and (in some years) western rims of the Labrador Sea, spread out to the centre of the Labrador Basin in 2004, filling the whole eastern part of the basin between 100 and 800 m. As a result, temperature and salinity at 700 m in the eastern part of the Labrador Sea increased by 0.6°C and 0.05 in one year.

Although the 2005 spring occupation did not show a further increase in the volume of these Irminger Sea waters, the upward trends in both temperature and salinity in the upper 2000 m over most of the AR7W line did persist (Figs. 4, 5). The Labrador Sea is approaching the conditions last seen in the late 1960s. If these trends continue, the Labrador Sea temperatures could soon become the warmest ever recorded. Even if the mean water temperature is still lower than the record high (Fig. 2), the sea level (estimated as the steric height, discussed below) in the central region of the Labrador Sea has already approached the record high levels observed between 1969 and 1972.

LSW Production and Contribution to the North Atlantic Deep Water

As we already mentioned, LSW is not just found in the Labrador Sea—it is the principal intermediate water mass of the subpolar North Atlantic gyre and spreads southward into the subtropical gyre and beyond within the deep western boundary current (Talley and McCartney 1982; Yashayaev et al. 2004). Within the subpolar gyre, LSW can be easily identified as a layer of low salinity and stability below 500 m (Yashayaev et al. 2004). Deep convection does not just create salinity, temperature and density anomalies at the intermediate depths through the formation of LSW, it also carries climatologically and biologically active substances such as greenhouse gases and nutrients out of the seasonally active surface and subsurface layers.

Because the North Atlantic was well surveyed in 1995-1997 (following the most voluminous LSW production) as part of WOCE, and there was an extensive observational effort in the same region in 1966-1972 (these featured the record low LSW volume), the total volume of recently ventilated LSW within the subpolar gyre could be estimated. Assuming that this ventilation took place over the entire 25-year period (1970-1995), we estimated the 25-year mean annual LSW production to be ~2×10^6 m^3 s^{-1} or ~2 Sv (Yashayaev et al. 2004). However, as discussed above, LSW production is not a continuous steady process but is more episodic in nature, meaning that for a year with developed winter convection, this estimate is a lower bound for a LSW production rate. (There are also other reasons for considering this value as an underestimation, e.g., quick removal of the LSW by the boundary currents outside of the domain, entrainment of the LSW by other water masses). Our recent analysis shows that just between 1987 and 1992 (the beginning of the recent development of the deep LSW), the average LSW production rate was at least 4.5 Sv, which is about a third of the expected average transport associated with the North Atlantic overturning circulation.

Because the LSW is found throughout the subpolar gyre, it is also mixed with the various Arctic components of the North Atlantic Deep Water (NADW) when these waters enter the North Atlantic through the Faeroe Banks channels and Denmark Strait or over the Faeroe–Iceland ridge. These dense waters from the Nordic Seas enter the North Atlantic at depths of less than 900 m and form boundary currents as they descend the continental slope to their equilibrium depths. There is a great deal of mixing associated with these overflows, and one of the water masses that the overflows are mixed with is the LSW[9].

Through this mixing and via NADW, freshwater, greenhouse gases, nutrients and other substances enter the abyssal oceans (which are the deep reservoirs for such substances), thereby forming an effective pathway from the surface layers to the deep ocean where these substances can be isolated from the atmosphere for centuries. This pathway only functions as long as winter convection occurs to depths of greater than 1000 m in the Labrador Sea.

Changes in the Deep Waters of the Labrador Sea

NADW represents a vast body of all intermediate and deep Atlantic waters that are collectively formed within the arctic and subarctic domains and is a common entity in large-scale analyses and generalizations. However, in regional studies, we operate with water mass definitions typifying the masses by their regions of origin and evolution histories.

Both vertical sections of salinity (Fig. 3) and plots showing the depth-dependent temporal evolution of salinity (Fig. 4) exhibit a relatively salty water mass below the LSW. This is the Northeast Atlantic Deep Water (NEADW). NEADW can be

[9] After its formation, LSW takes ~2 y to reach the northern parts of the Irminger Sea and ~5 y to reach the Iceland Basin.

easily identified as the salinity maximum below 1500 m (Figs. 3, 4). This water mass originates from the dense overflow entering the North Atlantic through the deep trenches in the Scotland–Shetland–Faeroe–Iceland ridge. The relatively cold, dense and fresh water below NEADW is the Denmark Strait Overflow Water (DSOW). DSOW enters the Irminger Sea from the Greenland Sea as a narrow, cold and dense flow at the sills of the Denmark Strait. DSOW is the densest water found in the Irminger Sea, Labrador Sea and Newfoundland basins. It is seen on vertical sections as a thin layer of relatively cold and fresh water found near the bottom of these basins (Fig. 3).

Between the 1960s and the late 1990s, the deep layers of the entire subpolar North Atlantic experienced widespread and sustained freshening (Dickson et al. 2002). Our Labrador Sea observations indicate that this tendency has recently changed. In 2000, NEADW reached its all-time freshest state and since then it has been becoming saltier (Fig. 4). Although the individual annual increases of NEADW salinity were small and about equal, they have been highly persistent, resulting in a significant trend over the last 5 years. Since NEADW arrives from the eastern North Atlantic by way of the Irminger Sea, the change seen in the Labrador Sea suggests that NEADW was also becoming saltier in the rest of the subpolar North Atlantic.

The near-bottom (DSOW) layer of the Labrador Sea exhibits significant interannual variations of temperature and salinity. Changes are largely caused by anomalously cold and fresh events (seen between 3300 m and 3600 m in Fig. 4) arriving in the eastern Labrador Sea from the Irminger Sea and exiting the southwestern part of the Labrador Sea. The most recent cooling and freshening of the DSOW layer was observed in the Labrador Sea in 2005. We combined our near-bottom temperature and salinity series with the "upstream" measurements from a mooring array across the slope of Greenland in the Irminger Sea, about 200 km south of the Denmark Strait, and lag-correlated the anomalies from different sites. All cooling and freshening events, first seen in the "upstream" DSOW records from the Irminger Sea moorings, arrived in the Labrador Sea with a delay, generally increasing to the west. The passage of such signals through the deep layers of the Labrador Sea provides an indication of the operational state of the abyssal branch of the meridional overturning circulation in the Atlantic Ocean.

Observed and Predicted Sea Level in the Central Labrador Sea

The section-wide changes in the water mass properties and stratification led to significant variations in the steric height (the water column thickness based on its temperature and salinity) in the central Labrador Sea that are also seen in the observed sea level (Fig. 2, lower plot; the steric height and sea-level anomalies were calculated for the same region). The sea-level anomalies (SLA) shown in Figure 2 were computed from SLA values extracted from the globally gridded SLA maps (1/3°×1/3°) computed with respect to a seven-year mean. These maps (downloaded from http://www.jason.oceanobs.com/html/donnees/produits/msla_uk.html) were based on the observations available from the Topex/Poseidon and Jason satellite missions since 1992. Temporal variations of the steric height and sea level agree well and reflect most of the major changes seen in the Labrador Sea hydrography. The intense cooling of the early 1990s resulted in a 9-cm drop of steric height in the central Labrador Sea, and the subsequent restratification over the past decade raised the steric height to its earlier levels. The warming observed between 1994 and 2005 led to the sea level rise. In 2005, the sea level in the central Labrador Sea was about 7-8 cm higher than in 1994, approaching the record highest level observed between the late 1960s and the early 1970s.

Conclusion

This 16-year series of annual occupations, first undertaken as a contribution to WOCE and continued as part of the CLIVAR and Global Ocean Observing System (GOOS) projects, is the key tool for observing the interannual variability of the North Atlantic within and near the high latitude source regions of the meridional overturning circulation. The value of this program to the understanding of ocean climate lies in the long-term sustained nature of the sampling because the variability is significant over years, decades and even longer.

The monitoring of the Labrador Sea is also a key task in the Arctic-Subarctic Ocean Flux (ASOF) action plan aiming "to measure and model the variability of fluxes between the Arctic Ocean and the Atlantic Ocean with the view to implementing a longer-term system of critical measurements needed to understand the high-latitude ocean's steering role in decadal climate variability" (http://asof.npolar.no/). During the International Polar Year, we hope to extend our observations to the north of the AR7W line and to study the effects of the Arctic outflows and regional climate change on the physical processes and ecosystem in the Labrador Sea and shelf regions.

Acknowledgements

The authors are grateful to many colleagues who have contributed to the hydrographic programs in the Labrador Sea and appreciate the helpful comments and suggestions from John Loder (BIO) and the AZMP Bulletin reviewers on this report.

References

Dickson, B., Yashayaev, I., Meincke, J., Turrell, B., Dye, S., and Holfort, J. 2002. Rapid freshening of the deep North Atlantic over the past four decades. Nature 416(6883): 832-837.

Hendry, R. 2006. Upper-ocean variability in the Labrador Sea in recent years. AZMP/PMZA Bulletin 5: 10-12.

Lazier, J.R.N. 1980. Oceanographic conditions at Ocean Weather Ship Bravo, 1964-1974. Atmos.-Ocean 18: 227-238.

Lazier, J., Hendry, R., Clarke, A., Yashayaev, I., and Rhines, P. 2002. Convection and restratification in the Labrador Sea, 1990-2000. Deep-Sea Res. I 49(10): 1819-1835.

McCartney, M.S., and Talley, L.D. 1982. The subpolar mode water of the North Atlantic Ocean. J. Phys. Oceanogr. 12(11): 1169-1188.

Talley, L.D., and McCartney, M.S. 1982. Distribution and circulation of Labrador Sea Water. J. Phys. Oceanogr. 12(11): 1189-1205.

Yashayaev, I., Lazier, J.R.N., and Clarke, R.A. 2003. Temperature and salinity in the central Labrador Sea. ICES Mar. Sci. Symp. Ser. 219: 32-39.

Yashayaev, I., Bersch, M., van Aken, H., and Clarke, A. 2004. A new study of the production, spreading and fate of the Labrador Sea Water in the subpolar North Atlantic, Arctic/Subarctic Ocean. Fluxes Newsletter. No. 2, pp. 20-23.

Modelling Plankton Dynamics with an Adaptive Physical–Biological Model: an Example with AZMP Station 2

A. F. Vézina, M. Pahlow, B. Casault and H. Maass
Bedford Institute of Oceanography, Box 1006, Dartmouth, NS, B2Y 4A2
VezinaA@dfo-mpo.gc.ca

Sommaire

Nous résumons ici les progrès accomplis dans le développement d'un modèle multi-disciplinaire (physique-biologie) pour assister l'interprétation des données acquises par le Programme de Monitorage de la Zone Atlantique. Le modèle se distingue par l'utilisation de fonctions adaptives qui simulent l'adaptation des organismes et des communautés planctoniques face aux changements environnementaux (ex. température). Le modèle simule bien l'évolution observée de la productivité hivernale et de l'intensité des blooms printaniers entre 1999 et 2004. Par contre, le modèle ne reproduit pas encore assez bien l'évolution pendant les périodes estivales et automnales. Le développement du modèle se concentre présentement sur l'étude de différentes fonctions pour décrire le broutage par le zooplancton.

The Department of Fisheries and Oceans, like most similar governmental agencies in the western world, is moving towards ecosystem-based management of the marine environment. This increases the demand not only for sustained observations of ecosystem properties but also for tools to integrate these observations and to eventually produce ecological forecasts. In that context, models that link simulations of the physical and ecological environments, generally referred to as physical–biological models, will play a significant role. In particular, physical–biological models can be designed to assimilate data from observing systems and thus combine the intelligent interpolation and extrapolation provided by the models with the reality check provided by the data. Here, we briefly summarize recent research activities related to the development of such assimilative models for the northwestern Atlantic. We focus our modelling studies on the AZMP Station 2 of the Halifax Section, situated approximately 50 km southwest of Halifax, Nova Scotia.

The physical–biological modelling system we use in our studies is illustrated in Figure 1. At this point, we model the physical environment and the ecosystem therein as a vertical column (1-D model). This may seem risky in coastal environments that can have vigorous horizontal circulations. However, our emphasis here is on evaluating different ways to simulate ecological processes, and 1-D models are really the only option given limitations of computer resources. The physical model is driven by analyzed weather observations (NCEP, http://www.cdc.noaa.gov), and the simulated temperature and salinity are continuously adjusted to ocean observations from Station 2 to compensate for the lack of full physics (e.g., no horizontal advection). Therefore, the physical model is not predictive and is used to produce simulated temperatures and mixing that reflect daily fluctuations in marine weather. These data are then passed to the ecological model, augmented by a temporally averaged vertical velocity from Petrie and Yeats (2000) to account for the vertical mixing and transport of ecological constituents and for the effect of temperature on

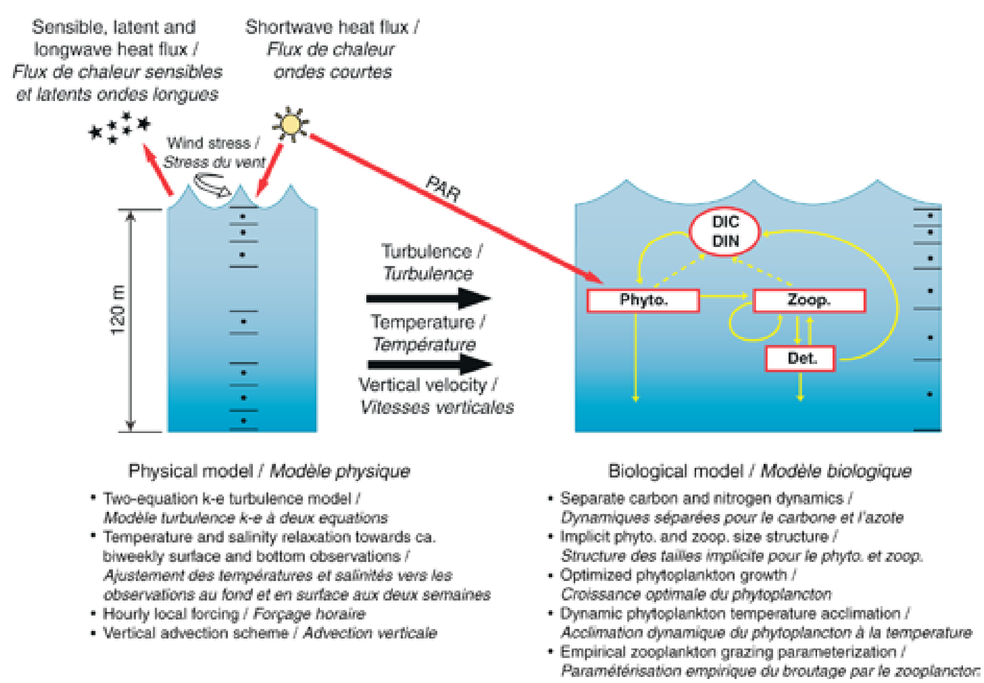

Fig. 1 Interdisciplinary model used to simulate seasonal to interannual variability in physical and ecological conditions on the Scotian Shelf. A full description of the model is currently being prepared for publication (Pahlow and Vézina, in prep.).

Modèle interdisciplinaire utilisé pour simuler la variabilité saisonnière et interannuelle dans les conditions physiques et écologiques sur le plateau Néo-Écossais. Une description complète du modèle est en préparation pour publication (Pahlow et Vézina, en prép.).

ecological processes. In these simulations, nitrate is kept constant (14 μM) at the bottom boundary of the model domain at 140 m and surface irradiance was reconstructed from NCEP daily means.

The ecological model includes phytoplankton, zooplankton, nutrients and detritus (the so-called PZND model) and does not include any higher trophic levels (Fig. 1). This is appropriate since our focus is on the impact of weather and climate on ocean productivity and nutrient cycling: plankton do most of the work in that regard. In principle, such lower trophic level models can pass information to higher trophic level models just as the physical model affects the plankton model. Although our ecological model has the PZND structure common to this type of interdisciplinary modelling, it has some unique features. In particular, we incorporate some of the complexity found in real ecosystems without increasing the number of boxes in the model. For example, our phytoplankton and zooplankton boxes (Fig. 1) are actually made up of size fractions that evolve during the simulation based on empirical rules (e.g., Li 2006). We also include principles that allow ecosystem components to adapt to changes in their simulated environment just as organisms or communities can in their real environment. For example, our adaptive temperature function simulates the effect of competition among different species that are adapted to different temperatures.

A model simulation of physical and ecological conditions at Station 2 from 1999 to 2004 is shown in Figure 2. For each year, the simulation reproduces the annual cycle typical of mid-latitudes. Temperatures are minimum and surface nutrients maximum during the winter, reflecting increased mixing with nutrient-rich bottom waters driven by strong cooling and winds. This is followed by a brief, intense spring bloom of phytoplankton (high chlorophyll) that uses up the surface nutrients. The warm summer period features low surface chlorophyll concentrations with a subsurface maximum at 20-30 m. The cycle is closed by small increases in phytoplankton biomass during the fall (fall blooms) as the surface waters cool and nutrients are mixed into the surface layer. In addition, the simulation also shows noticeable interannual variability, with colder winter temperatures during the latter part of the period concurrent with increased winter nutrients and stronger spring blooms. There is also a perceptible trend towards stronger subsurface chlorophyll maxima and fall blooms towards the end of the monitoring period.

The simulated interannual changes in temperature mirror reality since the physical model is adjusted to match the measurements for the time they were collected. However, the parame-

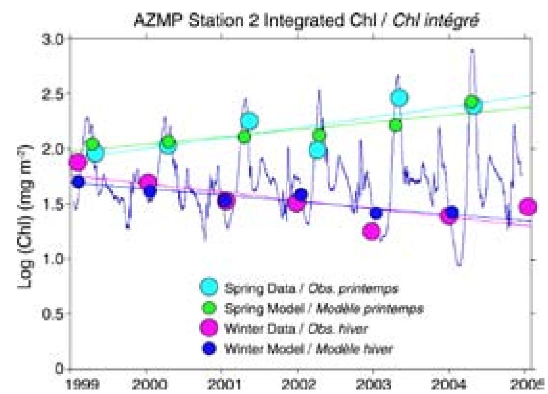

Fig. 3 Simulated integrated chlorophyll (solid blue line) along with seasonal averages for spring (March to May, model: green; data: cyan) and winter (December to February, model: blue; data: magenta). The straight lines indicate interannual trends for modelled and observed spring and winter averages. Slopes and standard deviations are given in Table 1.

Chlorophylle intégrée sur la colonne d'eau simulée par le modèle (ligne pleine bleue) avec les moyennes saisonnières pour le printemps (mars à mai, modèle : vert; données : cyan) et l'hiver (décembre à février, modèle : bleu; données : magenta). Les lignes droites indiquent les tendances interannuelles pour les moyennes printanières et hivernales observées et simulées. Les pentes et les écarts types de ces droites sont fournies au tableau 1.

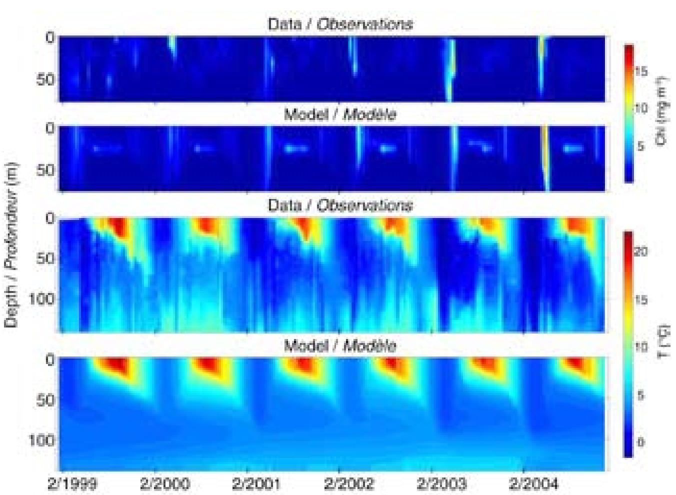

Fig. 2 Contour plots of observed and modelled chlorophyll (upper two panels) and temperature (lower two panels) for the period 1999 to 2004. The fluctuations in warmer temperatures below 100 m in the third panel indicate upwelling or onshore intrusions of slope water that cannot be reproduced by this model.

Évolution dans le temps des profils verticaux de la chlorophylle (deux panneaux du haut) et de la température (deux panneaux du bas) observées et simulées pour la période 1999 à 2004. Les variations dans les températures plus chaudes sous 100 m dans le panneau 3 indiquent des remontées d'eau ou des intrusions d'eaux de la pente continentale qui ne peuvent être reproduites par ce modèle.

Table 1 Trend over the 1999-2004 period (change yr^{-1}) and interannual variability (standard deviations in parentheses) in spring and winter integrated Chl (shown in Fig. 3).

Tendance sur la période 1999-2004 (changement an^{-1}) et variabilité interannuelle (écarts types entre parenthèses) dans la chlorophylle intégrée au printemps et en hiver (voir Fig. 3).

Change yr^{-1} (SD)	Spring	Winter
Changement an^{-1} (ET)	*Printemps*	*Hiver*
Data / *Données*	0.094 (0.22)	−0.075 (0.20)
Model / *Modèle*	0.067 (0.14)	−0.058 (0.12)

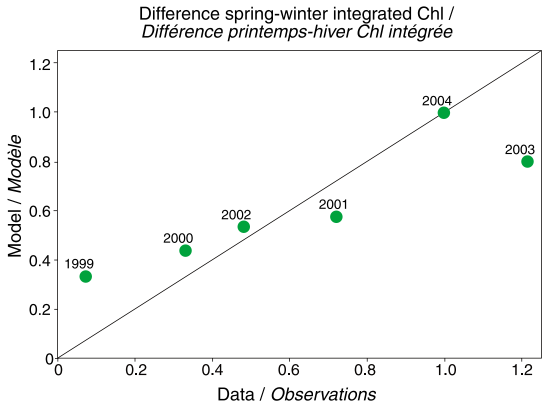

Fig. 4 Observed and modelled spring–winter differences in integrated chlorophyll for each year from 1999 to 2004. The root mean squared difference was calculated with respect to the 1:1 line. Numbers indicate years. Overestimates at the low end and underestimates at the high end indicate that the long-term variability is not well reproduced by the model.

Différences printemps–hiver dans la chlorophylle intégrée observée et simulée pour chaque année entre 1999 et 2004. La différence de la moyenne quadratique a été calculée par rapport à la ligne 1:1. Les nombres indiquent les années d'observations. La sur-évaluation pour les valeurs faibles et la sous-évaluation pour les fortes valeurs indiquent que la variabilité à long terme n'est pas bien reproduite.

ters of the ecological model were adjusted to match the average seasonal cycle in nutrients, chlorophyll and zooplankton over that period. Therefore, the simulated interannual variability of these ecological variables is an independent test of the model's sensitivity to simulated physical changes. Figure 3 shows interannual changes in vertically integrated chlorophyll simulated by the model and as observed at Station 2. The model correctly reproduces the general pattern of interannual trends and year-to-year variability for the spring and winter seasons (Fig. 3 and Table 1). Modelled spring-winter differences also largely follow the observed pattern (Fig. 4), but the model overestimates summer biomass and predicts increasingly strong fall blooms over the period whereas the data indicate that fall blooms have weakened over that same period (Fig. 2, upper two panels). The model estimates the change over the 1999-2004 period better than the year-to-year variability (Fig. 4 and Table 1). We are making substantial progress but work on improving the model must continue. To that end, we performed sensitivity analyses to investigate which aspects of this inter-disciplinary model should be given priority for further development. In general terms, our results indicate that improving the physical and ecological models should be given equal attention. More specifically, a better representation of vertical advection (upwelling, downwelling; see Fig. 2, third panel) seems critical to improve the results, both in terms of the seasonal cycle and interannual variability (Greenan et al. 2004). On the ecological side, the representation of zooplankton grazing turns out to be critical. With the same physics, changing the way grazing works in the model has dramatic impacts on the simulated seasonal and interannual patterns. Widely used models of grazing (e.g., Ivlev, Michaelis-Menten) do less well in reproducing the observed chlorophyll dynamics than an empirical model (Peters 1994). There is a strong need to develop new and more realistic grazing functions for ecological models.

References

Greenan, B.J.W., Petrie, B.D., Harrison, W.G., and Oakey, N.S. 2004. Are the spring and fall blooms on the Scotian Shelf related to short-term physical events? Cont. Shelf Res. 24: 603-625.

Li, W.K.W. 2006. Plankton populations and communities. *In* Marine Macroecology. *Edited by* Witman, J., and Roy, K. University of Chicago Press, in press.

Peters, F. 1994. Prediction of planktonic protistan grazing rates. Limnol. Oceanogr. 39: 195-206.

Petrie, B., and Yeats, P. 2000. Annual and interannual variability of nutrients and their estimated fluxes in the Scotian Shelf - Gulf of Maine region. Can. J. Fish. Aquat. Sci. 57: 2536-2546.

Phytoplankton Monitoring in Bedford Basin, the Scotian Shelf and the Labrador Sea: a Large-Scale Multi-Year Coherence

William K. W. Li, W. Glen Harrison and Erica J. H. Head
Bedford Institute of Oceanography, Box 1006, Dartmouth, NS, B2Y 4A2
LiB@mar.dfo-mpo.gc.ca

Sommaire

L'abondance du phytoplancton a été enregistrée pour des périodes de 13, 9 et 12 ans respectivement dans le bassin de Bedford, dans trois régions du plateau Néo-Écossais (plateau ouest, centre et est), et dans trois régions de la mer du Labrador (bassin central du Labrador, plateau du Labrador et plateau du Groenland). Cinq autres stations de la région de Western Isles dans la baie de Fundy ont également été étudiées pendant quelques mois. Les cellules phytoplanctoniques ont été comptées par cytomètre en flux et les résultats de ces analyses fournissent une perspective de la communauté photo-autotrophe qui est différente de celle offerte par les mesures de biomasse ou de dénombrement par microscopie des diatomées et des dinoflagellés. L'ensemble de ces données indique une cohérence générale en ce qui a trait au développement saisonnier du phytoplancton dans les différentes régions étudiées. Ces données indiquent également une grande cohérence dans l'évolution annuelle de l'abondance du phytoplancton au cours de plusieurs années, suggérant que des organismes avec des temps de reproduction aussi courts (e.g., les microbes) peuvent répondre d'une façon cohérente à un mécanisme de forçage environnemental commun. Dans ce contexte, le bassin de Bedford, qui est échantillonné de façon hebdomadaire, peut donc s'avérer un outil important de surveillance permettant de bien intégrer la réponse régionale du phytoplancton faces aux changements environnementaux.

Phytoplankton are unicells. They contain light-harvesting chromophores that make it possible to detect them remotely by visible spectral radiometry or in bulk samples by precise pigment quantification or crude colorimetric estimation. Thus, the respective use of satellite ocean colour, particulate chlorophyll concentration and Continuous Plankton Recorder green index to monitor the biomass of phytoplankton by proxy are important elements of AZMP (Atlantic Zone Monitoring Program). However, detection of phytoplankton as single cells requires visual examination by light microscopy or electronic discrimination by flow cytometry. Only these latter methods are useful for understanding biodiversity because they explicitly recognize phytoplankton as phylogenetically distinct biotic units expressive of evolutionary traits and ecological interactions. Phytoplankton cells are entities that undergo binary fission susceptible to selection pressures. These cells are also the entities eaten by consumers: small ones are engulfed by protistan zooplankton and large ones are captured by metazoan zooplankton. Conventional light microscopy is labour-intensive and biased towards the larger phytoplankton (microplankton such as diatoms and dinoflagellates). Flow cytometry is semi-automated and biased toward the smaller phytoplankton (pico- and nanoplankton). A combination of both methods provides detailed characterization of the phytoplankton community.

The abundance of phytoplankton is scaled to cell mass according to an allometric rule with a power exponent of negative ¾ (Belgrano et al. 2002). This highly uneven distribution is counterbalanced by the scaling of metabolic rate to cell mass according to a power exponent of positive ¾ (West et al. 2002). The equal and opposite scaling of abundance (cells m^{-3}) and cellular photosynthesis (mg C $cell^{-1}$ d^{-1}) ensures that their product, primary production (mg C m^{-3} d^{-1}), is invariant with size. Here, we report on the flow cytometric monitoring of phytoplankton abundance in different parts of the western North Atlantic Ocean. The results indicate a perspective of phytoplankton coherence across the entire region that is not evident in analyses of bulk pigment or microphytoplankton alone.

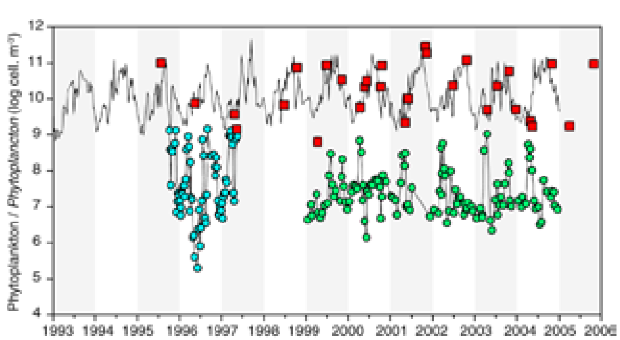

Fig. 1 Phytoplankton abundance in Bedford Basin and Halifax Station 2 (HL2). Measurements were made by flow cytometry (Bedford Basin = continuous line; HL2 = red squares) and by light microscopy (Bedford Basin = blue circles; HL2 = green circles).

Abondance du phytoplancton dans le bassin de Bedford et à la station 2 du transect de Halifax. (HL2). Les mesures ont été effectuées par flux cytométrie (bassin de Bedford = ligne continue; HL2 = carrés rouges) et par microscopie optique (bassin de Bedford = cercles bleus; HL2 = cercles verts).

Phytoplankton is monitored in three regions of the Canadian Atlantic zone using sampling and flow cytometric techniques described elsewhere (Li and Harrison 2001). Bedford Basin is the inner portion of Halifax Harbour and has been sampled once every week since 1992 at the Compass Buoy station (Li and Dickie 2001). The Scotian Shelf has been sampled once every spring (April or May) and every fall (October) since 1997 along a western section (Browns Bank Line, BBL), a central section (Halifax Line, HL), and an eastern section (Louisbourg Line, LL), all normal to the coast and each comprising seven stations (Therriault et al. 1998). At station 2 of the Halifax Line (HL2), there is supplementary sampling once every two weeks in order to delineate higher frequency events. The Labrador Sea has been sampled every spring or early summer (May-July) since 1994 along the AR7W transect (Lazier et al. 2002). Ice conditions permitting, 28 stations are sampled starting from Hamilton Bank on the Labrador Shelf (LS), through the central Labrador Basin (LB), ending at Cape Desolation on the Greenland Shelf (GS).

The 52-week cycle of phytoplankton in Bedford Basin is consistent from year to year (Fig. 1). Although week-to-week variations are large, the climatological cycle indicates a direct progression from the winter minimum on week 6 to the maximum on week 37, which is near the autumnal equinox (Li and Dickie 2001). A short series of microphytoplankton counts from fall 1995 to spring 1997 (Fig. 1) indicates diatom and dinoflagellate blooms (Li et al. 1998). The mean abundance of microphytoplankton is 2.5 x 10^8 cells m^{-3} and that of the other phytoplankton is 2.5 x 10^{10} cells m^{-3}: a ratio of exactly 1 to 100.

At HL2, the record of phytoplankton counts by flow cytometry is much less complete, but available observations appear to correspond well to those in Bedford Basin (Fig. 1). The semi-monthly microscope counts of microphytoplankton at HL2 establish a continuous time series since 1999 (Fig. 1); HL2 is characterized by intense diatom blooms in spring. The mean abundance of microphytoplankton at HL2 is 7.0 x 10^7 cells m^{-3}, which is about 700 fold less than the mean abundance of other phytoplankton.

Over the entire Scotian Shelf, the semi-annual counts of phytoplankton at HL, BBL and LL all show cross-shelf 7-station average values that are low in spring and high in fall, with concentrations not greatly different from those in Bedford Basin at the given times of the year (Fig. 2). In the Labrador Sea (Fig. 3), the 12-station average phytoplankton abundance in LB and the 10-station average in LS also show convincing agreement with the Bedford Basin time series. The 5-station average in GS was less well matched.

A consolidation of the data viewed as a 366-day cycle (Fig. 4a) emphasizes the general coherence of phytoplankton seasonality at virtually all the monitoring sites. The low bias in the GS values is clearly evident here. There may be a delay of about a month in the peak of phytoplankton on the shelves and open ocean compared to the inshore, but this cannot be confirmed until the former are sampled during the autumnal equinox.

In the Western Isles region of the Bay of Fundy, counts of phytoplankton were made by flow cytometry in the summer and fall of 2001 (Li et al. 2002). The developmental progression of

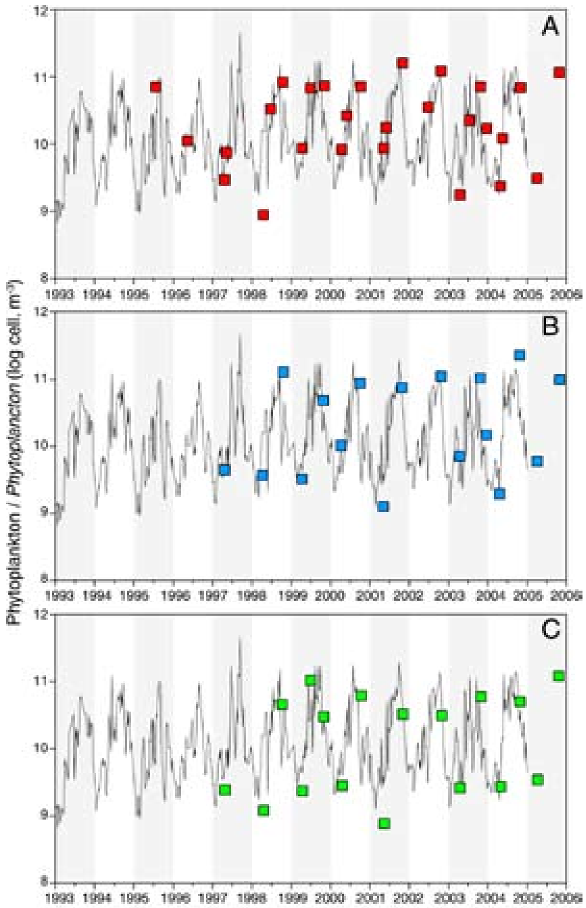

Fig. 2 Phytoplankton abundance in surface waters of Bedford Basin (continuous line) and the Scotian Shelf (coloured symbols) on the (a) Halifax Line, (b) Browns Bank Line, (c) Louisbourg Line. The Bedford Basin time series was constructed from weekly samples taken at 5 m depth. On each Scotian Shelf section, the values represent an integrated sample (average of 0, 5, 10 m) averaged over seven stations distributed along the different lines.

Abondance du phytoplancton dans les eaux de surface du bassin de Bedford (ligne continue) et du plateau Néo-Écossais (symboles colorés) le long du transect de Halifax (a), du transect de Browns Bank (b) et de celui de Louisbourg (c). La série temporelle de données pour le bassin de Bedford a été construite à partir des échantillons récoltés hebdomadairement à une profondeur de 5 m. Pour chaque transect du plateau Néo-Écossais, les valeurs utilisés représentent une intégration moyenne des échantillons (moyenne de 0, 5 et 10 m) provenant de 7 stations situées le long du transect.

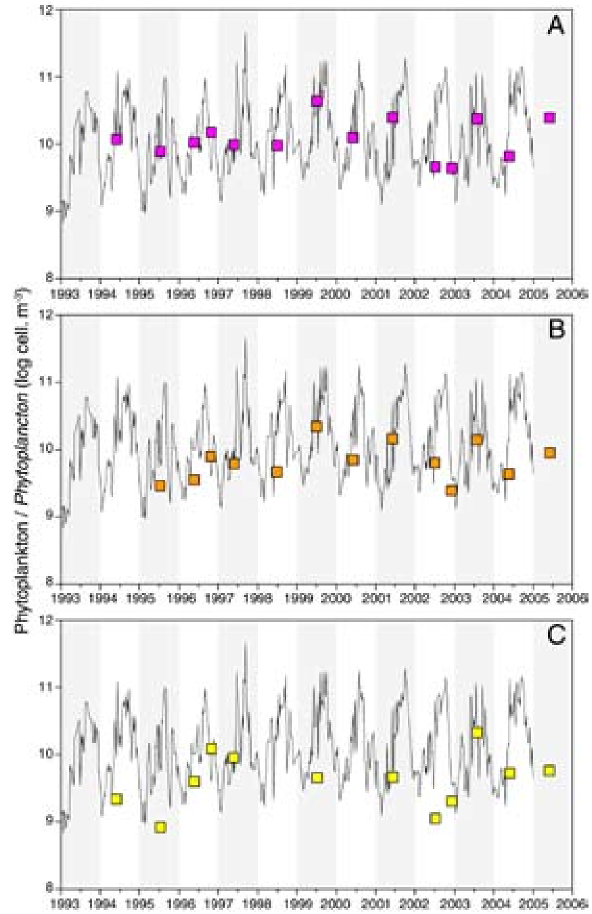

Fig. 3 Phytoplankton abundance in surface waters of Bedford Basin (continuous line) and the Labrador Sea (coloured symbols) in the (a) Labrador Basin, (b) Labrador Shelf and the (c) Greenland Shelf. The Bedford Basin time series was constructed from weekly samples taken at 5 m depth. In each subarctic region, the values represent integrated samples (average of 0, 5, 10 m) averaged over several stations distributed along the AR7W transect.

Abondance du phytoplancton dans les eaux de surface du bassin de Bedford (ligne continue) et de la mer du Labrador (symboles colorés) dans les régions du bassin du Labrador (a) du plateau du Labrador (b) et du plateau du Groenland (c). La série temporelle de données pour le bassin de Bedford a été construite à partir des échantillons récoltés hebdomadairement à une profondeur de 5 m. Pour chaque région subarctique, les valeurs utilisées représentent une intégration moyenne des échantillons (moyenne de 0, 5 et 10 m) provenant de plusieurs stations situées le long du transect AR7W.

phytoplankton at the five New Brunswick stations was almost perfectly matched to that in Nova Scotia (Fig. 4b). Moreover, the counts in Brandys Cove and mid Passamaquoddy Bay were almost identical to those in the Bedford Basin, which is situated much further away.

The coherence of regional phytoplankton on a seasonal basis (Figs. 2-4) appears to extend to a multi-year scale as well (Fig. 5). Here, we seek evidence for change in phytoplankton abundance on a year-to-year basis at the seasonal level. In Bedford Basin, phytoplankton in spring (average of Mar-Apr-May values) has been increasing at a rate of 6.6% y^{-1}. A similar increase (6.8% y^{-1}) is also occurring in the fall (average of Sep-Oct-Nov values). On the Scotian Shelf, the spring increase is 4.4% y^{-1} and the fall increase is 3.0% y^{-1}. In the Labrador Sea, the spring increase is 4.2% y^{-1}. It appears that phytoplankton abundance is not changing as fast on the shelves and open ocean as it is in Bedford Basin, but the statistical significance of these trends is very weak. A conclusive comparison cannot be expected until all the time series become longer. Notwithstanding uncertainties in the rate of change, it is remarkable that the direction of change is positive everywhere.

The seasonality of phytoplankton abundance (cells m^{-3}) and phytoplankton biomass (mg carbon m^{-3} or mg chlorophyll m^{-3}) are very different (Li and Dickie 2001). The former has a single peak that occurs at the autumnal equinox. The latter has two peaks: the first at the vernal equinox and the second at

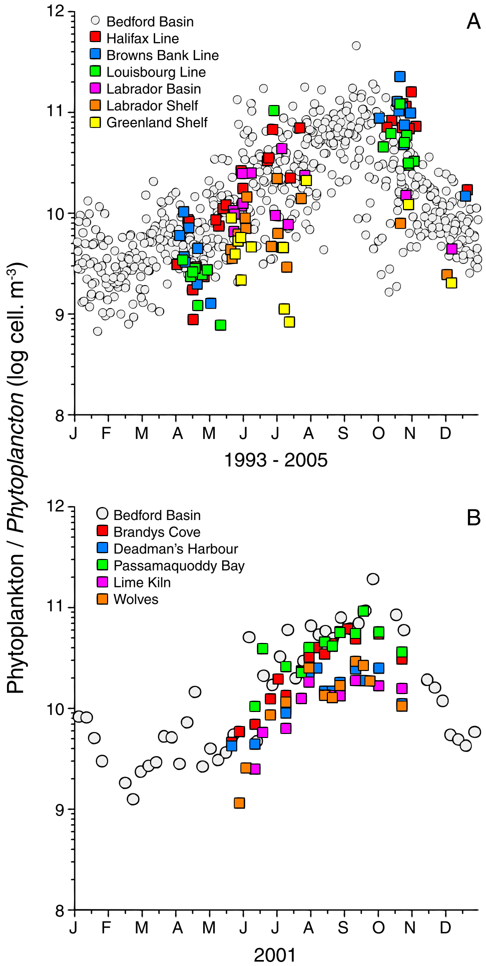

Fig. 4 (a) Annual cycle of phytoplankton in the Bedford Basin, Scotian Shelf and Labrador Sea consolidated over all years of observation and (b) phytoplankton development during 2001 in Bedford Basin and five sites in the Western Isles region of the Bay of Fundy.

(a) Cycle annuel du phytoplancton dans le bassin de Bedford, le plateau Néo-Écossais et la mer du Labrador construit à partir de toutes les années d'observation et (b) développement du phytoplancton au cours de l'année 2001 dans le bassin de Bedford et à cinq sites dans la région de Western Isles dans la baie de Fundy.

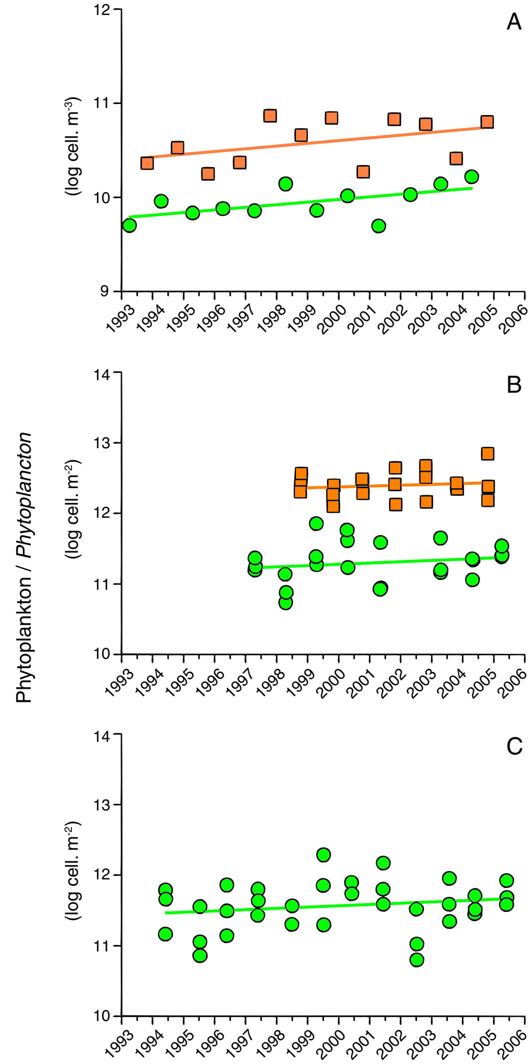

Fig. 5 Multi-year trends of phytoplankton abundance during spring (green circles) and fall (orange squares) in the (a) Bedford Basin: volumetric abundance (cells m^{-3}) at 5 m depth, (b) the Scotian Shelf: depth-integrated abundance (cells m^{-2}) from surface to 100 m at HL, BBL and LL, and (c) the Labrador Sea: depth-integrated abundance (cells m^{-2}) from surface to 100 m at LB, LS and GS.

Tendances multi-annuelles de l'abondance du phytoplancton au printemps (cercles verts) et à l'automne (carrés oranges) dans (a) le bassin de Bedford : abondance volumétrique (cellules m^{-3}) à 5 m, (b) le plateau Néo-Écossais : abondance intégrée de la surface jusqu'à 100 m (cellules m^{-2}) à HL, BBL, et LL, et (c) la mer du Labrador : abondance intégrée de la surface jusqu'à 100 m (cellules m^{-2}) à LB, LS et GS.

the autumnal equinox. The spring peak of biomass is due to a relatively small number of large cells (mainly diatoms), while the fall peak of biomass is due to a large number of small cells (mainly cyanobacteria and diverse eukaryotic picoplankton). In general, waters having high concentrations of chlorophyll are characterized by a relatively equitable distribution of cells across different size categories. On the other hand, waters having low concentrations of chlorophyll are heavily dominated by large numbers of small cells and contain only small numbers of large cells (Li 2002). Essentially, biomass is the product of abundance and cell mass: the macroecological inter-relationships of these three quantities may be explored in a straightforward manner (Li 2006).

Long-term change in the phytoplankton of marine ecosystems is often viewed from the perspective of biomass (e.g., Reid et al. 1998). An alternative is to view the number of reproductive entities, which is the basis for evolutionary change. In the northeast Atlantic, there is already evidence of multi-decadal change in microphytoplankton abundance (Richardson and Schoeman 2004) and phenology (Edwards and Richardson 2004) associated with climate change. Our observations in the northwest Atlantic have been carried out for a much shorter duration, and there is only a weak hint of change. However, the coherence in the seasonal development of phytoplankton cells across diverse environments (Fig. 4) and the coherence in directional change across many years (Fig. 5) suggest that organisms with short generation times (i.e., microbes) may be responding in a coherent fashion to a large-scale common forcing. Multiyear trends of chlorophyll concentration discerned from repeating annual cycles can be meaningfully interpreted in the context of climate variability (McClain et al. 2004). In other coastal oceans, a significant average increase (10% y^{-1}) in recent years has been described as a possible response to enhanced coastal upwelling or anthropogenic influences (Gregg et al. 2005).

It appears that Bedford Basin may be a useful sentinel for the regional phytoplankton response. It is sampled at a frequency twice that at which remotely sensed ocean colour is composited at BIO for regional maps, and it has a time series of considerable length. Few datasets of this nature exist, almost none of which include total phytoplankton abundance.

References

Belgrano, A., Allen, A.P., Enquist, B.J., and Gillooly, J.F. 2002. Allometric scaling of maximum population density: a common rule for marine phytoplankton and terrestrial plants. Ecol. Letters 5: 611-613.

Edwards, M., and Richardson, A.J. 2004. Impact of climate change on marine pelagic phenology and trophic mismatch. Nature 430: 881-884.

Gregg, W.W., Casey, N.W., and McClain, C.R. 2005. Recent trends in global ocean chlorophyll. Geophys. Res. Lett. 32: L03606, doi:10.1029/2004GL021808.

Li, W.K.W. 2002. Macroecological patterns of phytoplankton in the northwestern North Atlantic Ocean. Nature 419: 154-157.

Li, W.K.W. 2006. Plankton populations and communities. *In* Marine macroecology. *Edited by* Witman, J., and Kaustuv, R. Univ. Chicago Press, in press.

Li, W.K.W., and Dickie, P.M. 2001. Monitoring phytoplankton, bacterioplankton and virioplankton in a coastal inlet (Bedford Basin) by flow cytometry. Cytometry 44: 236-246.

Li, W.K.W., and Harrison, W.G. 2001. Chlorophyll, bacteria and picophytoplankton in ecological provinces of the North Atlantic. Deep-Sea Res. II 48: 2271-2293.

Li, W.K.W., Dickie, P.M., and Spry, J.A. 1998. Plankton monitoring program in the Bedford Basin, 1991-1997. Can. Data Rep. Fish. Aquat. Sci. 1036: vii+342 pp.

Li, W.K.W., Martin, J.L., and Ringuette, M.M. 2002. Monitoring of picoplankton, nanophytoplankton and bacterioplankton in the Western Isles region of the Bay of Fundy during 2001. *In* Environmental studies for sustainable aquaculture (ESSA): 2002 Workshop report. *Edited by* Hargrave, B.T. Can. Tech. Rep. Fish. Aquat. Sci. 2411, pp. 49-50.

Lazier, J., Hendry, R., Clarke, A., Yashayaev, I., and Rhines, P. 2002. Convection and restratification in the Labrador Sea, 1990-2000. Deep-Sea Res. I 49: 1819-1835.

McClain, C.R., Signorini, S.R., and Christian, J.R. 2004. Subtropical gyre variability observed by ocean-color satellites. Deep-Sea Res. II 51:281-301.

Reid, P.C., Edwards, M., Hunt, H.G., and Warner, A.J. 1998. Phytoplankton change in the North Atlantic. Nature 391: 546.

Richardson, A.J., and Schoeman, D.S. 2004. Climate impact on plankton ecosystems in the northeast Atlantic. Science 305: 1609-1612.

Therriault, J.-C., Petrie, B., Pepin, P., Gagnon, J., Gregory, D., Helbig, J., Herman, A., Lefaivre, D., Mitchell, M., Pelchat, B., Runge, J., and Sameoto, D. 1998. Proposal for a northwest Atlantic Zonal Monitoring Program. Can. Tech. Rep. Hydrogr. Ocean Sci. 194: vii+57 pp.

West, G.B., Woodruff, W.H., and Brown, J.H. 2002. Allometric scaling of metabolic rate from molecules and mitochondria to cells and mammals. Proc. Nat. Acad. Sci. 99: 2473-2478.

MERICA-Nord Program: Monitoring and Research in the Hudson Bay Complex

Michel Harvey[1], Michel Starr[1], Jean-Claude Therriault[1], François Saucier[2] and Michel Gosselin[2]

[1] Institut Maurice-Lamontagne, P.O. Box 1000, Mont-Joli, QC, G5H 3Z4

[2] Institut des sciences de la mer (ISMER), Universtié du Québec à Rimouski, 310 allée des Ursulines, Rimouski, QC, G5L 3A1

HarveyM@dfo-mpo.gc.ca

Sommaire

Le complexe de la baie d'Hudson (comprenant la baie d'Hudson, le détroit d'Hudson ainsi que le bassin de Foxe) représente probablement le plus grand estuaire nordique du monde. Cet estuaire est une composante importante du courant du Labrador qui exerce une influence prédominante sur le climat de la partie est de l'Amérique du Nord. La dynamique de circulation des masses d'eau dans cette région nordique est fortement influencée par les écoulements d'eau douce provenant notamment des bassins de drainage de la baie d'Hudson et de l'arctique. Cette région abrite près de la moitié des populations Inuits du Nunavut et du Nunavik, et est caractérisée par une forte biodiversité reflétant l'influence significative des eaux arctiques et subarctiques de l'Atlantique Nord. Cet écosystème nordique a été identifié comme un « point chaud » pour la conservation de la biodiversité marine, mais aussi comme l'une des régions les plus sensibles aux changements et à la variabilité climatique.

Afin de pouvoir détecter, comprendre, suivre et prédire les changements environnementaux dans cette région nordique, les scientifiques du MPO, région du Québec, ont initié en 2003 un programme de monitorage appelé MERICA-nord (pour études des MERs Intérieures du CAnada). Ce programme de monitorage complémente celui effectué dans la mer intérieure du golfe du Saint-Laurent (MERICA-sud). Dans sa conception, sa réalisation et son échantillonnage de base, ce programme de monitorage s'inspire du Programme de Monitorage de la Zone Atlantique. Il accommode en plus plusieurs programmes de recherche associés qui sont effectués par des partenaires tant à l'interne qu'à l'externe du MPO, comme par exemple le secteur universitaire. MERICA-nord est supporté par le Centre national d'excellence pour la recherche aquatique dans l'Arctique (N-CAARE en anglais). Un élément clé du programme est l'intégration des besoins des scientifiques avec l'expertise et la capacité de support logistique de la Garde côtière canadienne; ce programme a en effet profité jusqu'à maintenant de temps de navire offert par la Garde côtière canadienne sur une base d'opportunité. MERICA-nord permet finalement au MPO d'assumer ses obligations nationales et internationales de base en ce qui concerne l'étude des milieux marins nordiques, afin de répondre aux enjeux sociaux et globaux émergents que soulèvent l'impact de l'activité humaine (ex., les développements hydroélectriques) ou encore des changements climatiques. Dans ce contexte, l'environnement du complexe de la baie d'Hudson est encore bien peu connu.

Trois missions MERICA ont eu lieu jusqu'à présent en 2003, 2004 et 2005. Nous décrivons dans cet article quelques résultats préliminaires obtenus en 2003-2004. Ces résultats indiquent que la faible teneur générale en éléments nutritifs représente le principal facteur qui limite la croissance du phytoplancton dans la baie d'Hudson pendant l'été. De plus, les estimations de production primaire montrent des valeurs beaucoup plus faible dans le nord de la baie d'Hudson que dans le détroit d'Hudson (129 vs. 1526 mg C $m^{-2} d^{-1}$). La production estivale de phytoplancton était aussi beaucoup plus faible dans la partie nord de la baie d'Hudson (ca. 15 g C m^{-2}) que dans le détroit d'Hudson (ca. 180-230 g C m^{-2}), une région caractérisée par un mélange vertical favorisant l'enrichissement en éléments nutritifs. En ce qui concerne la biomasse totale de zooplancton, intégré sur l'ensemble de la colonne d'eau, nos résultats montrent qu'elle était 6 fois plus faible dans la baie d'Hudson que dans le détroit d'Hudson et le bassin de Foxe. À l'opposé, l'abondance (nombres d'individus) du mésozooplancton était plus élevée dans la baie d'Hudson que dans deux autres régions. Cette différence est reliée au fait que les espèces de copépodes de petite taille se retrouvent relativement en plus grand nombre dans la baie d'Hudson que dans les deux autres endroits. D'autres études sont encore nécessaires pour expliquer ces observations.

Introduction

The Hudson Bay (HB) complex (Hudson Bay, Hudson Strait and Foxe Basin) probably represents the largest northern estuary in the world and has a strong influence on the climate in the eastern part of North America. Water mass characteristics and circulation in this northern region are strongly influenced by the freshwater dynamics linked to the fluvial inputs from the large Hudson Bay and arctic drainage basins, the sea-ice formation and melting processes, and the inflow of less saline waters coming from the Pacific via the Northwest Passage. Of particular interest are the low salinity waters flowing out of Hudson Strait that have a significant influence on the Atlantic coast of Canada (including the Gulf of St. Lawrence), as well as on the deep circulation in the Labrador Sea by lowering the density of the surface waters in the regions where deep convection occurs (Fig. 1). Deep convection in the Labrador and Nordic seas supplies intermediate and deep waters to much of the North Atlantic Ocean. In that context, studying the variability of freshwater distribution and circulation processes in this northern system contributes to the basic understanding of circulation and climate processes that influence the arctic as well as the Atlantic region of interest to the Atlantic Zone Monitoring Program (AZMP). On the global scale, the arctic water outflow directly affects the climate via its indirect effect on the oceanic "conveyer belt."

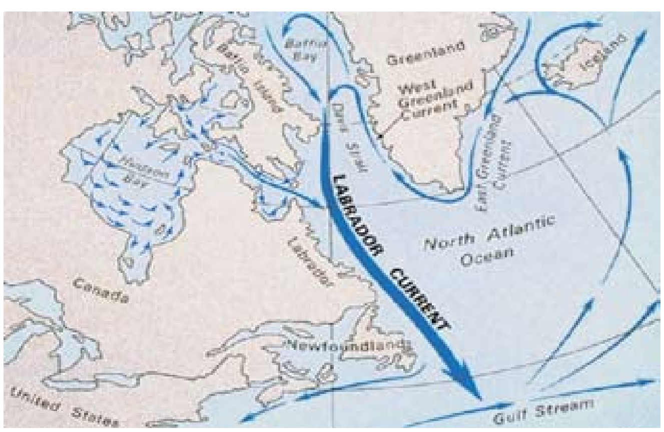

Fig. 1 The dominant oceanic currents in the North Atlantic.

Les courants océaniques dominants dans l'Atlantique Nord.

The Hudson Bay complex is home to approximately half of the Inuit population of Nunavut and Nunavik. This region is used for hunting and fishing, for ensuring transportation of supplies and goods during the ice-free season, and for fostering economic development in general. Its high biodiversity reflects the significant influence of both subarctic Atlantic and arctic waters. For this reason, the HB ecosystem has been identified as an arctic "hot spot" for marine conservation by the Canadian Arctic Resources Committee (CARC; Beckmann 1994). Recent studies have reported significant physical and biological shifts in most polar environments. The HB complex is no exception and is identified as one of the most sensitive regions subjected to climate change and variability (IPCC 2001, Laidre and Heide-Jørgensen 2005). Both northern and southern communities must face the consequences of climate change in the HB complex. Climate change scenarios for increasing greenhouse gas concentrations in the atmosphere suggest that the HB complex is undergoing a large climate shift toward steady near ice-free conditions by the end of this century (e.g., Boer et al. 2000). This raises important questions about the accuracy of global circulation model predictions of the details of this shift and the impacts such changes can have on the local sea-ice formation and water mass circulation, freshwater transport to the Labrador Sea, biological productivity of this marine environment, regional weather and climate, and local habitats (Saucier et al. 2004a).

Building on the expertise acquired through the AZMP and recognizing the pressing need to monitor environmental changes in the HB complex, DFO–Québec Region initiated a pilot field and modelling program four years ago aimed at detecting, understanding and predicting climate change and variability in the Hudson Bay complex in the context of understanding global climate changes and variability. This monitoring–research program is called MERICA-nord (études des MERs Intérieures du CAnada, Hudson Bay northern component – complementing the Gulf of St. Lawrence southern component; Saucier et al. 2004b). DFO Québec Region is trying to establish MERICA-nord as a continuous monitoring program to detect, understand, follow and predict environmental changes in this northern environment. Continuous measurements are essential to provide the time series needed to address climate change and provide complementary information to the AZMP. MERICA-nord also represents the nucleus of a pre-proposal that received full support from the International Polar Year Directorate.

Figure 2 shows the location of the standard hydrographic sampling stations (black dots) during the MERICA-nord cruise in August 2003. Stations were located along two sections in Hudson Bay and in Hudson Strait, and at strategic individual locations in Foxe Basin and in connecting channels between Foxe Basin and Hudson Bay. Similar oceanographic cruises were carried out in August 2004 and September 2005. However, for the 2005 cruise, the Hudson Strait section was moved slightly toward the southeast, where the Strait is nar-

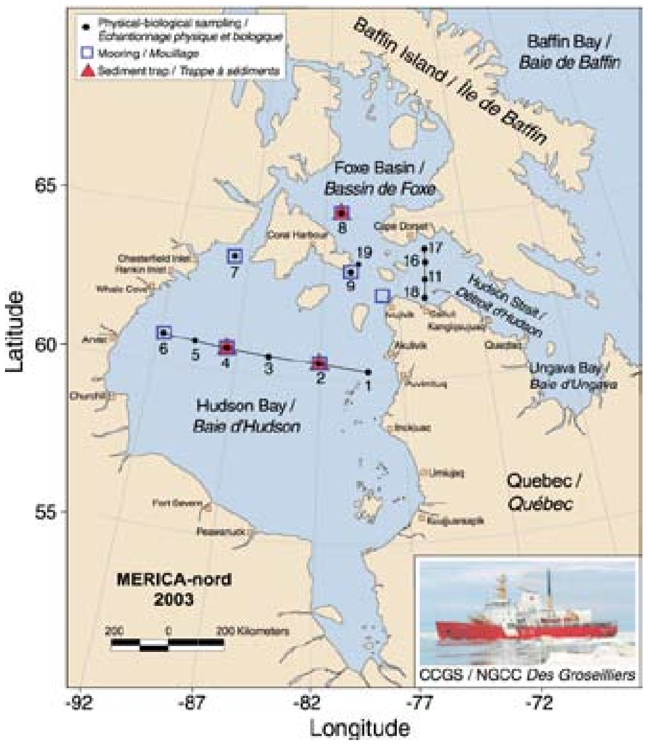

Fig. 2 Location of the sampling stations in the Hudson Bay complex during MERICA-nord 2003. The black dots indicate the location of standard sampling stations (CTD, bottles and plankton nets), the blue squares indicate the location of current meter moorings, and the red triangles are the location of sediment trap moorings. The inset shows the CCGS *Des Groseilliers*.

Localisation des stations d'échantillonnage dans le complexe de la baie d'Hudson durant la mission MERICA-nord 2003. Les points noirs indiquent la position des stations d'échantillonnage standard (CTD, bouteilles et filets à plancton), les carrés bleus indiquent la position des mouillages de courantomètres, et les triangles rouges indiquent la position des mouillage de trappes à sédiments. En médaillon: le navire NGCC Des Groseilliers.

rowest. The basic oceanographic variables measured during the three cruises were salinity, temperature, chlorophyll, primary production, nutrients, oxygen and various other chemical tracers (e.g., oxygen-18 isotopes, alkalinity, dissolved organic and inorganic carbon). Other standard measurements included phytoplankton, zooplankton and larval fish abundances and biomasses, as well as the abundance and biomass of benthic organisms at several stations. Current meters, CTDs, ADCPs and thermistor chains were also moored at seven locations (blue squares in Fig. 2) for a full year. In addition, optical characteristics of the water column were measured at a number of stations to calibrate satellite observations. Finally, sediment traps collecting suspended particulate matter at regular intervals over the entire year were deployed at two stations in Hudson Bay and one station in Foxe Basin (red triangles in Fig. 2) to obtain data on the seasonal variability of the carbon flux and particle sedimentation. The MERICA-nord program involved research projects of scientists from the different DFO research institutes, Canadian universities and the Woods Hole Oceanographic Institute (see Appendix 1). During the upcoming International Polar Year, it is anticipated that several new contributors and partners will join the program.

Preliminary Results

Salinity and Temperature

Figure 3 shows the distribution of salinity and temperature along the Hudson Bay (HB) and Hudson Strait (HS) sections in 2003. Single vertical profiles of salinity and temperature are also presented for the Foxe Basin (FB) stations. The main feature of the Hudson Bay section is the presence of colder and lower salinity waters in the near-surface layer (upper 40 m) on the eastern side of the Bay. The Hudson Strait section shows colder and lower salinity waters at the surface on the southern side of the section. During this mission, HB was free of ice except at the two easternmost stations of the HB section. The large near-surface freshwater content on the east side of the HB section and the south side of HS was associated with sea ice and continental melt waters moving from the southeastern region of HB along the eastern shore and leaving along the south shore of HS. From the surface to approximately 75 m in HB and to about 120 m in the southern HS, we observed a winter water layer with temperatures below -1°C. Between 75 and 150 m on the eastern side of HB, we observed warmer intermediate waters that could have come from the Strait, where warmer and more saline waters were observed below the surface winter layer. Near the bottom of HB and on the western side of HB, the water

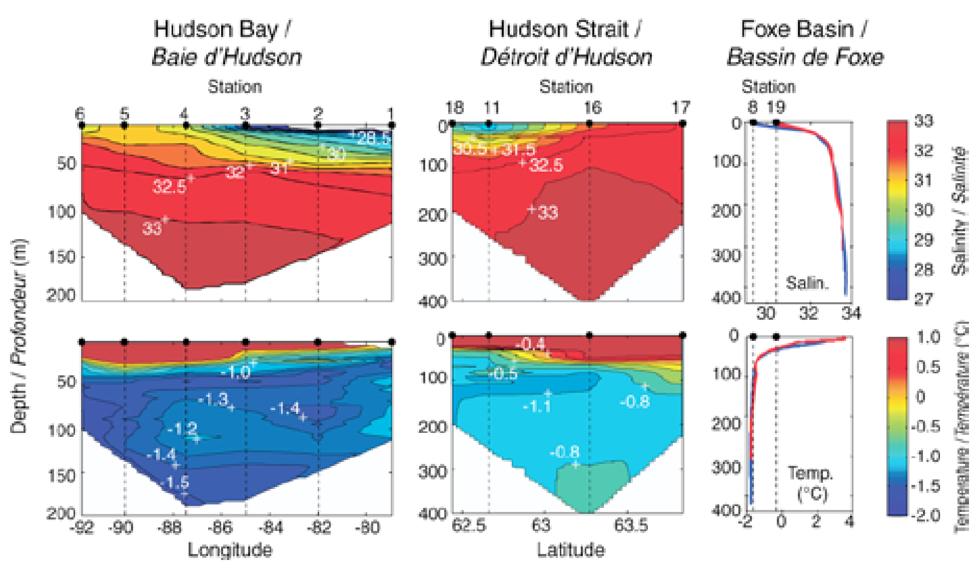

Fig. 3 Salinity and temperature data acquired in August during the MERICA-nord 2003 cruise along the Hudson Bay section (left), across the head of Hudson Strait (middle), and in Foxe Basin (right).

Profils de température et de salinité obtenus en août pendant la mission MERICA-nord 2003 le long du transect de la baie d'Hudson (gauche), à la tête du détroit d'Hudson (centre) et dans le bassin de Foxe (droite).

was generally colder at depth due to deep convection in the northwestern region of HB and in Foxe Basin. The salinity and temperature -profiles in FB confirm the production of dense and cold waters at depth, probably associated with brine rejection during winter. Cold waters found near 80 m in eastern HB were consistent with the estuarine-like circulation and mixing of cold waters from FB into eastern HB during summertime (Saucier et al. 2004a). These results are consistent with the counterclockwise circulation pattern in Hudson Bay that is shown in Figure 1 (adapted from Prinsenberg 1986 and Drinkwater 1990 for Hudson Bay complex region).

Phytoplankton Standing Stock and Primary Production

Figure 4 shows that the lowest standing stock of phytoplankton, as reflected by the integrated chlorophyll *a* concentrations in the upper 100 m (mg chl *a* m^{-2}), was observed on the eastern side of the HB section, where the water in the upper 50 m was fresher and colder, and where some melting ice was still present at the beginning of August 2003. Much higher chlorophyll concentrations were observed in the center and western side of HB. These regions were characterized by less turbid warmer and saltier waters, and were ice free. In HS, the highest phytoplankton biomasses were observed on the southern side, where the surface layer was highly stratified (Fig. 4). In FB, the phytoplankton standing stock showed intermediate chlorophyll concentrations in comparison with HB and HS.

Phytoplankton production and biomass were also measured in the three regions of the HB complex in August 2004 (data not shown). Phytoplankton production was higher in HS (954-3444 mg C m^{-2} d^{-1}) than in HB (54-344 mg C m^{-2} d^{-1}) and FB (325 mg C m^{-2} d^{-1}). In HB, primary production decreased gradually eastward. The phytoplankton community was generally dominated by small (0.7-5 µm) phytoplankton cells in HB and FB, and by large (≥ 5 µm) cells in HS. Phytoplankton biomass in the euphotic zone was lower in HB (6-51 mg chl *a* m^{-2}) than in HS and FB (62-78 mg chl *a* m^{-2}). The phytoplankton production to biomass ratio was higher in HS (17-44 mg C mg chl *a* d^{-1}) than in the two other regions (2-15 mg C mg chl *a* d^{-1}). Ammonium addition stimulated dark CO_2 fixation by the natural phytoplankton, indicating that the cells were physiologically nitrogen limited.

Particulate production was negatively correlated with the Brunt-Väisälä frequency, an index of the strength of the stratification of the upper 80 m of the water column. This suggests that phytoplankton production was mainly controlled by the vertical mixing processes governing the introduction of dissolved nitrogen into the upper brackish layer.

Zooplankton Standing Stock (Biomass)

In 2003, the total zooplankton biomass integrated over the water-column depth showed a quasi-monotonic decrease from the western to the eastern side of the HB section (Fig. 5). The lowest zooplankton biomass was observed on the eastern side, coinciding with the lower chlorophyll concentrations (Fig. 4). Much higher (up to 6 times) integrated zooplankton biomasses were observed in HS and in FB. The ratio of macrozooplankton (length > 2 mm, large carnivorous species other than copepods) to mesozooplankton (mostly copepods) biomass was close to 1:10 in HS and FB but varied between 1:1 and ~1:3 in HB. A ratio of 1:10 is typical in most aquatic ecosystems (e.g., Gulf of St. Lawrence, Harvey et al. 2005; western Antarctic Peninsula, Calbet et al. 2005). This stresses the importance of a more thorough understanding of the nutritional processes of zooplankton in the HB complex.

Mesozooplankton

In contrast to the biomass values, the mesozooplankton abundance (number of individuals) integrated over the water-column depth was generally higher in HB than in HS and FB, with a peak of abundance on the western side of HB (Fig. 6). The community was dominated by small copepod species such as *Oithona* spp., *Oncaea* spp. and *Microcalanus pusillis* in HB and by large species such as *Pseudocalanus* spp., *Calanus finmarchicus*, *C. glacialis* and *Metridia longa* in the other two regions. Large species represented 40-70% and 5-17% of the total mesozooplankton abundance in HS/FB and HB, respectively.

Macrozooplankton

The total integrated abundance of macrozooplankton did not show large variations among the three regions (Fig. 7). However, the two southern stations on the HS section showed a macrozooplankton abundance that was ~2 times lower than on the northern side of the section. The macrozooplankton

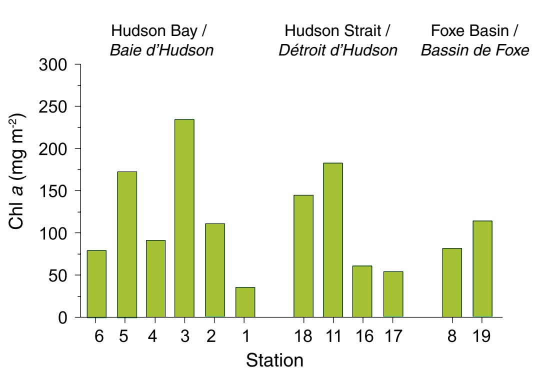

Fig. 4 Chlorophyll *a* concentration (integrated from 0 to 100 m) during the MERICA 2003 cruise.

Concentration en chlorophylle a *intégrée (0 à 100 m) pendant la mission MERICA 2003.*

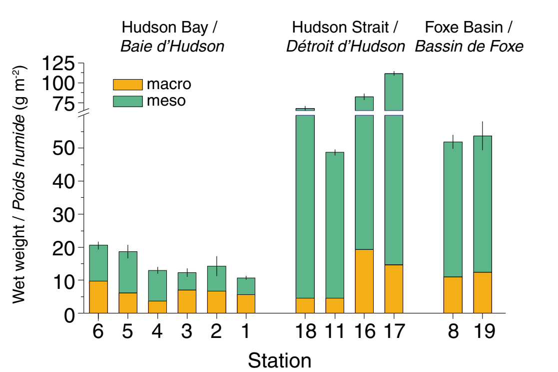

Fig. 5 Mean (± SE) total zooplankton biomass (integrated from bottom to surface) during the MERICA 2003 cruise.

Biomasse moyenne totale (± erreur type) du zooplancton (intégrée du fond à la surface) pendant la mission MERICA 2003.

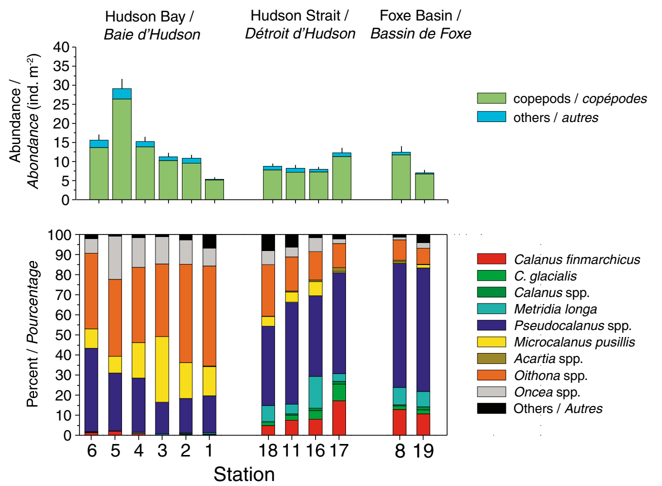

Fig. 6 Integrated values of abundance (bottom to surface) and specific composition of the mesozooplankton (copepods) evaluated during the MERICA 2003 cruise.

Valeurs intégrées de l'abondance (du fond à la surface) et composition spécifique du mésozooplancton (copépodes) pour la mission MERICA 2003.

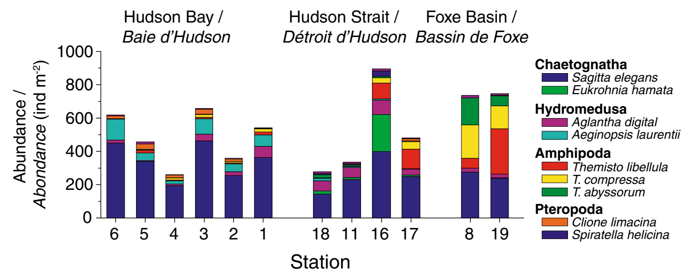

Fig. 7 Integrated values of abundance (bottom to surface) and specific composition of the macrozooplankton evaluated during the MERICA 2003 cruise.

Valeurs intégrées de l'abondance (du fond à la surface) et composition spécifique du macrozooplancton pour la mission MERICA 2003.

was also relatively more abundant in FB than in HB. The chaetognath *Sagitta elegans* was the most abundant macrozooplankton species and was found in all three regions, except at station 19 in FB, where the hyperiid amphipod *Themisto libellula* was more abundant. The hydromedusa *Aeginopsis laurentii* was the second most abundant macrozooplankton species in HB, but this species was nearly absent in HS and FB. On the other hand, the chaetognath *Eukrohnia hamata* as well as other mysid, euphausiid and decapod species were only found in the HB and FB regions. The hyperiid amphipods *Themisto libellula*, *T. abyssorum* and *T. compressa* were more abundant in FB and at the two northernmost stations of the HS section than at any other sampled stations.

Conclusion

The preliminary results obtained during the MERICA 2003 cruise indicate that the summer phytoplankton community in HB was nutrient limited. The primary production in the northern region of HB is about one order of magnitude lower than in HS. The total summer phytoplankton production was much lower in the northern region of HB than in HS, a system characterized by high turbulent vertical mixing during the summer, implying higher nutrient fluxes. The total zooplankton biomass integrated over depth was ca. 6 times higher in HS and FB than in HB. In contrast with biomass values, the mesozooplankton abundance (number of individuals) integrated over depth was generally higher in HB than in HS and FB. The zooplankton community was dominated by small copepod species in HB and by large species in the other two regions, implying different trophic structures.

MERICA-nord is a multi-disciplinary program that the region has not seen in a long time. Prior to this program, the most recent biological–physical results had come from individual studies that took place in the late 1980s–1990s (Drinkwater 1990, Harvey et al. 1997, 2001). MERICA-nord should assist DFO in responding to emerging social and global issues linked to climate change and variability while meeting its national and international obligations in the North. In this context, MERICA-nord represents a keystone activity, allowing the compilation of the oceanographic databases necessary to improve our knowledge and understanding of the largest inland sea of North America.

Acknowledgements

The first three years of MERICA (summers 2003, 2004 and 2005) were supported by a combination of funding from DFO, PERD and SARCEP. The oceanographic cruises were conducted using ship time provided by the Canadian Coast Guard (Central & Arctic and Québec regions). MERICA also integrates the northern component of DFO–Québec Region Species at Risk Act program (SARA) and represents an important component of N-CAARE (National Centre for Arctic Aquatic Research Excellence). The authors acknowledge the help provided by several research scientists, professionals and technicians from different organizations that are too numerous to be named here, and by several science managers who strongly believed in and supported the project. Particular thanks are also addressed to several Canadian Coast Guard managers for their support as well as to the navigating personnel of the CCGS icebreakers *Des Groseilliers* and *Pierre Radisson*.

References

Beckmann, L. 1994. Marine conservation in the Canadian Arctic. Northern Perspectives 22: 33-39.

Boer, G. J., Flato, G. M., and Ramsden, D. 2000. A transient climate change simulation with greenhouse gas and aerosol forcing: projected climate change in the 21st century. Climate Dynamics 16: 427-450.

Calbet, A., Alcaraz, M., Atienza D., Broglio, E., and Vaqué, D. 2005. Zooplankton biomass distribution patterns along the western Antarctic Peninsula (December 2002). J. Plankton Res. 27: 1195-1203.

Drinkwater, K.F. 1990. Physical and chemical oceanography. *In* Proceeding of the marine ecosystem studies in Hudson Strait. Montréal, 9-10 November 1989. *Edited by* J.A. Percy. Can. Tech. Rep. Fish. Aquat. Sci. 1770, pp. 87-97.

Harvey, M., Therriault J.-C., and Simard, N. 1997. Late-summer distribution of phytoplankton in relation to water mass characteristics in Hudson Bay and Hudson Strait (Canada). Can. J. Fish. Aquat. Sci. 54: 1937-1952.

Harvey, M., Therriault, J.-C., and Simard, N. 2001. Hydrodynamic control of late summer species composition and abundance of zooplankton in Hudson Bay and Hudson Strait (Canada). J. Plankton Res. 23: 481-496.

Harvey, M., St.-Pierre, J.-F., Devine, L., Gagné, A., Gagnon, Y., and Beaulieu, M.F. 2005. Oceanographic conditions in the Estuary and the Gulf of St. Lawrence during 2004: zooplankton. Can. Sci. Adv. Sec. Res. Doc. 2005/043.

IPCC. 2001. Climate change 2001; synthesis report: contribution of Working Groups I, II and III to the third assessment report of the Intergovernmental Panel on Climate Change. Cambridge University Press, Cambridge.

Laidre, K.L., and Heide-Jørgensen, M.P. 2005. Arctic sea ice trends and narwhal vulnerability. Biological Conservation 121(4): 509-517.

Prinsenberg, S.J. 1986. The circulation pattern and current structure of Hudson Bay. *In* Canadian inland seas. *Edited by* I.P. Martini. Elsevier, Amsterdam, pp. 187-204.

Saucier, F.J., Senneville, S., Prinsenberg, S., Roy, F., Smith, G., Gachon, P., Caya, D., and Laprise, R. 2004a. Modelling the sea ice - ocean seasonal cycle in Hudson Bay, Foxe Basin and Hudson Strait, Canada. Climate Dynamics 23: 303-326.

Saucier, F.J., Starr, M., Harvey, M., and Therriault, J.-C. 2004b. Expédition MERICA 2003: Suivi et étude du climat et de la productivité de la baie d'Hudson. Nat. Can. 128: 108-110.

Appendix 1.

List of main investigators who have participated in the MERICA-nord program / *Liste des principaux investigateurs qui ont participé au programme MERICA-nord*

Philippe Archambault[1], Kumiko Azetsu-Scott[2], Anne de Vernal[6], Jacques Gagné[1], Michel Gosselin[4], Michel Harvey[1], Christine Michel[3], Patrick Ouellet[1], François Saucier[4], Michael Scarratt[1], Michel Starr[1], Gary Stern[3], Fiamma Straneo[5], Jean-Claude Therriault[1], and Bruno Zakardjian[4].

[1] Department of Fisheries and Ocean, Institut Maurice-Lamontagne
[2] Department of Fisheries and Oceans, Bedford Institute of Oceanography
[3] Department of Fisheries and Oceans, Freshwater Institute
[4] Institut des Sciences de la Mer, Université du Québec à Rimouski
[5] Woods Hole Oceanographic Institute, USA
[6] Université du Québec à Montréal

Ten Years of Monitoring Winter Water Masses in the Gulf of St. Lawrence by Helicopter

Peter S. Galbraith, Rémi Desmarais, Roger Pigeon and Sylvain Cantin
Institut Maurice-Lamontagne, P. O. Box 1000, Mont-Joli, QC, G5H 3Z4
GalbraithP@dfo-mpo.gc.ca

Sommaire

Une mission océanographique héliportée a lieu à la fin de l'hiver dans le golfe du Saint-Laurent depuis maintenant dix ans. Cette mission a permis de monitorer les conditions extrêmes froides du Golfe ainsi que leurs variabilités interannuelles, et ce de façon plus représentative qu'avec les anciennes données qui étaient biaisées vers des conditions d'échantillonnage libre de glace. L'évolution des techniques d'échantillonnage est décrite, des premières années où le travail se faisait après avoir atterrie sur la glace, pour terminer avec un échantillonnage fait en grande majorité en vol stationnaire à l'aide d'un treuil électrique. L'efficacité de l'hélicoptère comme plate-forme pour ces travaux légers est sommairement discutée. Des résultats typiques de la mission sont présentés, tels que préparés pour l'examen annuel de l'état océanographique du golfe du Saint-Laurent. Ceux-ci inclus une prévision de l'indice de la couche intermédiaire froide (CIF) calculée à partir du volume total d'eau froide observé lors de la mission d'hiver. Ces données d'hiver aident à comprendre pourquoi les variations de la CIF se produisent.

Oceanographic sampling is most commonly done from ships; however, conditions sometimes make shipboard sampling very difficult if not impossible. We describe an oceanographic survey that has been conducted by helicopter every winter for the last 10 years. We shall discuss the rationale for the survey, as well as the methods that we have refined over the years to optimize the collection of samples and data.

Prior to 1996, wintertime oceanographic data from the Gulf of St. Lawrence (GSL) were sparse and biased toward warmer, ice-free conditions. However, complete monitoring of the Gulf requires knowledge of cold winter extremes. In the fall and winter, the surface layer releases large quantities of heat to the atmosphere. The layer becomes progressively colder and thicker until it reaches its coldest annual state at the end of winter. During the 1996-2005 period, the wintertime surface-layer temperatures in the Gulf were near-freezing over a mean thickness of 75 m; in some areas this layer was 100 to 200 m thick (Galbraith 2006). The volume of cold water (< 1°C) in the Gulf in late winter as determined from this helicopter survey varied between 10 and 15 × 10³ km³ (larger than any earlier estimates), representing 30 to 45% of all GSL waters (Galbraith 2006). This cold layer is not only pervasive during winter but characterizes the GSL for the rest of the year as well. In the spring, the surface restratifies in temperature and salinity, leading to a three-layer system (the warmer and saltier waters that underlie the winter cold layer are slowly advected along the Laurentian Channel from the continental slope). Beneath the summertime warm layer is the Cold Intermediate Layer (CIL), a remnant of the previous winter featuring a temperature minimum that varies from year to year by as much as 2°C (Gilbert and Pettigrew 1997). Since most exploited fish and invertebrate resources inhabit the CIL at various life stages, it is important to understand the causes of its variability. The helicopter survey, in addition to quantifying the winter water masses in the GSL, has also allowed us to begin to predict CIL conditions for the following summer. This information is useful to those doing stock assessments of this ecosystem.

Fig. 1 Taking a temperature-salinity profile through a hole in the ice after landing (March 1996).

Échantillonnage d'un profil de température et de salinité à travers un trou dans la glace après l'atterrissage (mars 1996).

Sampling Methods

The March survey was initiated in 1996 and uses a Canadian Coast Guard Bell-212 helicopter. For the first two years, stations were only done from the sea ice. For sea-ice stations, the pilot lands the helicopter on a suitable ice floe but maintains power and lift while the science personnel go onto the ice to drill and measure the ice thickness and report the information back to the pilot. If satisfied with the ice conditions, the pilot then proceeds to shut down the helicopter while the science personnel watch attentively for anything unusual. Only when the helicopter is completely shut down does the station work begin: profiling and sampling the water column through a hole in the ice (Figs. 1, 2). In addition to measuring temperature and salinity, Niskin bottles can be deployed through the holes to collect water samples at various depths. The water can be preserved for plankton taxonomy studies or filtered and frozen for later nutrient analyses. The on-ice stations worked very well in 1997 due to the extensive ice cover but were less successful in 1998, when a much reduced cover and thinner ice made regular landings impossible. Towards the end of the 1998 survey, 15 stations were done while hovering some 25 m above sea level and lowering and raising the CTD profiler (Sea-Bird Electronics SBE19) by hand to a depth of about 100 m (Fig. 3); the maximum depth was extended to 115 m the following year. The objective was to sample the surface cold layer in its entirety; the underlying warmer waters vary much more slowly. The survey began to shift from a higher percentage of stations being sampled from the ice to more stations done while hovering. The latter method allows the collection of CTD data regardless of ice cover; however, water samples were only collected when we landed on the ice, but complete ice cover rarely occurs in the Gulf.

The sampling depth of 100-115 m was adequate until 2001, when a much thicker cold layer intruded into the Gulf from the Strait of Belle Isle. We then landed on the ice in the northeastern Gulf and lowered the CTD to the end of its rope at 200 m, only to find that it was still within the cold layer. There was also a need to sample deeper than 115 m from stationary flight without using more flight time. A winch was designed and built in-house for 2002 that was powered by an off-the-shelf 18-volt cordless drill. The powered winch allowed us to sample to a depth of 200 m (or more if necessary). Additionally, a Niskin water-sampling bottle was rigged upside-down with flotation attached 2 m above the bottle; the flotation trips the bottle to close at a depth of 2 m (instead of using a weighted messenger to trip the closing mechanism by pushing on it). This last innovation allowed us to collect near-surface water samples (for nutrient analyses, plankton samples and salinity calibration) at every station since it could be deployed during stationary flight. Late winter is the optimal time to measure the nutrient concentrations in the surface mixed layer: winter mixing has replenished the surface with nutrients from deeper waters and a single near-surface measurement is representative of the entire mixed layer, so few samples are required. These nutrients will drive the coming spring bloom, which represents a significant portion of the annual primary production.

Fig. 2 On-ice station: a hole is drilled through the ice and the CTD probe is lowered to the bottom. Water samples can also be collected for later nutrient and phytoplankton analyses.

Station sur la glace : un trou est percé dans la glace et une sonde CTD y est descendue jusqu'au fond. Des échantillons d'eau peuvent aussi être récoltés pour analyse ultérieure des éléments nutritifs et du phytoplancton.

At each stationary-flight station, a CTD profiler (Sea-Bird Electronics SBE19) is quickly lowered to a depth of about 5 m. The instrument is held there for one minute to allow the sensors to equilibrate. The CTD profiler is then raised close to the surface and lowered at a rate of approximately 1 m s^{-1} to the bottom or a maximum of about 200 m (less than 200 m prior

Fig. 3 Hand-powered in-flight sampling: the CTD probe is lowered into the water, 25 m below, where it is held close to the surface for one minute and then lowered to a depth of 100 to 115 m. It is then pulled back up by hand over a small pulley.

Profillage à force de bras: la sonde CTD était descendue dans l'eau à partir d'une altitude d'environ 25 m, puis descendue à 5 m de profondeur pendant une minute en vue de stabiliser la température de l'instrument. Ensuite la sonde était descendue jusqu'à une profondeur de 100 à 115 m et remontée à la main à l'aide d'un système de poulie.

to the use of the electric winch), sampling the entire surface mixed layer. Since the lowering rate is decoupled from the sea-surface motion, it is unaffected by large waves. In fact, sampling has been done in open water with winds up to 45 knots. Windy conditions are preferred to calm conditions since wind provides lift for the helicopter. A station is completed within 10 minutes.

Cost-Effectiveness

The use of a helicopter for such a narrowly focussed survey (T, S, surface nutrients and plankton) is cost-effective, perhaps a third of the cost of a ship-based survey. First, a small team of two scientists and two Coast Guard helicopter crew cover about 70 stations in the Gulf in less than two weeks (see Fig. 5). This represents considerably less resources than required by a ship-based survey, albeit fewer variables are sampled. Second, the frequent winter storms that occur at this time of year do not impact the costs very much since most of the expense is associated with helicopter flight time as opposed to the number of days in the field. Approximately 40 hours of flight time are required for the survey, with roughly 12 hours of hovering and the rest for flying the grid. The Bell 212 aircraft has a flight

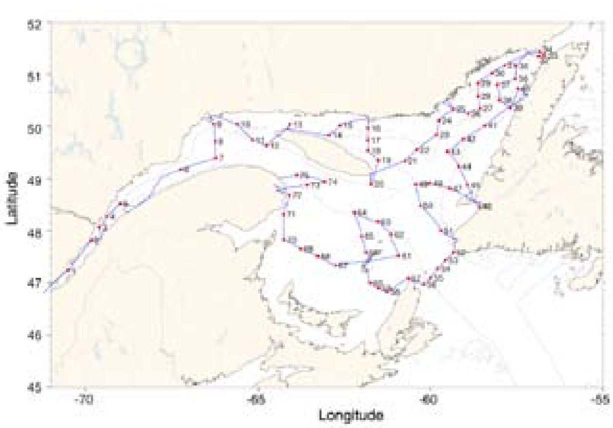

Fig. 5 Stations and survey track locations for the March 2004 survey.

Localisation des stations et trajet effectués en mars 2004.

Fig. 4 Sampling using a winch powered by a cordless drill from the helicopter: the left-hand panel shows the helicopter on the ice with the CTD sampling through a hole. In-flight sampling (all other panels) is done in a similar fashion except that a second person observes the descent and gives the pilot directions to stay on-station.

Échantillonnage à partir de l'hélicoptère en utilisant une perceuse à batterie 18V conventionnelle comme moteur de treuil. Sur l'image de gauche, l'hélicoptère est en fait sur la glace et l'échantillonnage se produit à travers un trou dans la glace. La technique est similaire en vol stationnaire (sur les autres images), excepté qu'une seconde personne surveille la descente dans l'eau et guide le pilote pour maintenir la position.

autonomy of about 3.5 hours (using about 1000 kg of jet fuel), which is well-suited to the size of the Gulf of St. Lawrence. Overall, little time is wasted in detours for fuel: Figure 5 shows that few detours back to coastal fueling locations were made without sampling along the way. In addition, ice presence is an asset instead of a hindrance as it is when sampling from ships.

Survey Results

Figure 6 shows the surface temperature and salinity, the depth of the cold mixed layer, and the estimate of the volume of Labrador Shelf water that flowed in through the Strait of Belle Isle for 2004. At this time of year, the winter water masses (including the very salty Labrador Shelf water) have not mixed with surrounding waters very much and retain their characteristics, making them easier to identify. The temperature and salinity data show a warm and saline intrusion into the Gulf on the Newfoundland side of Cabot Strait. This area had a cold layer thickness of zero (Fig. 6C). A thick intrusion of Labrador Shelf water entered the Gulf through the Strait of Belle Isle (Fig. 6D). The high surface salinity in that area indicates that the intrusion also reached the surface. The areas north and northeast of Anticosti Island have the thickest cold mixed layer and are the regions of the greatest vertical transfer of oxygen and heat to the intermediate layers of the Gulf of St. Lawrence.

The total wintertime volume of the cold layer (< -1°C) can be obtained by integrating the layer thickness (in Fig. 6C) over the area of the Gulf. This volume varied between 10 and 15 $\times 10^3$ km^3 between 1996 and 2005 (Fig. 7). It was shown to be related to the following summer's CIL index, accounting for 54 to 80% of the variance (Galbraith 2006). Using that relation, we are able to predict the coming summer's CIL index immediately after the winter survey. This timing usually coincides

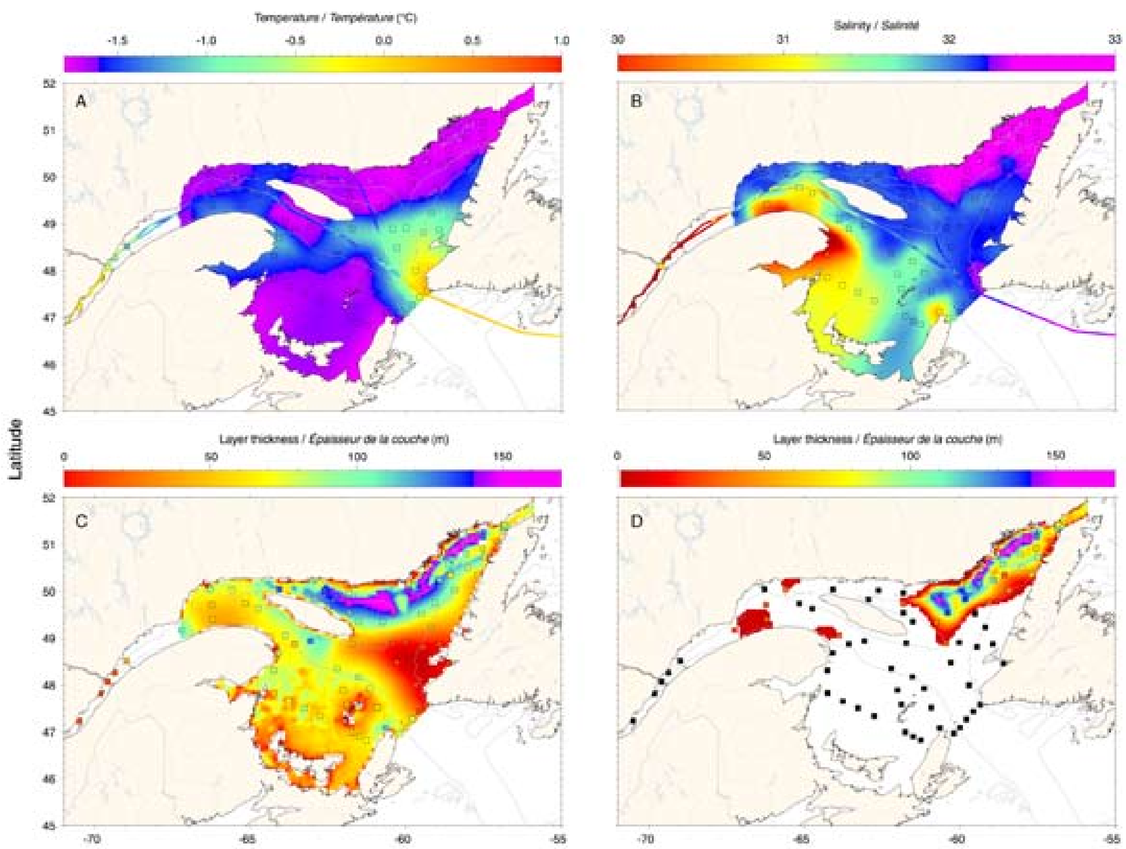

Fig. 6 Distribution maps of (A) surface temperature, (B) salinity, (C) cold layer thickness (< -1° C), and (D) thickness of the layer of cold and salty Labrador Shelf waters during the 2004 winter survey. The surface temperature and salinity data are complemented by ship-borne thermosalinograph data from the MV *Cicero* (see Galbraith et al. 2002) obtained during the same period.

Cartes de répartition (A) de la température et (B) de la salinité de surface, (C) de l'épaisseur de la couche d'eau froide (< -1° C) et (D) de l'épaisseur de la couche d'eau froide et saline en provenance du plateau du Labrador durant la mission hivernale de 2004. Les mesures de température et de salinité de surface sont complétées par des données d'un thermosalinographe recueillies à partir du navire Cicero *(voir Galbraith et al. 2002) obtenues pour la même période.*

with the Fisheries Oceanography Committee meeting, where various fisheries quotas are recommended. Since the environmental state of the Gulf is a factor influencing the recommendations, our results and predictions are very timely for this resource management process. The helicopter data allow us to predict with some degree of accuracy and confidence the next summer's temperature conditions in the Gulf's water column and help us understand why the change occurred.

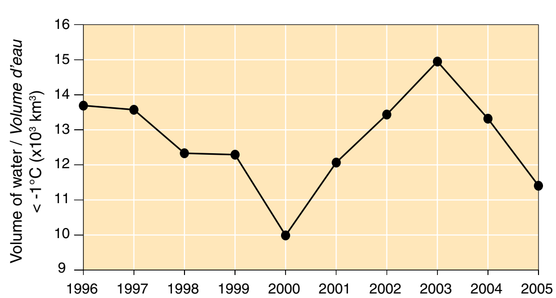

Fig. 7. Volume of the cold surface mixed layer (< -1°C) in the Gulf of St. Lawrence during each survey (adapted from Galbraith 2006 and updated for 2005).

Volume de la couche de mélange froide en surface (< -1°C) dans le golfe du Saint-Laurent pour chaque relevé annuel (adapté de Galbraith 2006 et mis-à-jour pour l'année 2005).

In summary, the helicopter-based survey is yielding late-winter temperature and salinity data for the Gulf of St. Lawrence and is contributing to a better understanding of winter conditions and their variability. The wintertime volume of cold water accounts for as much as 45% of all waters in the Gulf and is used as a predictor of the summer's cold-intermediate layer conditions.

Acknowledgements

The authors thank helicopter pilots Yvan Côté, Bernard Lemieux, Robert Delisle and Daniel Dubé as well as the aircraft technicians Michel Raymond, Pierre Ouellet, Yvan P. Côté, Michel Gionet, Alain Lambert and Bertran Murray, without whom this survey would never have gotten off the ground. We also thank Jean Du Sablon and Pierre Lemieux (CCG) for their support of the survey.

References

Galbraith, P.S. 2006. Winter water masses in the Gulf of St. Lawrence. J. Geophys. Res. In press.

Galbraith, P.S., Saucier, F.J., Michaud, N., Lefaivre, D., Corriveau, R., Roy, F., Pigeon, R., and Cantin, S. 2002. Shipborne monitoring of sea-surface temperature and salinity in the Estuary and Gulf of St. Lawrence. AZMP Bulletin PMZA No. 2, pp. 26-30.

Gilbert, D., and Pettigrew, B. 1997. Interannual variability (1948-1994) of the CIL core temperature in the Gulf of St. Lawrence. Can. J. Fish. Aquat. Sci. 54 (Suppl 1): 57-67.

Seasonality of Plankton on the Newfoundland Grand Banks

Gary Maillet and Pierre Pepin
Northwest Atlantic Fisheries Centre, Box 5667, St. John's, NL, A1C 5X1
MailletG@dfo-mpo.gc.ca

Sommaire

Nous avons examiné le moment d'occurrence des périodes de production du plancton à partir des données du CPR (*Continuous Plankton Recorder*) qui ont été récoltées sur les Grands Bancs de Terre-Neuve entre 1961 et 2003. Ces données montrent que le cycle saisonnier du plancton sur les Grands Bancs de Terre-Neuve se caractérise par une stabilité relative pour une variété importante de taxons et de niveaux trophiques. Ces résultats sont en contraste avec les patrons observés dans le nord-est de l'Atlantique et sur plateau Néo-Écossais. Les résultats obtenus dans la partie centrale de la mer du Nord et le plateau Néo-Écossais indiquent en effet que plusieurs taxons montrent une période de production plus hâtive de nos jours qu'au cours des dernières décades. Le temps d'occurrence plus hâtif de la période de production du plancton dans ces régions a été associé à une tendance générale au réchauffement des océans. Nos résultats suggèrent donc que le cycle saisonnier de production du plancton sur les Grands Bancs de Terre-Neuve est demeuré relativement stable dans le temps au cours des décennies 1960-1970 et 1990-2000 et cela, malgré le patron général de réchauffement des océans observé au cours de la dernière décade à la grandeur de l'Atlantique nord.

Introduction

The Continuous Plankton Recorder (CPR) surveys[1] provide long-term observations of the abundance and geographic distribution of planktonic organisms ranging from large phytoplankton cells to macrozooplankton (Warner and Hays 1994). CPR collections in the northwest Atlantic began in 1959 and continued with some interruptions until 1986. Collections were renewed in 1991 and continue to the present. The CPR is towed by ships of opportunity along a number of standard commercial routes throughout the North Atlantic. The CPR device collects plankton at a nominal depth of 7 m; organisms are retained on a moving band of silk material and preserved. Sections of silk representing an 18.5-km tow distance and ca. 3 m^3 of water filtered are examined microscopically. Every second section is analyzed, providing a horizontal scale of ca. 37 km. Many taxa are identified to the species level, while others are identified to coarser levels such as genus or family.

The timing of plankton production may have important implications for the transfer of energy from primary to secondary and tertiary producers (Cushing 1990, Harrington et al. 1999). Recent studies suggest that the timing of plankton cycles in temperate marine systems is a sensitive indicator of climate change (Edwards and Richardson 2004). It is hypothesized that the general trend of rising ocean temperatures in the eastern North Atlantic during the later part of the 1990s and into this century will modify trophic interactions among key planktonic taxa, resulting in the alteration of the food-web structure and leading to ecosystem-level responses (Beaugrand et al. 2003, Edwards and Richardson 2004). Similar trends in ocean warming have been documented in the western North Atlantic (Colbourne and Foote 2000, Colbourne 2004, ICES 2004). In this paper, we examine the timing of production cycles for major plankton taxa on the Newfoundland Grand Banks using data from the CPR surveys during the periods of 1961-1977 and 1991-2003.

The data extend from 1961 to 2003 with an intervening gap from 1978 to 1990. The sampling distribution was uneven in both space and time owing to variations in shipping routes and CPR funding. We did not differentiate the data based on bathymetry (e.g., shelf versus slope) and included all the data bounded by NAFO Divisions 3L and 3Ps (Fig. 1).

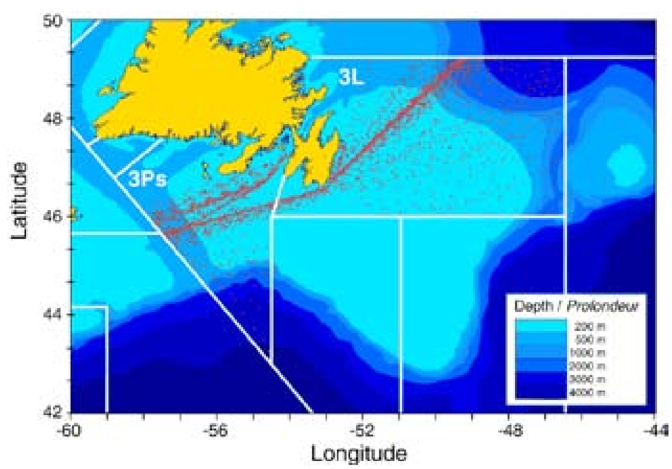

Fig. 1 Overlay of Continuous Plankton Recorder (CPR) stations within NAFO Divisions 3L and 3Ps (Newfoundland Grand Banks) from 1961 to 2003. Note the concentration of stations along the main commercial shipping lanes.

*Localisation des stations d'échantillonnage des données CPR (*Continuous Plankton Recorder*) dans les Divisions de l'OTAN 3L et 3Ps (Grands Bancs de Terre-Neuve) entre 1961 et 2003. Noter la concentration des stations le long des principales routes commerciales.*

The CPR estimates of plankton abundance used in this study are means of transformed counts [$x = \log_{10}(n+1)$] in 3 m^3 samples, averaged over each available month and year from 1961-1977 and 1991-2003. We excluded data from the analysis when more than two consecutive months were missing. We examined the seasonality of plankton on the Grand Banks using a temporal

[1] See the SAHFOS web site at (http://192.171.163.165/) for a description of the CPR Program collected for the Sir Alister Hardy Foundation for Ocean Science of Plymouth, England.

index developed by Colebrook (1979) and used by Edwards and Richardson (2004). The index, T_{CM}, is the centre of mass of the monthly counts based on the entire year's data. We have:

$$T_{CM} = (\sum_{i=1}^{12} M \cdot x_m)/(\sum_{i=1}^{12} x_m)$$

where M is the month number (January = 1 to December = 12) and x_m is the monthly mean abundance (log-transformed). Many factors may influence this parameter, including changes in timing or amplitude of the seasonal peak, or shifts in the average abundance and the community composition of the plankton. The occurrence of multiple peaks (e.g., spring and autumn blooms) in some years and the uneven sampling distribution may also result in variations in the centre of gravity index.

We used linear regression analysis to detect trends in the centre of gravity index within each time period during the 1961-2003 time series. The Kruskal-Wallis test (non-parametric) was used to compare the mean values of the seasonal peaks estimated by T_{CM} between the 1961-1977 and 1991-2003 time periods.

Plankton Production

The temporal indexes of the major phytoplankton production were relatively stable on the Grand Banks during the entire period (Fig. 2a). T_{CM} of large-celled diatom and dinoflagellate phytoplankton ranged from the early spring arrival of *Coscinodiscus* spp., followed by *Chaetoceros* spp. and *Ceratium arcticum* in late May-early June, through to autumn for *Ceratium fusus*. No significant linear trends were detected during either time period with the exception of *Chaetoceros* spp., which gradually shifted to a later occurrence during the 1960-1970s. Contrasts between the time periods indicated a transition to later time for *Ceratium arcticum* in the 1990s and recent years. The number of phytoplankton taxa increased during the 1990-2000s with the appearance of the large-celled diatoms *Coscinodiscus* and *Rhizosolenia* spp., which were not prevalent on the Grand Banks during the 1960-1970s, although they have been enumerated in the CPR since the late 1950s.

The seasonality of the dominant CPR mesozooplankton, consisting mainly of copepods, also showed remarkable consistency from year to year on the Grand Banks (Fig. 2b). The T_{CM} values for the mesozooplankton are mainly confined to late spring-summer (i.e., May-July) except for early life stages of copepods (nauplii), with values corresponding to March-April (Fig. 2b). Interannual variability in the T_{CM} of mesozooplankton was particularly high for certain CPR taxa (e.g., *Paracalanus/Pseudocalanus* spp.). The only trends were observed for the early life stages of *Calanus* spp. (CI-CIV; composed mainly of *Calanus finmarchicus*), which occurred later during the 1960-70s relative to the 1990-2000s, and vice versa for *Oithona* spp. Significant differences were observed between the two time periods for the late *Calanus* stages (CV-CVI) and *Calanus finmarchicus*, both showing a shift in T_{CM} to later in the year during the 1990-2000s. The number of mesozooplankton taxa also increased during the later period, with the appearance of *Metridia* spp. on the Grand Banks in comparison to limited observations of this copepod during the 1960-1970s (Fig. 2b).

The temporal centre of mass of dominant macrozooplankton taxa remained largely unchanged although interannual variability was high (Fig. 2c). The T_{CM} values of macrozooplankton occurred from May through August. Interannual variability of Chaetognatha and Euphausiacea revealed abrupt changes from summer to spring during the early to mid-1960s (Fig. 2c). These taxa also showed evidence of a systematic and gradual move back to summer production during the later part of the 1970s. The index of the Euphausiacea shifted gradually to later in the year during the 1960-1970s, but this pattern changed for both Chaetognatha and Euphausiacea during the 1990-2000s, with a shift back to an earlier occurrence during the year. No significant differences were observed between the respective time periods except for the Larvacea, which indicated a shift to later seasonality during the 1990-2000s. Shelled pteropods (*Limacina* spp.) also became prevalent on the Grand Banks during the 1990-2000s in contrast to lower abundances observed during the earlier time period.

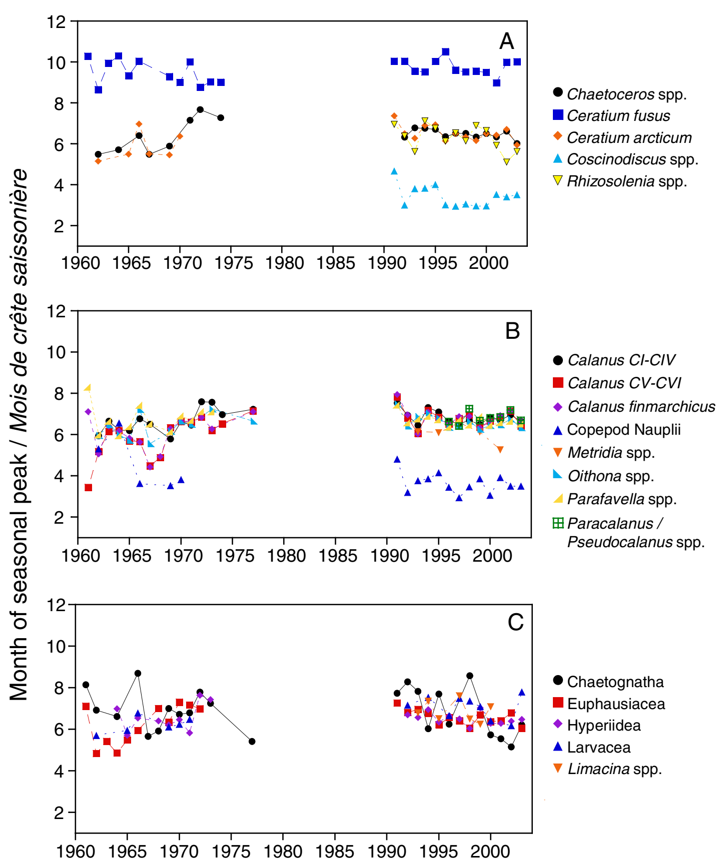

Fig. 2 Annual value of the T_{CM} index (annual centre of mass of the monthly plankton counts) for (a) phytoplankton, (b) mesozooplankton, and (c) macrozooplankton taxa collected during the Continuous Plankton Recorder (CPR) survey on the Grand Banks during the 1961-1977 and 1991-2003 time periods.

*Graphiques montrant le moment de l'année où se produisent les pics de production saisonniers (a) du phytoplancton, (b) du méso-zooplancton et (c) du macrozooplancton déterminés à partir des données CPR (*Continuous Plankton Recorder*) sur les Grands Bancs de Terre-Neuve au cours des périodes 1961-1977 et 1991-2003.*

Conclusion

Our results indicated that only 5 of 18 CPR plankton taxa on the Grand Banks showed significant trends in T_{CM} during the 1961-1977 and 1991-2003 time periods. All functional groups of plankton were represented, including phytoplankton, mesozooplankton, and macrozooplankton. In those taxa with significant linear trends, the slope values (range ± 0.2) indicated only a relatively small change in T_{CM} over the duration of the respective time periods (Fig. 3). Given the monthly resolution of the plankton data, the analyses suggest that the temporal index of plankton on the Grand Banks has remained stationary over the length of each period. In those five CPR taxa, the T_{CM} of plankton during the early period (i.e., 1961-1977) shifted later in the year (positive T_{CM} values) while this trend was reversed (negative T_{CM} values) in the second period. Where contrasts in the average T_{CM} values could be made between the respective time periods, only 4 of 13 comparisons showed significant differences (Kruskal-Wallis test), with *Ceratium arcticum*, *Calanus* CV-CVI, *Calanus finmarchicus*, and Larvacea all shifted to a later value in the 1990-2000s relative to the earlier period.

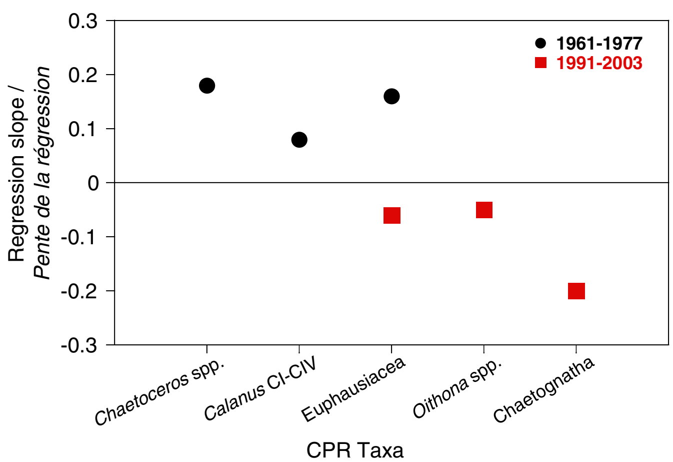

Fig. 3 Change in the T_{CM} index (annual centre of mass of the monthly plankton counts) for plankton collected during the Continuous Plankton Recorder (CPR) survey on the Grand Banks during the 1961-1977 and 1991-2003 time periods. For each CPR taxa, linear regression analysis was used to estimate the change in slope between the respective time periods, 1961-1977 and 1991-2003 (only significant changes in CPR taxa are shown). A negative slope indicates that the trend in seasonality or abundance is becoming earlier or decreasing while positive values suggest the reverse.

*Variations de l'indice T_{CM} (centre de masse annuel des décomptes mensuels de plancton) pour le plancton récolté au cours des traits d'échantillonnage CPR (*Continuous Plankton Recorder*) sur les Grands Bancs de Terre-Neuve au cours des années 1961-1977 et 1991-2003. Pour chacun des taxons échantillonnés par le CPR, une analyse de régression linéaire a été utilisée pour estimer le changement de pente entre les différentes périodes respectives : 1961-1977 et 1991-2003 (seulement les données montrant des différences significatives sont montrées ici). Une pente négative indique un pic saisonnier qui apparaît plus tôt en saison ou une abondance qui décroît, tandis des valeurs positives suggèrent le contraire.*

Overall, the small changes in the T_{CM} of the dominant CPR plankton on the Grand Banks contrasts with observations in the central North Sea (Edwards and Richardson 2004), where long-term variability of the parameter was driven by an earlier seasonality during the main production cycle (e.g., late spring-summer). For the period from 1958 to 2002, Edwards and Richardson (2004) reported that the T_{CM} values of North Sea plankton late in that period occurred one to two months earlier than they had at the start of the observation period. A shift to earlier timing was reported for the production cycle of phytoplankton and zooplankton during the 1990s compared to the 1960-1970s on the Scotian Shelf (Sameoto 2001), but that may have been confounded by a shift in the CPR route from the inshore to the offshore half of the shelf. In contrast, our analysis indicates remarkable stability in the seasonality of plankton on the Grand Banks (Fig. 3). Despite the general trend in ocean warming observed over the whole of the North Atlantic since the late 1990s (ICES 2004), the seasonal cycles of most phyto- and zooplankton species on the Grand Banks remained relatively stable. The CPR and AZMP programs will continue to provide valuable information regarding the response of the marine pelagic community to climate change. However, given that T_{CM} can be affected by the many factors noted above, we plan further analyses that will separate their influence and potentially refine our view of the annual and interannual variability of plankton dynamics on the Newfoundland Shelf.

References

Beaugrand, G., Brander, K.M., Lindley, J.A., Souissi, S., and Reid, P.C. 2003. Plankton effect on cod recruitment in the North Sea. Nature 426: 661-664.

Colbourne, E.B. 2004. Decadal changes in the ocean climate in Newfoundland and Labrador waters from the 1950s to the 1990s. J. Northw. Atl. Fish. Sci. 34: 41-59.

Colbourne, E.B., and Foote, K.D. 2000. Variability of the stratification and circulation on the Flemish Cap during the decades of the 1950s-1990s. J. Northw. Atl. Fish. Sci. 26: 103-122.

Colebrook, J.M. 1979. Continuous Plankton Records: Seasonal cycles of phytoplankton and copepods in the North Atlantic Ocean and the North Sea. Mar. Biol. 51: 23-32.

Cushing, D.H. 1990. Plankton production and year-class strength in fish populations: an update of the match/mismatch hypothesis. Adv. Mar. Biol. 26: 250-293.

Edwards, M., and Richardson, A. 2004. Impact of climate change on marine pelagic phenology and trophic mismatch. Nature 430: 881-884.

Harrington, R., Woiwod, I., and Sparks, T. 1999. Climate change and trophic interactions. Trends Ecol. Evol. 14: 146-150.

ICES. 2004. The annual ICES Ocean Climate Status Summary 2003/2004. ICES Cooperative Research Report, No. 269, 32 pp.

Sameoto, D. 2001. Decadal changes in phytoplankton color index and selected calanoid copepods in continuous plankton recorder data from the Scotian Shelf. Can. J. Fish. Aquat. Sci. 58: 749-761.

Warner, A.J., and Hays, G.C. 1994. Sampling by the Continuous Plankton Recorder survey. Prog. Oceanogr. 34: 237-256.

Using Size Structure as a Monitoring Index of Zooplankton Population Dynamics and Ecosystem Production

Alex W. Herman
Bedford Institute of Oceanography, Box 1006, Dartmouth, NS, B2Y 4A2
HermanA@mar.dfo-mpo.gc.ca

Sommaire

Les mesures basées sur la taille ont récemment émergées comme un index intéressant pour caractériser la dynamique du zooplancton et la production d'un écosystème. Dans ce contexte, la collecte de données sur la taille des organismes obtenues par un compteur de plancton optique au laser (LOPC : *Laser Optical Plankton Counter*) mène tout naturellement au développement d'outils d'analyse très puissants qui sont basés sur l'utilisation d'une représentation log-log de la biomasse ou du spectre de taille de la biomasse normalisée (NBSS : *Normalized Biomass Size Spectrum*). La forme ou la courbature de NBSS peut nous fournir une mesure ou un index de l'état de pauvreté ou de productivité de la communauté planctonique. Récemment, le développement d'un modèle spécifique utilisant la pente de la courbe NBSS a conduit au calcul direct du nombre de niveaux trophiques dans la communauté zooplanctonique et des exemples de cette application sont présentés ici pour le transect de Halifax (PMZA) sur le plateau Néo-Écossais, au printemps et à l'automne. D'autres exemples illustrent également l'utilité de la courbe NBSS pour isoler les pics de distribution des stades *Calanus finmarchicus* IV-V et pour mesurer des concentrations aussi faible que 10-20 organismes m^{-3}. Un dernier exemple d'un développement récent consiste en un LOPC monté sur un dériveur Lagrangien (SOLO) qui a été déployé dans les eaux côtières Californiennes.

Introduction

Certain metrics for zooplankton communities have been emerging as valuable indices for population dynamics. Traditionally, one of these metrics has a taxonomic base while recently another has been size based (Yurista et al. 2005). Size structure and biomass can provide a valuable index of zooplankton population dynamics and ecosytem production (Zhou and Huntley 1997, Kerr and Dickie 2001, Edvardsen et al. 2002). The Laser Optical Plankton Counter (LOPC; Fig.1), described in Herman et al. (2004), and its predecessor, the OPC (Herman 1988, 1992, Herman et al. 1993), have been applied to zooplankton community studies in a number of ways, for example i) for the identification of species, specifically *Calanus finmarchicus* IV-V (Osgood and Checkley 1997, Heath 1999, Baumgartner 2004), ii) for modelling of normalized zooplankton biomass size spectra and for estimating growth, mortality and productivity in marine (Zhou and Huntley 1997, Zhou et al. 2001) and in freshwater environments (Sprules et al. 1998, Sprules 2002, Edvardsen et al. 2002), and more recently iii) in the application of zooplankton size-spectra data for assessment of ecological conditions in the Great Lakes (Yurista et al. 2005) and in the Chesapeake Bay (Kimmel and Roman 2003). Presented here are the background and various applications of biomass size spectra obtained with the LOPC and its utility in monitoring programs.

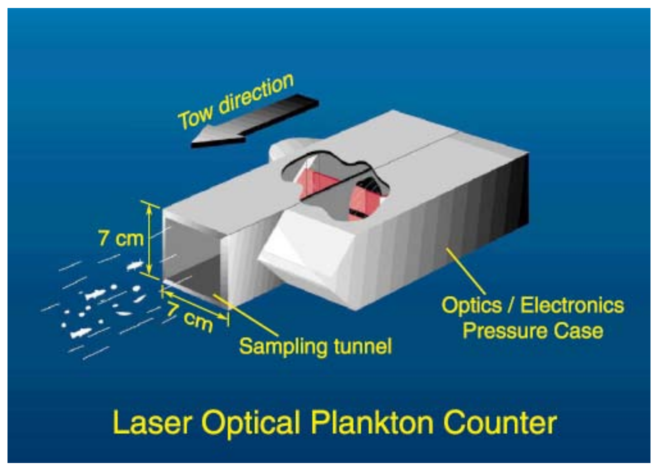

Fig. 1 Illustration of the Laser Optical Plankton Counter (LOPC) showing the laser beam (1x35 mm) traversing the sampling tunnel.

Illustration du compteur optique de plancton au laser (LOPC : acronyme anglais) montrant le rayon laser (1x35 mm) traversant le tunnel d'échantillonnage.

The Normalized Biomass Size Spectrum

As a result of its ability to measure zooplankton sizes rapidly over broad size ranges, the availability of LOPC size distribution data has revived some powerful analytical tools based on spectral analyses of turbulent wave energy and previously used for analyzing phytoplankton size distributions (Platt and Denman 1978). The biomass size spectrum provides a log-log representation of the biomass "probability" distribution over the entire size range of the zooplankton community sampled and provides "equal weighting" or "equal body intervals" of all sizes sampled (Normalized Biomass Size Spectrum, NBSS). The spectral shape or slope can represent departures from an equilibrium state indicating a depletion or net increase of particular taxa of plankton. The NBSS is a size-based analysis beginning with an LOPC particle size measurement. The LOPC measures the cross-sectional area of each particle and equates this area to an equivalent sphere with a corresponding equivalent spherical diameter (or esd) and hence its corresponding volume or biomass can then be calculated from its esd. Frequency distributions of particle biomasses are then calculated in equal logarithmic intervals representing the NBSS x-axis while the y-axis is represented by the corresponding biomass density (m^{-3}) divided by the logarithmic interval.

Examples of the NBSS are shown in Figure 2 for two regions (0-250 m) of the Gulf of St. Lawrence in 2001. NBSS are typically represented by their slopes and, in this case, the estuarine region, with a more negative slope of -1.01, has been shown to represent waters of higher production due to increases in zooplankton and additional aggregates or flocs. The clear benefit of NBSS is that it captures the entire zooplankton community in one measurement over a broad particle size range (100 µm to 3 mm esd) as represented by the x-axis (log biomass, Fig. 2). The spectral shape can yield information related to its zooplankton community status (e.g., productivity, biomass). The lower end of the x-axis of the estuarine zooplankton community (slope = -1.01) shows that there is a considerably greater number of small particle sizes present and that there is potential for "biomass-energy flow" from small sizes to large sizes, hence a potential for higher productivity. On the other hand, the open-water NBSS, with a slope of -0.47, represents a depleted zooplankton community that is not energetically sustainable.

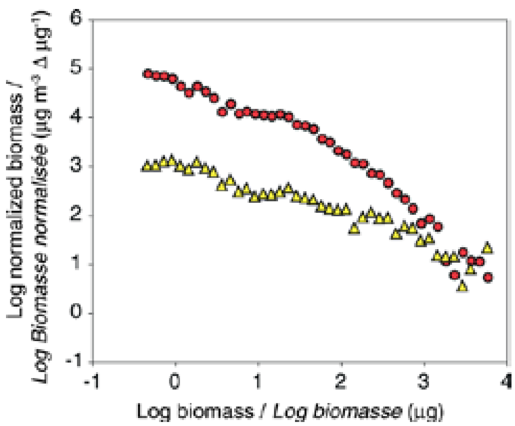

Fig. 2 Zooplankton normalized biomass size spectra (NBSS) for two representative stations in the Gulf of St. Lawrence. The profile in the Estuary (in red) showed high productivity, with a slope of -1.01, while the more oceanic waters in the Gulf (in yellow) are less productive, with a slope of -0.47.

Spectres de taille de la biomasse normalisée du zooplancton pour deux régions représentatives du golfe du Saint-Laurent. Le profil dans l'Estuaire (en rouge) montre une forte productivité avec une pente de -1.01 tandis que les eaux plus océaniques du Golfe (en jaune) sont moins productives avec une pente de -0.47.

It is difficult to characterize zooplankton populations solely from taxonomic data since singly quantified species cannot provide us the state of the zooplankton community, i.e., its structure determined by the rates of growth and the change in abundance, which in turn are determined by food availability and trophic relations. What indices can the NBSS provide for monitoring the zooplankton community? The area under the NBSS curve simply represents the static abundance or biomass of the zooplankton community. However, the NBSS slope or its shape has been hypothesized to be determined by growth rates, respiration, mortality and trophic dynamics. Observations indicate the slope should be approximately –1 (Platt and Denman 1978, Silvert and Platt 1978, Zhou and Huntley 1997). Assuming that the time-dependent variation of the biomass spectrum represents population dynamics within the plankton community, inverse mathematical methods were developed for solving individual body growth and mortality rates based on observations and theory (Heath 1995, Edvardsen et al. 2002, Zhou et al. 2002). A further model development by Zhou (under review) has led to linking the community assimilation efficiency (η) and trophic levels (*n*) to the slope of the biomass spectrum (sl), which can be expressed as:

$$n = -(1 + \eta)/(\eta \cdot sl) \qquad (1)$$

As an example, the grazing of copepods on phytoplankton biomass represents the first trophic level. In the case where zooplankton mortality loss and subsequent recycling by carnivorous zooplankton to maintain stability occurs, the parameter "*n*-1" is a measure of the number of recycles, i.e., where *n*=1, 2, 3, etc. Values of *n*=1 indicate the zooplankton community was dominated by herbivores, *n*=2 signifies a biomass recycling by carnivorous zooplankton of n-1 or 1x, while *n*=3 signifies a recycling of *n*-1 or 2x, and so on. For example, using published values of η=0.7, the NBSS slope of -0.47 in the Gulf of St. Lawrence (Fig. 2) yields *n*~5, indicating biomass recycled n-1 or 4x and therefore a community dominated by carnivorous zooplankton. The more negative NBSS slope of -1.01 in Figure 2 results in *n*=2.4 and indicates a biomass recycling of *n*-1 or 1.4x, implying that carnivorous zooplankton are an important but less dominant component in this stable community.

The trophic levels, *n*, were calculated (assuming η=0.7) for each profile (using a Moving Vessel Profiler) of the Halifax Section–Scotian Shelf (Fig. 3) for both spring and fall, consisting of approximately 70 profiles over a distance of 180 km. During the spring 2004, the mean number of trophic levels n ~2 indicated a biomass recycling of 1X, implying equal components of herbivorous and carnivorous zooplankton. The same region during fall (2003) had ~4-5 trophic levels, indicating biomass recycling of 3-4x and the dominance of carnivorous zooplankton. However, during fall (2003), *n* decreased considerably (~1-2) over Emerald Basin for ~25 km, indicating a localized dominance of herbivores. The estima-

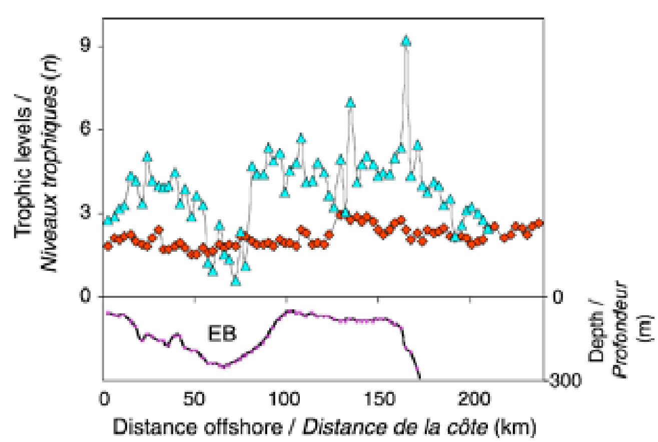

Fig. 3 Trophic levels (n) for the Halifax Line plotted for both the fall 2003 (in blue) and spring 2004 (in red) samplings. The lower plot shows the cross-sectional Scotian Shelf bathymetric profile, showing Emerald Basin (EB) and the shelf edge to the right.

Niveaux trophiques (n) pour le transect de Halifax pour les périodes d'automne 2003 (en bleu) et de printemps 2004 (en rouge). Le graphique du bas montre le profil bathymétrique d'une section transversale sur le plateau Néo-Écossais illustrant le bassin Emerald (EB) et la pente continental à la droite.

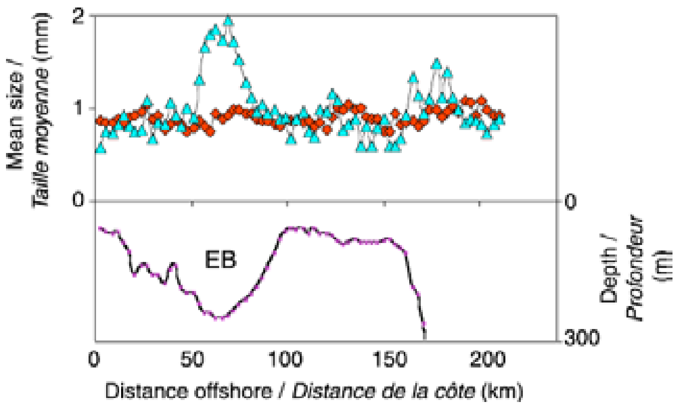

Fig. 4 Mean size (mm) of the NBSS zooplankton distribution as measured by the LOPC for the Halifax Line, plotted for both the fall 2003 (in blue) and spring 2004 (in red) samplings. The lower plot shows the cross-sectional Scotian Shelf bathymetric profile, showing Emerald Basin (EB) and the shelf edge to the right.

Taille moyenne (mm) du spectre de taille de la biomasse normalisée du zooplancton tel que mesuré par le LOPC pour le transect de Halifax à l'automne 2003 (en bleu) et au printemps 2004 (en rouge). Le graphique du bas montre le profil bathymétrique d'une section transversale sur le plateau Néo-Écossais illustrant le bassin Emerald (EB) et la pente continental à la droite.

tion of the parameter *n* (trophic levels) is based on well-developed modelling (Zhou, under review) but will still require vigorous field testing and validation. Although estimates of absolute values of *n* may not be currently established with full confidence, changes in *n* from season-to-season are well-established in zooplankton ecosystem modelling and will provide reasonable estimates for monitoring.

Other monitoring indices that may be derived from NBSS allow seasonal tracking of the community size. Figure 4 shows the mean size (mm) of the zooplankton as measured by the LOPC and derived from the NBSS. The mean size during spring is uniform across the Scotian Shelf at about 0.9 mm while during fall the mean size shows a sharp increase (of ~ 1 mm) over Emerald Basin and some increases at the shelf edge. Net samples indicated high concentrations of large *Calanus finmarchicus* (V-VI) situated deep in Emerald Basin (200-250 m) and at the shelf edge, and also indicated high concentrations of small euphausiids.

Taxonomic Identification using NBSS

Ideally, taxonomic identification of zooplankton would be complementary to NBSS analyses since it provides monitoring programs with the necessary knowledge to determine which species (or groups) are present as herbivores or carnivores. In eastern Canadian coastal waters, *Calanus finmarchicus* is a dominant herbivore continually monitored by AZMP via net tows. Because the NBSS is structured to represent "equal body intervals" (i.e., log biomass) within the zooplankton community, many individual species can often be isolated as peaks and quantified within the spectrum. Figure 5 shows an example of the size-frequency distribution of an LOPC profile taken in the Gulf of Maine in 2002, which sampled high density layers of *Calanus finmarchicus* V-VI between 100-150 m with densities of 2000-3000 m^{-3}. Figure 5a clearly shows a

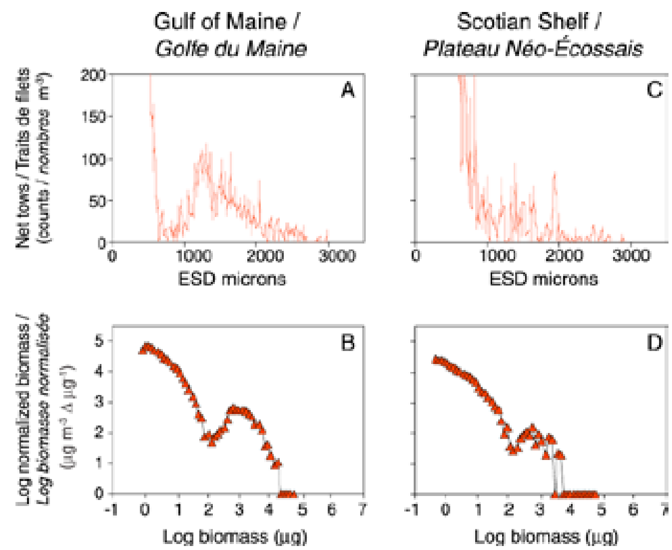

Fig. 5 LOPC data from the 100-150 depth stratum in the Gulf of Maine and on the Scotian Shelf. (A) Counts m^{-3} vs the equivalent spherical diameter (esd) showing a *Calanus finmarchicus* CV peak between 1200 and 2000 microns in the Gulf of Maine; (B) the NBSS plot of the same data showing a clear definition of the *C. finmarchicus* CV peak in the same range; (C) counts m^{-3} vs esd on the Scotian Shelf showing a concentration of *C. finmarchicus* CV about 1/10 of that shown in (A); (D) the NBSS plot of same data showing a clearer definition of the *C. finmarchicus* CV peak.

Données LOPC de la strate de 100-150 m de profondeur dans le golfe du Maine et sur le plateau Néo-Écossais. (A) décomptes m^{-3} *vs le diamètre sphérique équivalent (esd) montrant le pic de* Calanus finmarchicus *CV entre 1200 et 2000 microns dans le golfe du Maine; (B) graphique de la courbe NBSS pour les mêmes données indiquant une définition claire du pic de* C. finmarchicus *CV dans cette gamme de taille; (C) décomptes* m^{-3} *vs esd montrant une abondance de* C. finmarchicus *CV environ 1/10 de celle sur la Fig. A; (D) graphique de la courbe NBSS pour les mêmes données suggérant une définition plus claire du pic de* C. finmarchicus *CV.*

peak in the distribution between 1200-2500 µm esd while the corresponding NBSS (Fig. 5b) also shows the peak situated above the biomass curve. Figure 5c, on the other hand, shows a size-frequency distribution sampled in the Scotian Shelf, where the *C. finmarchicus* V-VI concentrations are 1/10th of those in the Gulf of Maine, and the peak is not clearly evident between 1200-2500 µm. The NBSS representation, however, clearly shows a peak present in the same biomass interval as that seen in Figure 5b. In a typical coastal profile, the NBSS representation is capable of measuring concentrations between 200 and 2000 m^{-3} (counts summed over the peak).

Distinguishing Aggregates/Flocs from Zooplankton

During the period surrounding spring blooms, a substantial quantity of aggregates or marine flocs are present simultaneously with zooplankton and increase LOPC-measured concentrations considerably over its size range. Aggregates typically disintegrate in nets due to their fragility (hence termed "fragile particles" or FPs) but can be reasonably quantified by camera imaging. Both FPs and zooplankton are captured by the LOPC, which provides an optical measurement; however, separating zooplankton and FP counts is difficult. Recent work in CalCOFI (California Cooperative Oceanic Fisheries Investigations) regional waters (Herman and Checkley – pers. comm.) has shown that the LOPC is able to separate FPs and

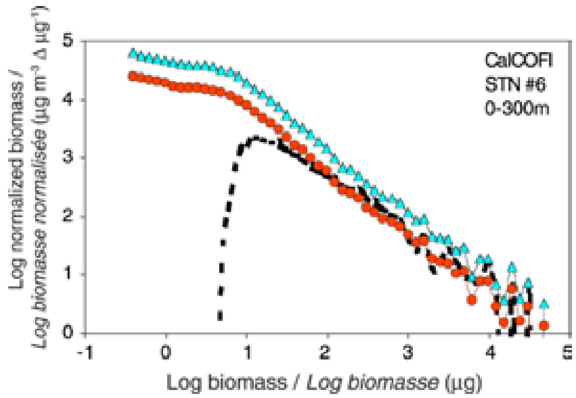

Fig. 6 NBSS plot representing in blue a station with high biomass (fragile particles [FP] and zooplankton) and in black the "partial" NBSS measured (by LOPC) for particles with a high transparency only. By extrapolating the black line towards the minimum size, we can generate a distribution representing the "FP" NBSS that, when subtracted from the "total NBSS," represents the NBSS of zooplankton only (in red).

Graphique NBSS représentant en bleu une station avec une biomasse forte (particules fragiles et zooplancton) tandis que la ligne noire montre le NBSS « partiel » mesuré (par LOPC) pour des particules avec une grande transparence seulement. Par extrapolation de la ligne noire vers la taille minimale, on peut générer une distribution représentant le NBSS des particules fragiles qui, lorsque soustrait du NBSS total, représente le NBSS du zooplancton seulement (en rouge).

zooplankton using estimates of opacity. Implementing a subtraction of FP biomass within the NBSS distribution, we can now obtain accurate estimates of zooplankton abundances. Figure 6 shows an NBSS (blue line) sampled in CalCOFI regional waters that was also identified by camera imaging as containing high concentrations of FPs and zooplankton. A separate NBSS (black line) can be generated for only those particles measured by the LOPC with high transparency in a biomass range >1.0 (log biomass on x-axis) that therefore represents the NBSS for FPs in that size range. A first-order estimate is applied by extrapolating the curve-slope for the NBSS FPs back to the smallest measurable size in Figure 6; we can then generate the estimated full range of the NBSS FP distribution. By subtracting the FP distribution from the "total NBSS," we can generate an NBSS attributed to zooplankton only (Fig. 6, red data).

The abundance estimates for *Calanus* spp. made by the LOPC are often higher than those abundance estimates determined from net tows due to the presence of FPs. A comparison between simultaneous net and LOPC tows in CalCOFI regional waters is shown in Figure 7, where raw counts from LOPC estimates (*C. pacificus* V-VI) are 2X higher than estimates from net tows (slope=0.43, blue data points). By applying the correction described in Figure 6, the linear fit results in a slope closer to unity. By utilizing the NBSS correction process described above, we are now able to reasonably extract abundances of *Calanus* spp. (V-VI) over the full range of concentrations 20-2000 m^{-3}. The correction method has also been applied successfully to abundance estimates of other taxonomic groups such as *Oithona* spp. and *Oncaea* spp. in the lower size ranges of 300-600 µm.

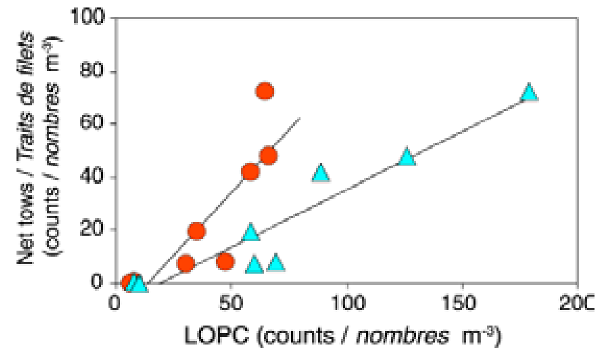

Fig. 7 Inter-comparison between abundances of *C. pacificus* V and VI from net tows and simultaneous LOPC measurements. Blue triangles represent raw data (slope=0.43) while red circles represent data (slope=0.94) where fragile particles (FPs) have been subtracted, resulting in a near 1:1 relationship (slope 0.94).

Comparaison entre l'abondance de C. pacificus *V et VI provenant des traits de filets et les mesures simultanées de LOPC. Les triangles bleus représentent les données brutes (pente = 0.43) tandis que les cercles rouges représentent les données auxquelles on a soustrait les valeurs des particules fragiles résultant presque en une relation 1:1 (pente = 0.94).*

Sampling Platforms: Present and Future

With the current 120 OPCs sold since 1990 and 25 LOPCs sold since 2003, there have been a large variety of sampling platforms for OPCs/LOPCs developed by users, ranging from those units installed in plankton nets to higher speed undulating vehicles. A recent and exciting development of Lagrangian drifter applications has emerged from collaboration between Scripps Institution of Oceanography and the Bedford Institute of Oceanography. The LOPC developed at BIO and the SOLO drifter float developed at SIO have been integrated and tested

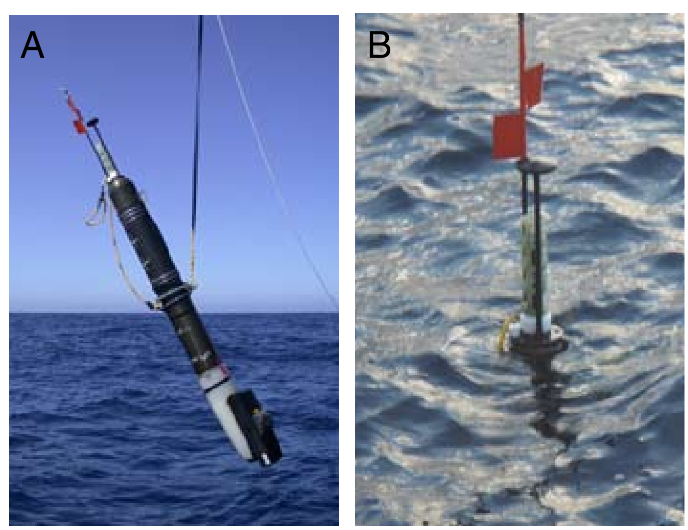

Fig. 8 Prototype "SOLOPC" consisting of an LOPC integrated with a SOLO drifter float: (A) deployed in CalCOFI regional waters in Sept. 2005; (B) breaking surface following a dive and beginning to transmit data to an Iridium satellite via its top-mounted antennas.

Prototype « SOLOPC » comprenant un LOPC intégré à une bouée dérivante SOLO (A) déployé dans les eaux régionales CalCOFI en septembre 2005; (B) faisant surface après une plongée et débutant la transmission des données vers un satellite Iridium via ses antennes montée sur le dessus.

in CalCOFI regional waters in a collaborative development project (D. Checkley, SIO; R. Davis, SIO; A. Herman, BIO; G. Jackson, TAMU). The first prototype SOLOPC, shown being launched from the R/V *Sproul* in Figure 8a, was successfully tested in Sept. 2005 over a period of three days, securing 64 profiles to 100 m. Once its sampling is completed, the SOLOPC breaks surface and transmits its data to an Iridium satellite using its top-mounted antennas shown in Figure 8b. A second unit is planned at SIO, one that will be deployed for a longer period of approx. 3-6 months. The need for continuous oceanic data in monitoring programs is being addressed by the evolving development of autonomous Lagrangian drifters such as the SOLOPC.

References

Baumgartner, M. F. 2004. Comparisons of *Calanus finmarchicus* fifth copepodite abundance estimates from nets and an optical plankton counter. J. Plankton Res. 25(7): 855-868.

Edvardsen, A., Zhou, M., Tande, K.S., and Zhu, Y. 2002. Zooplankton population dynamics: Measuring in situ growth and mortality rates using an Optical Plankton Counter. Mar. Ecol. Prog. Ser. 227: 205-219.

Heath, M.R. 1995. Size spectrum dynamics and the planktonic ecosystem of Loch Linnhe. ICES J. Mar. Sci. 52: 627-642.

Heath, M.R. 1999. The ascent migration of *Calanus finmarchicus* from overwintering depths in the Faroe-Shetland Channel. Fish. Oceanogr. 8(Suppl 1): 84-99.

Herman, A.W. 1988. Simultaneous measurement of zooplankton and light attenuance with a new optical plankton counter. Cont. Shelf Res. 8: 205-221.

Herman, A.W. 1992. Design and calibration of a new optical plankton counter capable of sizing small zooplankton. Deep-Sea Res. 39: 395-415.

Herman, A.W., Cochrane, N.A., and Sameoto, D.D. 1993. Detection and abundance estimation of Euphausiids using an optical plankton counter. Mar. Ecol. Prog. Ser. 94: 165-173.

Herman, A.W., Beanlands, B., and Phillips, E.F. 2004. The next generation of Optical Plankton Counter: the Laser-OPC. J. Plankton Res. 26(10): 1135-1145.

Kerr, S.R., and Dickie, L.M. 2001. The biomass spectrum: a predator-prey theory of production. Columbia University Press, N.Y.

Kimmel, D.G., and Roman, M.R. 2004. Long-term trends in mesozooplankton abundance and community composition in the Chesapeake Bay, USA: influence of freshwater input. Mar. Ecol. Prog. Ser. 267: 71-83.

Osgood, K.E., and Checkley, D.M. Jr. 1997. Observations of deep aggregations of *Calanus pacificus* in the Santa Barbara Basin. Limnol. Oceanogr. 42: 997-1001.

Platt, T., and Denman, K. 1978. The structure of marine pelagic ecosystems. Rapp. P.-V. Réun. Cons. Int. Explor. Mer 173: 60-65.

Silvert, W., and Platt, T. 1978. Energy flux in the pelagic ecosystem: a time-dependent equation. Limnol. Oceanogr. 23: 813-816.

Sprules, W.G. 2002 Spatial estimates of prey consumption by *Mysis relicta* Loven using an optical plankton counter. Ver. Internat. Verein. Limnol. 27: 3275-3278.

Sprules, W.G., Jin, E.H., Herman, A.W., and Stockwell, J.D. 1998. Calibration of an optical plankton counter for use in fresh water. Limnol. Oceanogr. 43: 726-733.

Zhou, M., and Huntley, M. 1997. Population dynamics theory of plankton based on biomass size spectra, Mar. Ecol. Prog. Ser. 159: 61-73.

Zhou, M., and Tande, K. (editors). 2002. A review of the optical plankton counter and an introduction to the next generation of laser-optical plankton counters. An International Global Oceans Ecosystem Dynamics (GLOBEC) Program Report of the Optical Plankton Counter Workshop. Tromso, Norway, June 17-20, 2001, 67 pp. (http://www.pml.ac.uk/globec/products/reports/globecrep.htm)

Yurista, P., Kelly, J.R., and Miller, S. 2005. Evaluation of optically acquired zooplankton size-spectrum data as a potential tool for assessment of condition in Great Lakes, Environmental Management 35(1): 34-44.

The Need for Ongoing Monitoring Programs in the Development of Ocean Forecasting Capabilities in Canada

Fraser J.M. Davidson[1], Daniel G. Wright[2], Denis Lefaivre[3] and Joël Chassé[2]

[1] Northwest Atlantic Fisheries Centre, Box 5667, St. John's, NL, A1C 5X1

[2] Bedford Institute of Oceanography, Box 1006, Dartmouth, NS, B2Y 4A2

[3] Institut Maurice-Lamontagne, Box 1000, Mont-Joli, QC, G5H 3Z4

DavidsonF@dfo-mpo.gc.ca

Sommaire

Le Programme de Monitorage de la Zone Atlantique (PMZA) est un atout important pour le développement de l'océanographie opérationnelle au Canada. Il permet d'obtenir des observations pouvant être utilisées autant comme valeurs à assimiler dans les modèles que comme références permettant de valider les sorties des modèles numériques de prévisions océaniques. Bien que toutes les observations du PMZA ne soient pas encore recueillies et transmises de façon automatique et en temps réel, les futurs systèmes de prévisions océaniques pourraient avec avantage faire usage des observations in situ recueillies en temps réel par le PMZA. Dans ce contexte, l'utilisation conjointe des observations satellitaires d'altimétrie et de la température de surface avec les observations in situ de profils de température et de salinité devrait faire partie de la première étape débouchant sur le développement de la prévision océanique sur les plateaux continentaux de l'est du Canada.

Ocean forecasting falls within the broader field of operational oceanography, which encompasses all systems that provide useful information about the present and future states of the ocean for marine applications. This information is typically provided by a combination of observations and modelling, including everything from statistical information based on ocean observations to model forecasts. In August 2002, a workshop entitled "Assessing Operational Global Marine

Environmental Prediction for Canada" was held under the auspices of the Center for Marine Environmental Prediction (CMEP) in Halifax, NS. The participants concluded that a data assimilative ocean–atmosphere forecasting system was needed in Canada and that inter-agency coordination and effort were required to bring a national system into service. Since then, government departments and academic partners have increased their efforts to establish improved regional and global-scale capabilities in operational oceanography. We provide a very brief overview of recent operational oceanography developments and a description of some potential contributions that the AZMP could make to new initiatives in ocean nowcasting and forecasting in Atlantic Canada.

The IML Example

In Canada, the Institut Maurice-Lamontagne (IML) is at the forefront of the development of useful ocean information products for commercial, social and scientific interests. The IML forecasting system is based on research models (e.g., Saucier and Chassé 2000, Saucier et al. 2003) migrated to the operational level. Products from the IML system are freely available on the St. Lawrence Observatory Web site (www.osl.gc.ca). The IML microcosm demonstrates the large range of activities and benefits associated with operational oceanography. They take advantage of information collected by other agencies (e.g., the Meteorological Service of Canada weather observations, Canadian Ice Service ice charts, the Canadian Hydrographic Service water level observations, the Great Lakes outflow forecast from Environment Canada, the flow forecast from the Ottawa River Board Secretariat) and maintain programs to make additional routine observations of the marine environment. This information together with ocean and coupled ocean–atmosphere–sea-ice forecast models are used to provide operational services for clients through web-based dissemination. Examples of services include the Gulf of St. Lawrence daily forecast of sea-ice concentration and thickness for ship routing, the St. Lawrence River surface currents and water levels for the Canadian Coast Guard Environmental Emergency Service to use in oil-spill trajectory forecasts, surface wave and current estimates for Search and Rescue systems, wave and freezing spray marine forecasts, 30-day water level forecast for the St. Lawrence River and freshwater flow nowcasting at Québec City. The system is an excellent example of what can be done with ocean information and how it can benefit Canadians.

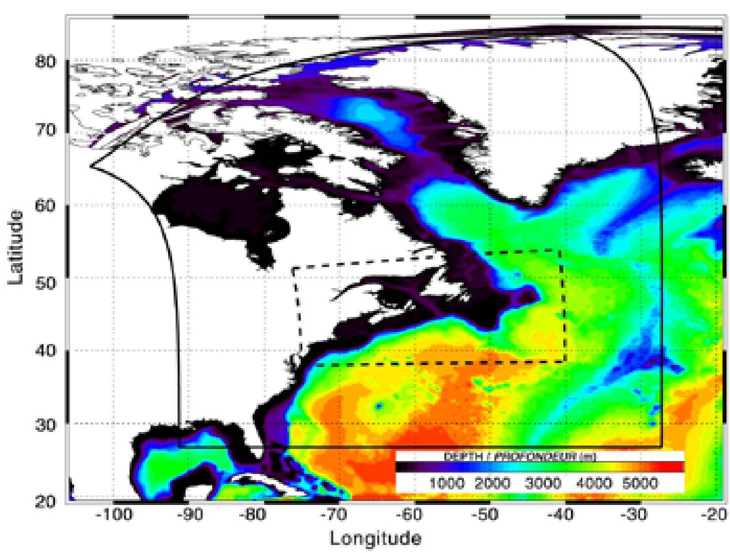

Fig. 1 Model domain showing the Northwest Atlantic Common Domain (outer black line) and the high resolution EAST domain (dotted black line). Colours represent the model depth in metres.

Domaine du système de prévision où la ligne noire extérieure représente le domaine commun dans la région nord-ouest de l'Atlantique. L'espace défini par la ligne noire pointillée correspond au domaine de haute résolution EAST. Le code de couleur correspond à la profondeur du modèle en mètres.

Data assimilation is used to improve the accuracy of the water-level forecast system to aid deep-draft ships navigating the St. Lawrence River. In contrast, the ocean circulation prediction system at IML includes models that are initialized and verified with data, but to date, data have not been merged with the forecast through data assimilation. This approach has produced very promising results for the Gulf of St. Lawrence, partly because the region of interest is a relatively small semi-enclosed system for which variability at the open boundaries is important but not dominant and also because surface fluxes and river inputs are relatively well known. For other regions, forcing through the open boundaries will play a more important role, and new techniques will be required to make up for less complete information on initial conditions and the fluxes through surface and open-ocean boundaries. This will undoubtedly require the assimilation of ocean observations into numerical models.

Zonal "Modelling" Program

There are already several operational (or quasi-operational) ocean modelling systems for the east coast of Canada. Successful initiatives have focussed on specific geographic and product development areas, and this approach to R&D will continue in the future. In addition, a new operational forecasting system for the Canadian east coast is presently under development, involving, at various levels of effort, participation from the Northwest Atlantic Fisheries Centre, the Bedford Institute of Oceanography, the Gulf Fisheries Centre and the Institut Maurice-Lamontagne. This initiative encompasses areas of interest to all of these regions and is tentatively referred to as the EAST (Enhanced Atlantic Shelf Territory) initiative. We hope that this system will help to consolidate DFO-led operational oceanography initiatives on the east coast and make it easier for various groups with overlapping interests to share both advances and the workload of developing and maintaining an operational system. It would thus provide a truly zonal modelling program to complement the AZMP. Eventually, this consolidation should also simplify the interactions between observational programs like AZMP and the modelling side of operations.

To cover the full region and reduce problems associated with open boundary conditions, we have included a relatively coarse resolution (initially 1/4 degree) outer domain that covers the entire Northwest Atlantic (black line, Fig. 1) with the finer resolution (initially 1/12 degree) EAST domain (dotted line, Fig. 1) embedded within it. The entire Northwest Atlantic domain is currently being nested within the Mercator North Atlantic operational system with a horizontal resolution of approximately 1/4 degree. Eventually, the NW Atlantic system could be embedded within other models, including a global operational coupled ocean–atmosphere–sea-ice system to be developed by an inter-agency initiative involving the Meteorological Service of Canada, the Department of Fisheries and Oceans, the Department of National Defence and members of the university community. Integration into the latter system would permit a two-way interaction between the global and regional modelling efforts.

The first near-operational version of the east coast forecasting system is being developed as an element of the Newfoundland Operational Ocean Forecast System (NOOFS) in St. John's with input from all four regions. It is expected to be functional in the summer of 2006, with ongoing system evolution and enhancement. Once functionality of the forecast system is established, the model resolution could be increased as computer resources permit. For example, an increase from 1/4 to 1/8 degree in the outer domain and from 1/12 to 1/24 degree within the embedded EAST domain would significantly enhance the utility of the system for shelf-related problems. AZMP data will assist in the development of this system by providing observations on the shelf to enable model hindcasts over the past 10 years for analysis and validation purposes. All temperature and salinity profiles collected by AZMP will either be entered in the analysis or retained for model validation. Once the modelling system enters the operational phase, AZMP will continue to make major contributions through the timely and routine supply of data.

Expanded Roles for AZMP

The AZMP operations can provide a foundation for the coordination of both systematic and opportunistic observations and the distribution of this observational information to ocean nowcast and forecast centres in Atlantic Canada. The nascent operational oceanography initiative is fortunate to have an established monitoring program to build on for this purpose; very few countries have such a well-established system for the routine collection of oceanographic information. With the current surge in ocean forecasting effort, it is anticipated that the importance of the AZMP for ocean monitoring and prediction will continue to increase over the coming years.

Ocean nowcasting and forecasting are natural complements to ocean monitoring programs. To interpret the data and provide the best estimates of past, present and future conditions on the Labrador Shelf, Newfoundland Shelf, Scotian Shelf and in the Gulf of St. Lawrence and Gulf of Maine will require continued data collection and assimilation into numerical ocean models. Further, it is anticipated that the need for new and/or modified data sets will become apparent as we learn more about what is required to efficiently and effectively constrain model results; the modelling system must evolve to better address the issues of interest to users. Forecasts of future conditions are particularly valuable, but are difficult to make successfully. Forecasts may extend from a few hours to a couple of weeks for smaller regions and possibly to seasonal time scales for the larger Canadian Atlantic zone. Ocean models

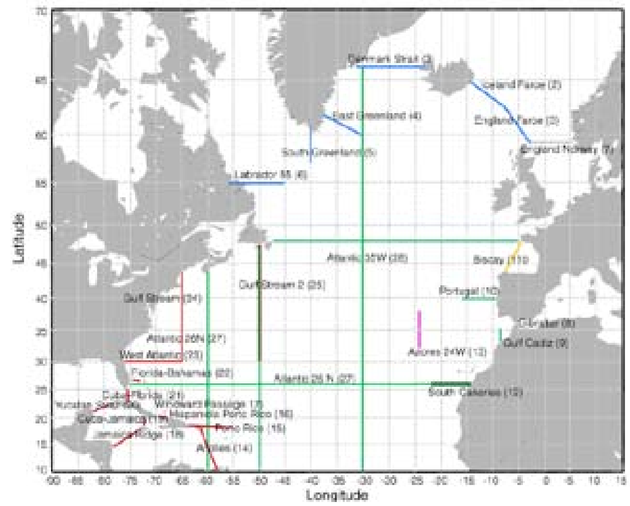

Fig. 2 Class 2 metrics along predetermined high-resolution transects for the comparison of models and observations in the European MERSEA project (Crosnier and Le Provost 2006).

Deuxième classe d'unités quantifiables le long de sections à haute résolution spécifiques pour la comparaison entre les observations et les résultats du modèle dans le cadre du projet européen MERSEA (Crosnier et Le Provost 2006).

must be properly initialized to have any hope of providing useful forecasts of future conditions; the AZMP will play a critical role in this regard.

To develop the best possible system, to check its reliability and to uncover problems, the model results must be compared with observations. The AZMP will be a fundamental contributor to model validation and improvement. For the North Atlantic there are numerous ocean forecast systems already running, including Mercator, HyComm, Topaz, Foam and NLOM. To facilitate the intercomparison of model results and representation of the real world, a set of metrics have been defined (and continue to be refined). Within the European Marine and Environmental Security for the European Area (MERSEA) ocean forecasting project for the North Atlantic, the following classes of metrics are defined:

- Class 1 metrics are based on horizontal slices of quantities such as temperature, salinity and velocity at 12 standard depths as well as the two-dimensional quantities such as sea-surface height, mixed-layer depth, barotropic stream function, wind stress, heat flux and evaporation–precipitation–runoff.

- Class 2 metrics encompass high-resolution transects of temperature, salinity and velocity for regions of the model domain that are of special dynamic interest (Fig. 2), observations from transects that are regularly occupied by ship routes (Fig. 3) and fixed-mooring locations and established monitoring sites (e.g., Station 27 off St. John's, Newfoundland).

- Class 3 metrics consist of integrated quantities such as the zonally integrated meridional overturning transport and the mean transports through transects defined by classes 1 and 2.

- Class 4 metrics include tests of performance and analysis of forecasts, inter-comparison of model output with available in-situ profiles, and drifting buoys and scoring mechanisms for ocean forecast accuracy.

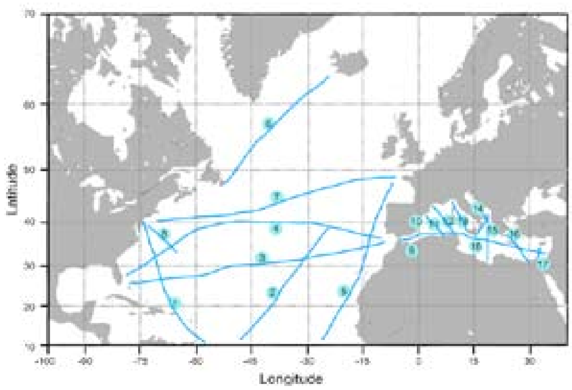

Fig. 3 Standard sampling transects on regular ships-of-opportunity routes across the North Atlantic (from Mercator-Ocean www.mercator-ocean.fr).

Transects d'échantillonnage standards suivant les trajets réguliers de navires d'opportunité dans l'Atlantique Nord (origine de Mercator-Ocean www.mercator-ocean.fr).

These metrics can be routinely produced by ocean models and compared with observational data—if the latter are available. They can include bio-physical parameters such as nutrients, oxygen and chlorophyll *a*, which must be nowcasted and forecasted for ecosystem research and integrated management. Various biological models, starting with nutrient–plankton–zooplankton models, will be integrated into the modelling system; the AZMP biological data will be essential to initialize and test model applications (e.g., Le Fouest et al. 2003). Scientists at IML, the Gulf Fisheries Centre (GFC) and the Bedford Institute of Oceanography (BIO) determine annual hindcasts of the oceanic conditions in the Gulf of St. Lawrence and northeast Scotian Shelf that provide complementary information for stock assessments and the review of environmental conditions. Forecasting the recruitment of selected fishes requires information on the drift, growth and survival of the early life stages; the AZMP provides some of the biological data (larvae, eggs) necessary for the initialization of the required bio-physical models. Such applications contribute to the comprehensive fishery information system used for ecosystem considerations and integrated management. The development of an ocean model with assimilation of physical observations will provide an improved framework for these bio-physical models.

Current AZMP transects (Fig. 4) represent valuable information for validation based on class 2 metrics. The data from these shelf transects can be compared to results from various North Atlantic operational forecast systems as well as to present and developing Canadian regional systems. With the anticipated development of operational ocean forecasts that cover the entire North Atlantic at a horizontal resolution of 7 km, even features such as the inshore branch of the Labrador Current are being resolved in basin-scale systems. The AZMP can thus provide valuable information for both the regional and the international forecasting community, particularly for sections that extend beyond the shelf break. Interests in using AZMP transect information for the evaluation of metrics has already been expressed by the MERSEA program.

We mentioned that our regional model will be coupled to a global coupled atmosphere–ocean–sea-ice model. This global model will not represent many of the small-scale processes and features present in the shelf and Gulf regions, but will provide an improved representation of the influence of large-scale changes on the embedded regions. Assimilation of archived hydrographic and satellite altimetry data has already made major improvements to the realism of basin-scale ocean models; further improvements are anticipated. These developments will be included in the basin-to-global initiative, so regional models will have access to the best possible open-boundary information. In addition, if two-way coupling is used in which the fine-resolution results are smoothed and passed back to the coarse grid, then the influence of small-scale processes in the EAST region on basin-scale variability will be better represented. Any improvements made in the regional models may thus be fed back to the basin-to-global scale models. In this manner, projects like AZMP have the potential of influencing the utility of model results on larger scales.

During this past year, basin-scale operational ocean forecasting systems currently being run for the North Atlantic have advanced to include assimilation of both altimetry and in-situ profiles; previously only altimeter data were used. While altimetric sea-surface measurements provide a measure of the depth-integrated effect of density changes, it is impossible to accurately determine the vertical distribution of changes without in-situ information. The effect of assimilating in-situ data with altimetry is thus significant. Prior to assimilating in-situ data, errors of 3-4ºC occurred in the upper water column on the Newfoundland Shelf. With the inclusion of in-situ data in the assimilation scheme, the errors have been reduced by up to a factor of ten, i.e., to 0.3-0.4ºC; further improvements in both shelf and deep-ocean regions are anticipated as the

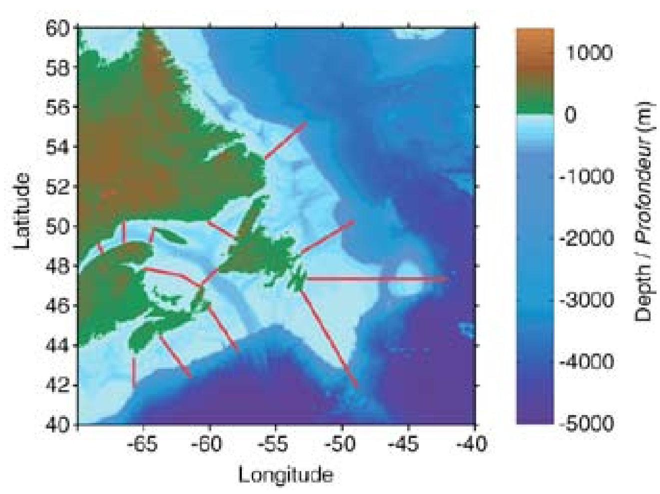

Fig. 4 AZMP standard survey transects for eastern Canada.

Transects standards du programme d'échantillonnage PZMA sur la côte est canadienne.

observations and assimilation methodologies are refined. Assimilation schemes for shelf waters are complicated by the presence of strong fronts coincident with abrupt topographic variations and degraded altimetry in the near-shore region (Mourre et al. 2004). It is clear that both higher-density observations and more sophisticated assimilation schemes will be required for the shelf regions. Again AZMP will be providing valuable data for fine tuning assimilation schemes for the shelf that are under development.

Conclusion

Clearly an expansion in Canadian operational oceanographic capacity will require increased input from AZMP and analogous programs. These data are essential to the development of an operational capacity and will become even more valuable as this system matures. There will be demands to have access to the data from AZMP surveys in near real time in order to ensure their use in short-term ocean forecasts for the regional and basin-scale forecasting systems. This will require further development from both the data acquisition and the modelling initiatives and will be possible only through intensive collaboration.

References

Crosnier, L., and Le Provost, C. 2006. Internal metrics definition for operational forecast systems inter-comparison: Example in the North Atlantic and Mediterranean Sea. *In* Ocean weather forecasting: an integrated view of oceanography. *Edited by* E. P. Chassignet and J. Verron, Elsevier, Springer, Berlin, pp. 455-465.

Le Fouest, V., Chifflet, M., Starr, M., Zakardjian, B., and Saucier, F. 2003. Toward prediction of the ecosystem: 3D simulations of the coupled biological production and hydrodynamics in the Estuary and Gulf of St. Lawrence. AZMP Bulletin PMZA 3: 37-41.

Mourre, B., De Mey, P., Lyard, F., and Le Provost, C. 2004. Assimilation of sea level data over continental shelves: an ensemble method for the exploration of model errors due to uncertainties in bathymetry. Dyn. Atmos. Oceans 38: 93-121.

Saucier, F.J., and Chassé, J. 2000. Tidal circulation and buoyancy effects in the St. Lawrence Estuary, Canada. Atmos.-Oceans 38(4): 1-52.

Saucier, F.J., Roy, F., Gilbert, D., Pellerin, P., and Ritchie, H. 2003. Modeling the formation and circulation processes of water masses and sea ice in the Gulf of St. Lawrence. J. Geophys. Res. 108: 3269-3289.

Liens entre la floraison printanière du phytoplancton et la croissance de la crevette nordique Pandalus borealis *: une première approche par télédétection spatiale*

César Fuentes-Yaco[1,2], Peter A. Koeller[1], Shubha Sathyendranath[1,2] et Trevor Platt[1]
[1] Institut d'Océanographie de Bedford, B.P. 1006, Dartmouth, NS, B2Y 4A2
[2] Department of Oceanography, Dalhousie University, Halifax, NS, B3H 4J1
Fuentes-YacoC@mar.dfo-mpo.gc.ca

Abstract

This work indicates a link between the latitudinal and temporal variations of the spring bloom of phytoplankton, as detected by satellite remote sensing of visible spectral reflectance (ocean colour), and the carapace length of the nordic shrimp *Pandalus borealis* on the Newfoundland and Labrador shelves. The variations in the spring bloom are determined by the use of ecological indicators such as the maximum chlorophyll *a* concentration, the time of occurrence of the bloom initiation and of the maximum (peak) chlorophyll *a* concentration, as well as by the duration of the spring bloom. We found significant correlations between the bloom intensity, the time of the occurrence of maximum phytoplankton concentration, and the size of the young shrimp for particular years. These results are discussed in the context of the observed decreasing trend in shrimp carapace length since the early 1990s for several stocks in the Northwest Atlantic (Fuentes-Yaco et al. 2006).

Introduction

La télédétection satellitaire utilisant la luminance spectrale visible (la couleur de l'océan) permet maintenant l'étude quantitative de la floraison printanière du phytoplancton dans la partie nord de l'océan Atlantique (Platt et al. 2003). Ce phénomène écologique est exceptionnel dans le contexte de l'océan mondial (Longhurst 1998). Toujours dans la même région, Koeller et al. (2006) ont observé, depuis le début des années 1990, une réduction significative de la taille et du taux de croissance des crevettes *Pandalus borealis* sur les plateaux de Terre-Neuve et du Labrador. Cette région est caractérisée par une relation positive, forte et persistante entre la taille de la carapace des crevettes et la latitude. Cette observation a été expliquée par l'âge plus avancé des crevettes récoltées dans la partie plus nordique de la zone étudiée (Shumway et al. 1985, Parsons et al. 1989, Nilssen et Hopkins 1991, Wieland 2004).

Dans le présent travail, nous utilisons la télédétection satellitaire pour étudier l'effet des variations de la disponibilité alimentaire, en l'occurrence du phytoplancton, sur la longueur de la carapace de *P. borealis* sur les plateaux de Terre-Neuve et du Labrador. L'information satellitaire provient du capteur *Sea-viewing Wide Field-of-view Sensor* (SeaWiFS) qui mesure la luminance spectrale visible des eaux superficielles (Fuentes-Yaco et al. 2005a). Cette mesure permet de dériver les concentrations en chlorophylle *a*, un indice de biomasse du phytoplancton. On sait que les larves de *P. borealis* consomment des quantités importantes de phytoplancton (Stickney et Perkins 1981, Pedersen et Storm 2002).

L'approche générale présentée dans cette étude a déjà été utilisée afin de trouver des relations entre le moment de l'initiation de la floraison printanière du phytoplancton tel que mesurée par télédétection, et le recrutement d'aiglefin

(*Melanogrammus aeglefinus*) (Platt et al. 2003). D'autres études ont également utilisé de telles mesures satellitaires pour étudier les crevettes (Lindner et Bailey 1968, Ramseier et al. 2000, Stein 2000). Cependant, nous croyons que le travail de Fuentes-Yaco et al. (2006) dont nous rapportons les principaux résultats ici représente la première tentative pour trouver des liens entre la floraison printanière du phytoplancton et la taille de la crevette nordique *Pandalus borealis*.

Matériel et méthodes

Les données de crevettes

Les données sur les crevettes pour cette étude proviennent d'échantillonnages réalisés au cours des missions de recherche multi-spécifiques en automne et des résultats de prises commerciales à différentes périodes de l'année. Les crevettes échantillonnées lors des missions de recherche proviennent surtout des zones situées au sud de la région A5 (Fig. 1). Par contre, les captures commerciales couvrent une région plus grande en latitude (A2 à A8). Les analyses statistiques sur les données de crevettes sont décrites en détail dans les travaux de Koeller et al. (2006) et Fuentes-Yaco et al. (2006).

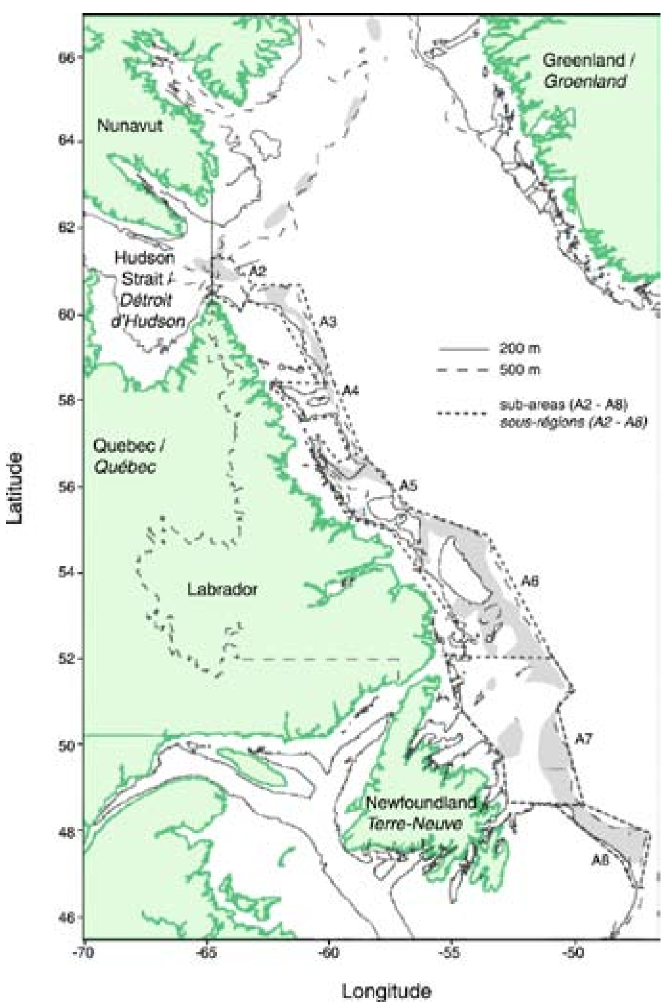

Fig. 1 Région d'étude et délimitation des régions de pêches à la crevette (en gris).

Study area and delineation of the main shrimp fishing areas (in grey).

Les indices écologiques de la floraison printanière du phytoplancton

Les indices écologiques de la floraison printanière du phytoplancton ont été dérivés en utilisant toutes données du capteur SeaWiFS qui étaient disponibles à l'Institut d'Océanographie de Bedford. L'algorithme OC4v4.3 de SeaDAS/NASA (O'Reilly et al. 2000) a alors été utilisé pour estimer les concentrations en chlorophylle *a* (Fuentes-Yaco et al. 2005b). Nous avons fait la moyenne de toutes les données valides couvrant le nord-ouest de l'océan Atlantique (39ºN à 62.5ºN et 42ºO à 71ºO) afin d'obtenir des images composites hebdomadaires avec une résolution spatiale de 1.5 km par pixel. Ces calculs ont été faits pour les mois de février à septembre pour chacune des années 1998 à 2003. Finalement, les images ont été lissées en calculant la médiane pour chaque 3 x 3 pixels, centrée sur le pixel concerné, afin de réduire les irrégularités.

La Figure 2 illustre les indices écologiques qui ont été utilisées pour caractériser la variabilité de la floraison de phytoplancton soit : i) l'intensité ou l'amplitude maximale de la concentration de chlorophylle *a*, ii) le moment d'initiation ou la semaine où la biomasse de phytoplancton excède pour la première fois le seuil de 20 % de l'amplitude maximale, iii) le moment dans le temps où l'amplitude maximale est atteinte et iv) la durée ou le temps où la biomasse demeure au dessus du seuil de 20 % (Platt et al. 2003). Tous ces indices ont été déterminés pour chacun des 1.5 million de pixels du domaine spatial d'intérêt sans compromettre la structure synoptique des données. L'analyse s'est répétée pour chaque année afin de construire une série temporelle et de montrer comment les caractéristiques de la floraison de phytoplancton varient entre les années 1998 et 2003. Ces résultats ont ensuite été comparés aux tailles mesurées des carapaces de crevettes pour chaque zone de pêche.

Résultats

Une première observation significative est que la floraison de phytoplancton débute plus tôt dans la partie sud de la zone étudiée. Cette floraison progresse ensuite graduellement vers le nord à mesure que la saison avance. La climatologie (moyenne pour les années 1998-2003) du temps de l'initiation de la floraison (Fig. 3a) et de l'occurrence de la concentration maximale du phytoplancton (Fig. 4a) illustrent bien cette

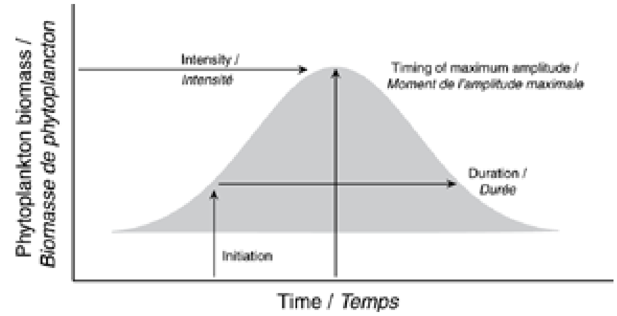

Fig. 2 Représentation graphique des indicateurs écologiques des floraisons de phytoplancton (voir le texte pour les explications).

Graphical representation of the ecological indicators of the phytoplankton blooms (see text for explanations).

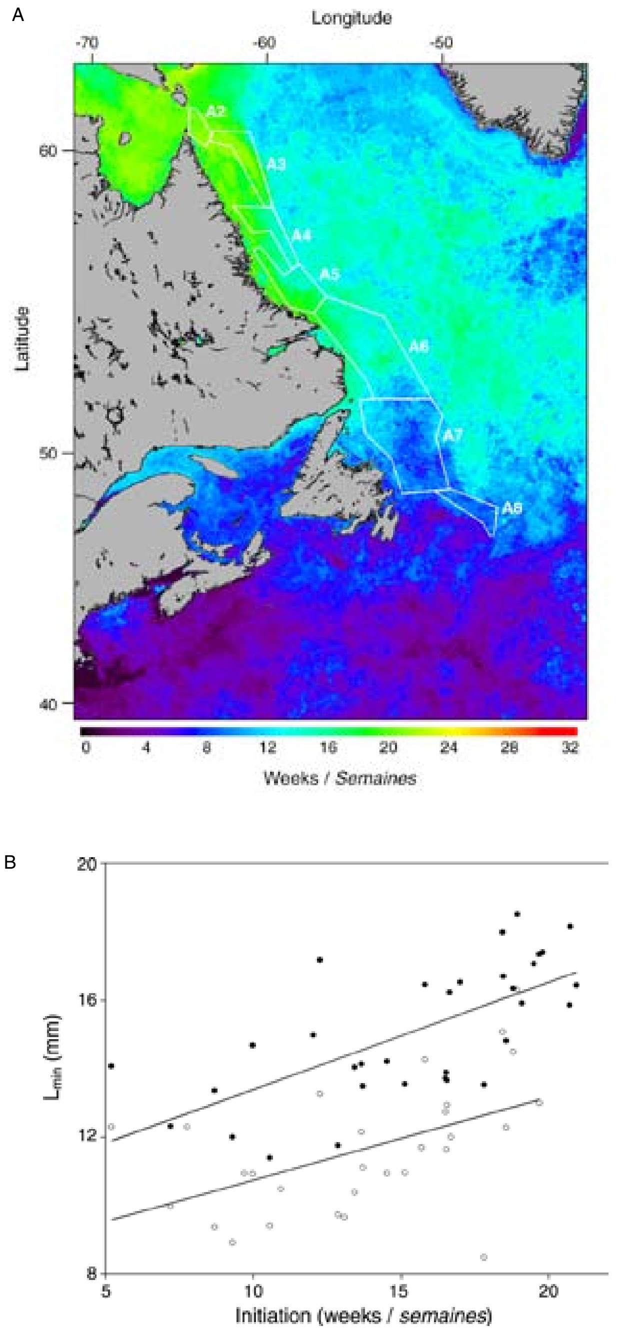

Fig. 3 a) Climatologie (moyenne entre 1998 et 2003) du moment de l'initiation de la floraison phytoplanctonique (nombre de semaines à partir du début février), selon la définition de la Figure 2. Les polygones représentent les régions de pêche à la crevette du nord (A2) vers le sud (A8); b) Relation entre le moment de l'initiation de la floraison du phytoplancton et la longueur moyenne des plus petites crevettes pour tous les échantillons par année et par région (L_{min}) pour les deux sources de données, de pêches commerciales (•) et de recherches scientifiques (○). Les lignes représentent des régressions linéaires (p<0.001).

a) Climatology (average from 1998 to 2003) of the time of initiation of the phytoplankton bloom (number of weeks from the beginning of February), as defined in Figure 2. The polygons represent shrimp fishing areas from north (A2) to south (A8); b) Relationship between the time of initiation of the phytoplankton bloom and the average length of the smallest shrimp for all samples per year and area (L_{min}) for both commercial (•) and research survey (○) data. The lines represent linear regressions (p<0.001).

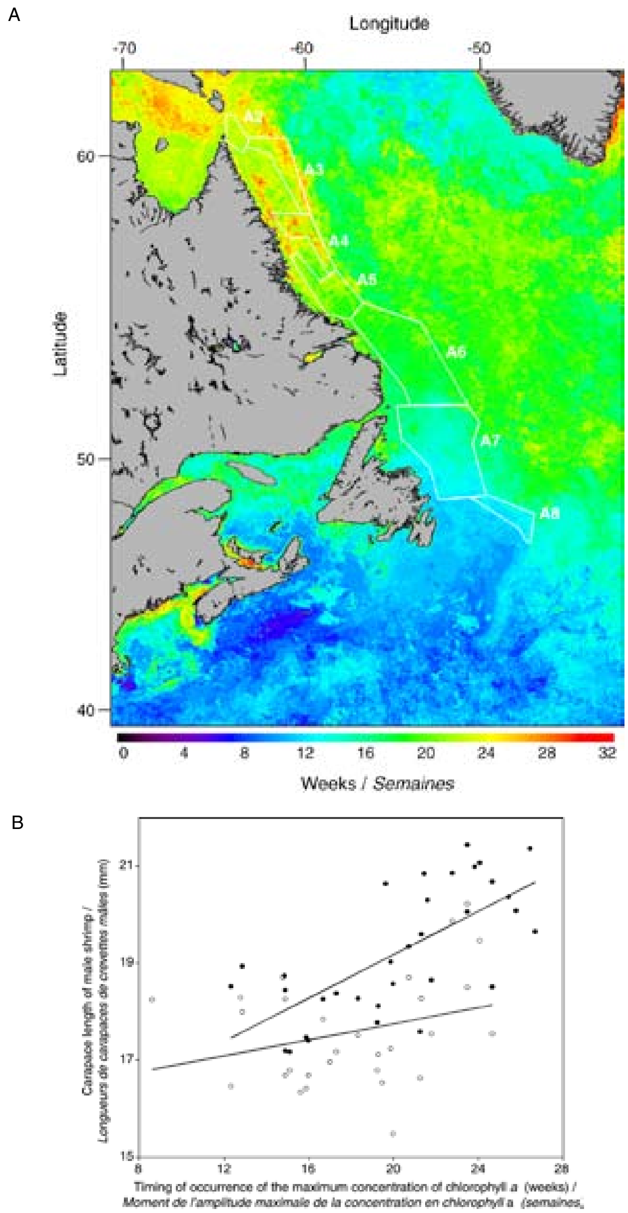

Fig. 4 a) Climatologie (moyenne entre 1998 et 2003) du moment de l'amplitude maximale de la concentration en chlorophylle *a* (en nombre de semaines à partir du début février), selon la définition de la Figure 2. Les polygones représentent les régions de pêche à la crevette du nord (A2) vers le sud (A8) ; b) Relation entre le moment de l'amplitude maximale de la concentration en chlorophylle *a* et les longueurs de carapaces de crevettes mâles pour les deux sources de données de pêches commerciales (•) et de recherches scientifiques (○). La longueur moyenne des carapaces pour les crevettes provenant des pêches commerciales = 19.2 mm et celles provenant des missions de recherche scientifique = 17.6 mm. Les lignes représentent des régressions linéaires (pêches commerciales, p<0.01).

a) Climatology (average from 1998 to 2003) of the time of occurrence of the maximum concentration of chlorophyll a *(in number of weeks from the beginning of February) as defined in Figure 2. The polygons represent shrimp fishing areas from north (A2) to south (A8); b) Relationship between the time of the occurrence of the maximum bloom intensity and the carapace length of male shrimp for all samples per year and area for both commercial (•) and research survey (○) data. The average carapace length is 19.2 mm for commercial fisheries and 17.6 mm for scientific surveys. Lines represent linear regressions (commercial fisheries,* p*<0.01).*

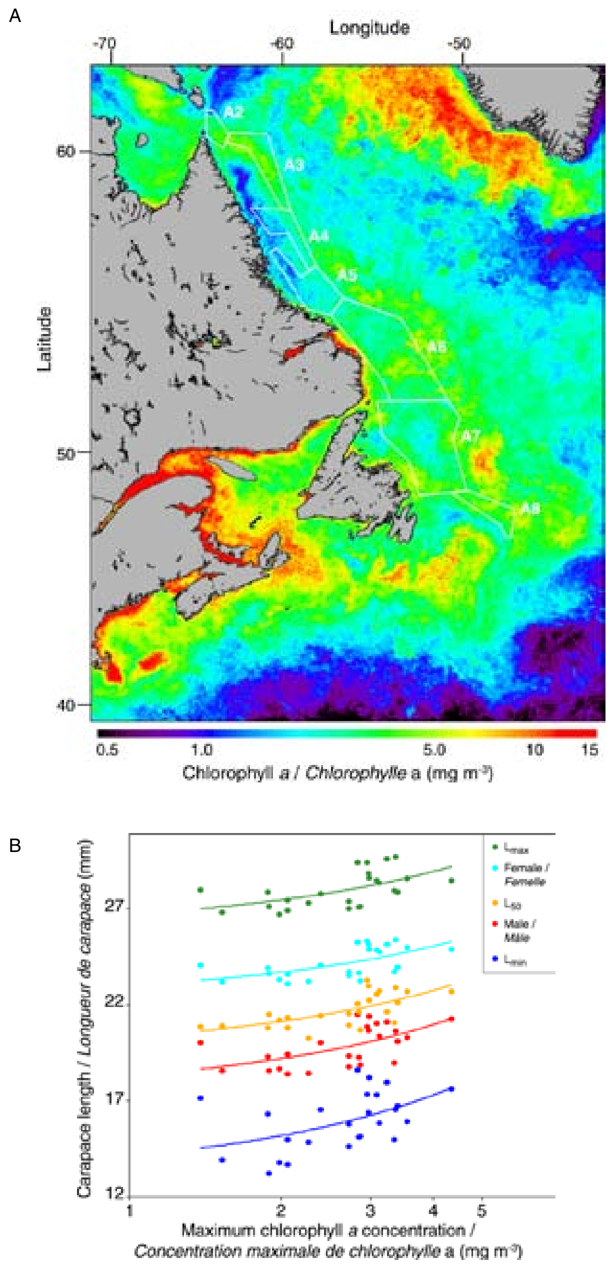

Fig. 5 a) Climatologie (moyenne entre 1998 et 2003) de la concentration maximale de chlorophylle *a* (mg m^{-3}). Les polygones représentent les régions de pêche à la crevette du nord (A2) vers le sud (A8) ; b) Relation entre la concentration maximale de chlorophylle *a* et la longueur des carapaces de crevettes pour L_{min} (moyenne des plus petites crevettes : en bleu foncé), les crevettes mâles (en rouge), L_{50} (la taille à laquelle la moitié des individus dans un échantillon étaient des femelles : en orange), les crevettes femelles (en bleu pâle) et L_{max} (moyenne de longueur des plus grandes crevettes de tous les échantillons, par année et par zone de pêche : en vert). Les lignes représentent des régressions linéaires (p<0.001).

a) Climatology (average from 1998 to 2003) of maximum chlorophyll a *concentration (mg m^{-3}). The polygons represent shrimp fishing areas from north (A2) to south (A8); b) Relationship between the chlorophyll* a *maximum and the carapace length for L_{min} (average of smaller shrimp: in dark blue), male shrimp (in red), L_{50} (the size at which half of the individuals in the sample were females: in orange), female shrimp (in light blue), and L_{max} (the average of the largest shrimp for all samples per year and area: in green). The lines represent linear regressions (*p*<*0.001).*

évolution. Les Figures 3b et 4b montrent les relations qui existent entre L_{min} (moyenne de la longueur des plus petites crevettes des échantillons, par année et par zone de pêche) et le temps de l'initiation de la floraison, ainsi qu'entre la longueur des carapaces des crevettes mâles et le temps où se produit la concentration maximale de chlorophylle *a*. L'intensité de la floraison suggère une distribution bimodale avec des valeurs fortes dans les zones de pêche au nord et au sud, et des valeurs relativement faibles dans les zones intermédiaires, A4 et A5 (Fig. 5a). Ces fortes valeurs de biomasses phytoplanctoniques au nord du plateau de Terre-Neuve sont bien connues. Elles sont attribuées aux processus de mélange locaux et à l'apport de nutriments par le détroit d'Hudson (Drinkwater et Harding 2001). Il est important de souligner qu'il existe une étroite correspondance (p<0.001) entre la longueur de la carapace des crevettes et l'intensité de la floraison (Fig. 5b).

Nous avons par ailleurs remarqué une corrélation négative entre la taille de la carapace des crevettes mâles et le moment d'occurrence de la concentration maximale de phytoplancton dans la région A6 (Fig. 1). Cette zone de pêche est la plus échantillonnée, représentant 60 % des spécimens commerciaux et 36 % des échantillons de recherche récoltés. La Figure 6a montre les anomalies par rapport à la climatologie (moyenne de toutes les années) du moment d'occurrence de la concentration maximale de phytoplancton pour la région A6. Les anomalies sont en général positives (initiation tardive) pour les années 2000 à 2002 et négatives (initiation avancée) pour 1998-99 et 2003. La Figure 6b illustre les relations négatives (p<0.01) entre le moment d'occurrence du maximum de biomasse phytoplanctonique et la longueur de la carapace des crevettes mâles. En fait, les longueurs des carapaces à l'âge de 1 et 2 ans montrées dans Koeller et al. (2006) suggèrent aussi un effet analogue entre le moment de l'initiation avancée ou tardive de la floraison printanière de phytoplancton et la croissance des crevettes. Ce patron d'anomalies est présent dans l'étude réalisée par Platt et al. (2003) avec le recrutement des larves d'aiglefin (*Melanogrammus aeglefinus*) sur le plateau Néo-Écossais. Cette étude témoigne de l'importance écologique du temps de l'initiation de la floraison printanière du phytoplancton. En somme, une floraison algale précoce peut encourager une croissance précoce des animaux, en comparaison avec les années où la floraison survient plus tard.

Discussion

Dans ce travail nous explorons les liens entre les variations de la disponibilité de nourriture (chlorophylle *a* / phytoplancton détecté par satellite) et la croissance de la crevette *Pandalus borealis* sur les plateaux de Terre-Neuve et du Labrador. De prime abord, nous voudrions faire une mise en garde parce que nous considérons que nos données ont des limitations spatiales et temporelles importantes. Nos interprétations et conclusions doivent donc être utilisées avec prudence. Dans un premier temps, l'abondance des données de crevettes pour les régions situées au nord est restreinte. De plus, les données de couleur de l'eau n'existent pas pour les années antérieures à 1998, lorsque les plus fortes diminutions en taille des crevettes ont été observées (Koeller et al. 2006). Par ailleurs, l'incertitude associée à la détermination de l'âge des plus grosses crevettes est telle que l'on ne peut pas attribuer facilement les variations de taille à une croissance rapide

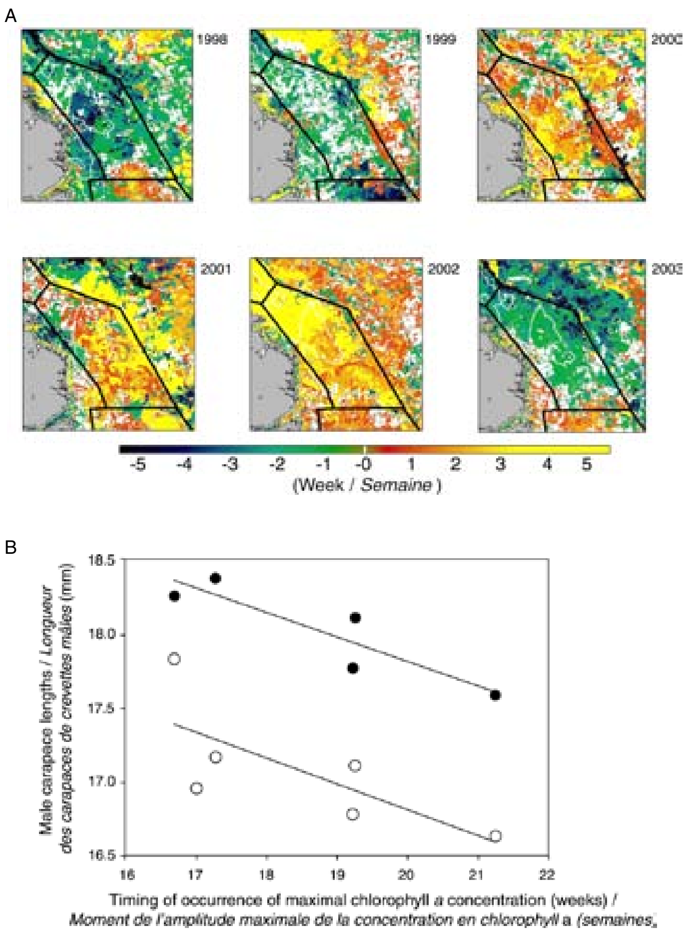

Fig. 6 a) Anomalies (année sous considération – climatologie) du temps pour atteindre la concentration maximale de chlorophylle *a* (en semaines) dans la zone A6 pour la période d'étude. Une valeur négative ou positive indique respectivement un moment d'occurrence plus tôt ou plus tard que la climatologie; b) Relation entre le moment de l'amplitude maximale de la concentration en chlorophylle *a* et la longueur des carapaces de crevettes mâles dans la région A6 pour les deux sources de données, de pêches commerciales (●) et de recherches scientifiques (○); (p<0.01).

a) Anomalies (year considered – climatology) of the timing of occurrence of the maximum chlorophyll a *concentration (in weeks) in region A6 for the study period. Negative and positive values indicate bloom periods earlier or later than the climatology, respectively; b) Relationship between the time of occurrence of the maximal chlorophyll* a *concentration and male carapace lengths in region A6 for both commercial (●) and research survey (○) data; (*p*<0.01).*

ou à une croissance lente associée à une longévité augmentée. Par conséquent, nos conclusions pourraient avoir des explications contradictoires, tout dépendant de l'hypothèse invoquée. Cependant, ces problèmes sont au delà des objectifs de ce travail mais ils pourraient être résolus avec : i) un échantillonnage plus important, ii) des mesures en continu de la luminance spectrale visible, iii) des méthodes plus précises pour la détermination de l'âge des crevettes, ainsi iv) qu'avec l'élaboration de bons modèles de croissance des crevettes.

Notre première hypothèse postule que l'augmentation de la longueur des carapaces de crevettes avec la latitude est attribuable à une longévité plus grande des crevettes dans les eaux froides (Parsons et al. 1989). Toutefois, ces auteurs soulignent que quelques observations dans la région de Terre-Neuve et Labrador ne soutiennent pas cette hypothèse. Aussi, les travaux de Colbourne et Mertz (1998) et Koeller et al. (2006) ont montré que pour des températures similaires sur le plateau où les crevettes passent la plus grande partie de leur vie, la température a probablement une influence mineure sur la variabilité de la croissance de la crevette. Il peut alors être postulé que la croissance des crevettes est plus lente dans la région nord de notre zone d'étude parce qu'il y a moins de nourriture dans cette partie de l'océan. Cette idée est compatible avec nos résultats puis qu'ils indiquent que la floraison du phytoplancton et l'éclosion des oeufs coïncident seulement dans la partie sud de notre zone d'étude, et que cette éclosion précède le moment d'apparition du maximum de concentration de chlorophylle *a* par presque trois mois au nord (Fuentes-Yaco et al. 2006). Selon cette hypothèse, les plus petites crevettes (L_{min}) capturées par les filets de pêche (prises de recherche et commerciales) dans ces régions nordiques ont une taille plus grande parce que les larves pélagiques et les stades juvéniles benthiques sont plus vieux quand ils sont attrapés (Koeller et al. 2006). Les crevettes juvéniles seraient donc trop petites quand elles descendent au fond pour être retenues par les filets, et seraient capturées un an plus tard, quand elles sont plus grandes. Cette hypothèse nous amène à conclure que le manque de nourriture limite la taille des organismes dans la région nord de la zone d'étude.

Notre seconde hypothèse propose que la crevette pourrait croître plus rapidement dans les eaux plus productives du nord. Les fortes relations positives entre l'intensité de la floraison de phytoplancton et la taille des carapaces dans les échantillons de pêche commerciale soutiennent cette idée. Selon cette hypothèse, les larves pélagiques de crevette dans la région nordique peuvent survivre pendant plusieurs mois avant le début de la floraison et lors de très fortes floraisons de phytoplancton, elles vont croître beaucoup plus rapidement qu'au sud et descendre au fond ayant atteint le stade juvénile. Ces larves qui seraient attrapées par les filets auraient ainsi le même âge que celles d'autres régions qui n'ont toutefois pas atteint le stade juvénile ou une plus grande taille en raison de la limitation en nourriture. Cette hypothèse n'explique cependant pas la petite taille des crevettes dans les régions situées au sud, qui ont eu l'avantage d'une éclosion coïncidant avec des floraisons de phytoplancton d'une intensité comparable à celles de la région nord.

D'autres facteurs ont aussi une influence certaine sur ces scénarios. Par exemple, dans les analyses spatiales, les moments de l'initiation et de l'occurrence de l'amplitude maximale de la floraison du phytoplancton ont des fortes corrélations positives avec la longueur des carapaces de crevettes. Par contre, il y a une corrélation temporelle négative entre ces mêmes paramètres. Selon la deuxième hypothèse, cela pourrait se produire si les grandes tailles (et âge) des crevettes du nord étaient déterminées génétiquement. Il est possible que les populations de *P. borealis* aient développé des taux de croissance plus rapides pour atteindre des tailles plus grandes avant le premier hiver, tel que démontré pour plusieurs espèces de poissons et d'invertébrés (voir Conover et al. 2005 et les références inclues). Nous attendons le développement de modèles de croissance plus précis des Pandalidés afin de trouver des réponses définitives à ces questions. Aussi, les relations fonctionnelles à la base des corrélations montrées ici entre les données satellitaires de phytoplancton et la taille des crevettes ne pourront être éclaircies que lorsque l'on comprendra mieux l'influence de la nutrition (e.g., phytoplancton, détritus, copépodes) sur les différentes phases de développement des crevettes en milieu océanique.

En conclusion, la démonstration de liens significatifs entre la floraison printanière du phytoplancton et la taille de la crevette *P. borealis* nous permet de formuler deux hypothèses vraisemblables sur les causes de la distribution régionale et temporelle de la taille des crevettes. Bien que nous n'apportions pas de conclusions définitives, en raison de la limitation imposée par les données que nous possédons présentement, nous avons tout de même pu démontrer que les variations à grande échelle et à long terme de la répartition du phytoplancton peuvent être mesurées et que l'impact de ces variations sur les espèces marines d'importance commerciale peut être testé.

Les recherches futures devraient nous emmener à considérer les processus de recrutement des crevettes, entre autre le rôle de l'advection des larves vers le sud, ainsi que l'importance de la glace dans le développement des floraisons phytoplanctoniques. Enfin, malgré les limitations importantes du présent ensemble de données, les résultats présentés (voir Koeller et al. 2006 et Fuentes-Yaco et al. 2006 pour plus de détails) sont importants pour l'industrie de la crevette puisqu'ils démontrent que les variations environnementales ont eu une influence significative sur la diminution de la taille des crevettes dans les années 1990. Il semble par ailleurs qu'une capture moins intensive n'aurait pas affecté les tendances observées. Pour la recherche scientifique sur la pêche à la crevette, les données satellitaires pourraient donc occuper une place importance entre autre, afin de faciliter l'étude de la dynamique des populations de crevettes dans certains milieux moins accessibles comme par exemple la baie d'Hudson.

Remerciements

L'utilisation des données SeaWiFS pour la recherche scientifique est une courtoisie de la NASA. Nous remercions les employés du Pêches et Océans Canada ainsi que le groupe d'observateurs sur les pêches commerciales qui ont participé à la récolte des échantillons de crevettes sur les missions de recherche et les sorties commerciales. Nous remercions également Steve Smith et Dave Orr pour leurs commentaires sur le travail, et Linda Payzant, Heidi Maass et George White III pour leur aide dans l'analyse des images satellitaires. Marie-Hélène Forget et Emmanuel Devred ont participé à la correction de ce document. Ce travail a été financé par l'Agence Spatiale Canadienne (programme GRIP).

References

Colbourne, E.B., et Mertz, G. 1998. Spatial and temporal variability of ocean temperature over the Labrador Shelf. Atmos.-Ocean 36(4): 299-317.

Conover, D.O., Arnott, S.A., Walsh M.R., et Munch, S.B. 2005. Darwinian fishery science: lessons from the Atlantic silverside (*Menidia menidia*). Can. J. Fish. Aquat. Sci. 62: 730-737.

Drinkwater, K.F., et Harding, G.C. 2001. Effects of the Hudson Strait outflow on the biology of the Labrador Shelf. Can. J. Fish. Aquat. Sci. 58: 171-184.

Fuentes-Yaco, C., Devred, E., Platt, T., Sathyendranath, S., Forget, M.E., et Son, S.H. 2005a. Principes physiques et interprétation de la réflectance spectrale marine (la couleur de l'océan) : applications aux données satellitaires. Physics in Canada 61(5): 215-226.

Fuentes-Yaco, C., Devred, E., Sathyendranath, S., Platt, T., Payzant, L., Caverhill, C., Porter, C., Maass, H., et White, J.G. III. 2005b. Comparison of in situ and remotely-sensed (SeaWiFS) chlorophyll-a in the Northwest Atlantic. Indian J. Mar. Sci. 34(4): 341-355.

Fuentes-Yaco, C., Koeller, P., Sathyendranath, S., et Platt, T. 2006. Shrimp (*Pandalus borealis*) growth and timing of the spring phytoplankton bloom on the Newfoundland-Labrador Shelf. Fish. Oceanogr. (sous presse).

Koeller, P., Fuentes-Yaco, C., et Platt, T. 2006. Decreasing shrimp sizes off Newfoundland and Labrador – environment or fishing? Fish. Oceanogr. (sous presse)

Lindner, M.J., et Bailey, J.S. 1968. Distribution of brown shrimp (*Penaeus aztecus aztecus* Ives) as related to turbid water photographed from space. Fish. Bull. 72(2): 289-293.

Longhurst, A. 1998. Ecological geography of the sea. Academic Press, San Diego.

Nilssen, E.M., et Hopkins, C.C.E. 1991. Population parameters and life histories of the deep-water prawn *Pandalus borealis* from different regions. ICES CM, 1991/K:2.

O'Reilly, J.E., Maritorena, S., Siegel, D., O'Brien, M.C., Toole, D., Mitchell, B.G., Kahru, M., Chavez, F.P., Strutton, P., Cota, G., Hooker, S.B., McClain, C.R., Carder, K.L., Muller-Karger, F., Harding, L., Magnuson, A., Phinney, D., Moore, G.F., Aiken, J., Arrigo, K.R., Letelier, R., et Culver, M. 2000. Ocean color chlorophyll *a* algorithms for SeaWiFS, OC2 and OC4: version 4. *In* SeaWiFS Technical Report Series. *Edited by* Hooker, S.B., and Firestone, E.R NASA Tech. Memo. 2000-206892, 11(3), pp. 8-22.

Parsons, D.G., Mercer, V.L., et Veitch, P.J. 1989. A comparison of the growth of northern shrimp (*Pandalus borealis*) from four regions of the Northwest Atlantic. J. Northw. Atl. Fish. Sci. 9: 123-131.

Pedersen, S.A., et Storm, L. 2002. Northern shrimp (*Pandalus borealis*) recruitment in West Greenland waters. Part II. Lipid classes and fatty acids in *Pandalus* shrimp larvae: implications for survival expectations and trophic relationships. J. Northw. Atl. Fish. Sci. 30: 47-60.

Platt, T., Fuentes-Yaco, C., et Frank, K.T. 2003. Spring algal bloom and larval fish survival. Nature 423: 398-399.

Ramseier, R.O., Garrity, C., Parsons, D.G., et Koeller, P. 2000. Influence of particulate organic carbon sedimentation within the seasonal sea-ice regime on the catch distribution of the northern shrimp (*Pandalus borealis*). J. Northw. Atl. Fish. Sci. 27: 35-44.

Shumway, S.E., Perkins, H.C., Schick, D.F., et Stickney, A.P. 1985. Synopsis of biological data on the pink shrimp, *Pandalus borealis* Krøyer, 1838. NOAA Technical Report NMFS 30, FAO Fisheries Synopsis 144.

Stein, M. 2000. Hydrographic and atmospheric conditions off East Greenland – their potential effect on the distribution of shrimp (*Pandalus borealis*). J. Northw. Atl. Fish. Sci. 27: 63-67.

Stickney, A.P., et Perkins, H.C. 1981. Observations on the food of the larvae of the northern shrimp, *Pandalus borealis* Krøyer (Decapoda, Caridea). Crustaceana 40(1): 36-49.

Wieland, K. 2004. Length at sex transition in northern shrimp (*Pandalus borealis*) off West Greenland in relation to changes in temperature and stock size. Fish. Res. 69: 49-56.

Activities of the Remote Sensing Laboratory at the Maurice Lamontagne Institute

Les activités du laboratoire de télédétection à l'Institut Maurice-Lamontagne

Pierre Larouche
Institut Maurice-Lamontagne, P. O. Box 1000, Mont-Joli, QC, G5H 3Z4
LaroucheP@dfo-mpo.gc.ca

Abstract

This article describes research projects and operational activities of the remote sensing laboratory at the Maurice Lamontagne Institute (DFO-Québec Region) since its beginning in 1988.

A Brief Historical Summary

The remote sensing laboratory of the Maurice Lamontagne Institute (IML), Department of Fisheries and Oceans, began its activities in 1988 by conducting various research projects using (1) satellite radar images to measure coastal currents (Larouche 1996) and detect ice ridges (Hudier and Larouche 2005), and (2) Landsat images to determine surface currents using drifting ice floes as tracers (Larouche and Dubois 1990). Starting in 1994, the activities of the IML remote sensing laboratory became operational with the installation of a receiving station on top of the Maurice Lamontagne Institute in Mont-Joli (Québec), which provided direct access to weather satellite data from NOAA (National Oceanic and Atmospheric Administration). In 1998, a second receiving station was installed in Resolute Bay (Northwest Territories) at the Arctic Weather Centre of Environment Canada. Direct access to these data fostered important developments, and IML's remote sensing laboratory has since engaged in several activities supporting DFO's operational needs as well as those of other departments (e.g., Natural Resources Canada, Environment Canada). The IML remote sensing laboratory also supports several research projects from DFO and university scientists. Today, one of its main clients is the Atlantic Zone Monitoring Program.

Operational Activities

The main operational activities of the laboratory are the reception, archiving and processing of the NOAA data to generate a set of products available through the St. Lawrence Observatory web portal (www.osl.gc.ca). Besides managing two receiving stations, the remote sensing laboratory also receives and processes the data acquired by an antenna located at the Institute of Ocean Sciences, on the Pacific coast. These three receiving stations allow a complete coverage of the Canadian territory, including Atlantic, Pacific and Arctic waters under

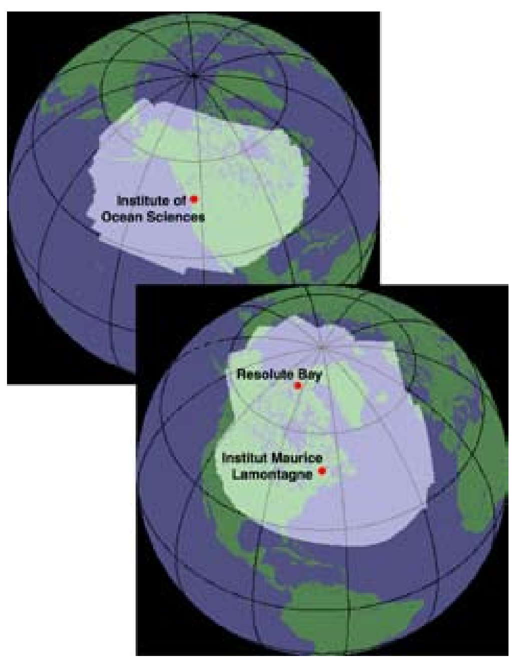

Fig. 1 Couverture géographique des images acquises par les trois stations de réceptions.

Geographical coverage of images acquired by the three receiving stations.

Sommaire

Cet article décrit les projets de recherche et les activités opérationnelles du laboratoire de télédétection de l'Institut Maurice-Lamontagne (MPO-région du Québec) depuis ses débuts en 1988.

Un bref historique

Le laboratoire de télédétection de l'Institut Maurice-Lamontagne (IML), Pêches et Océans Canada, a débuté ses activités en 1988 en menant divers projets de recherche qui utilisaient (1) les images satellitaires radar pour la mesure des courants côtiers (Larouche 1996) et pour détecter les crêtes de pression dans les champs de glace (Hudier et Larouche 2005), et (2) les images Landsat pour déterminer la vitesse des courants en utilisant la dérive des glaces comme traceur (Larouche et Dubois 1990). À partir de 1994, les activités du laboratoire de télédétection sont devenues opérationnelles avec l'installation d'une station de réception sur le toit de l'IML, à Mont-Joli (Québec), permettant l'accès direct aux données des satellites météorologiques NOAA (National Oceanic and Atmospheric Administration). En 1998, une seconde station a été installée à Resolute Bay (Territoires du Nord-Ouest) au Centre Météorologique Arctique d'Environnement Canada. L'accès direct à ces données a permis des développements importants et le laboratoire de télédétection de l'IML est depuis engagé dans diverses activités qui supportent les besoins opérationnels du MPO et de d'autres ministères (ex., Ressources Naturelles Canada, Environnement Canada). Le laboratoire de télédétection de l'IML supporte également plusieurs projets de recherche de scientifiques du MPO et du milieu universitaire. Aujourd'hui, l'un des principaux clients est le Programme de Monitorage de la Zone Atlantique.

Activités opérationnelles

Les principales activités opérationnelles du laboratoire de télédétection sont la réception, l'archivage et le traitement des données NOAA afin de générer un ensemble de produits rendus disponibles via l'Observatoire du Saint-Laurent (www.osl.gc.ca). En plus des deux stations qu'il gère, le laboratoire de télédétection reçoit et traite des images captées par une antenne localisée à l'Institut des Sciences de la Mer sur la

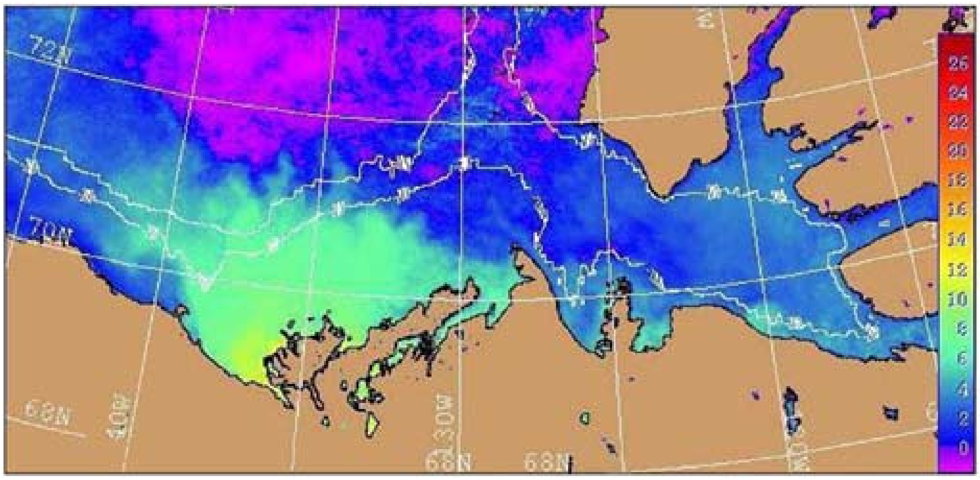

Fig. 2 Carte des températures de surface moyennes dans la mer de Beaufort pour la période du 16 au 31 août 2004 (192 passes incluses). L'extension du panache du fleuve Mackenzie est clairement visible en milieu côtier.

Composite sea-surface temperature map of the Beaufort Sea between August 16 and 31, 2004 (192 passes). The Mackenzie River plume extension is clearly visible in the coastal region.

Canadian jurisdiction (Fig. 1) and large freshwater lakes such as Lake Winnipeg and the Great Lakes (images available in 2006). Image processing is done automatically using a production system based on the TeraScan software. The laboratory has recently improved the system by developing a new acquisition interface totally based on Linux and allowing greater operational flexibility, particularly for the Resolute Bay station.

Maps of sea-surface temperature (SST), generated for each pass of a NOAA satellite, are the main products of the image processing system. The data are then processed into smaller regional maps to allow greater accessibility for local users. As clouds often obscure the sea surface, composite maps of

côte du Pacifique. Ces trois stations de réception permettent une couverture complète du territoire canadien, incluant les eaux Atlantiques, Pacifiques et Arctiques sous juridiction canadienne (Fig. 1) et les grandes surfaces d'eau douce tels que le lac Winnipeg et les Grands Lacs (images disponibles en 2006). Actuellement, le traitement des images s'effectue de façon automatique à l'aide d'un système de production basé sur le logiciel TeraScan. Le laboratoire a récemment amélioré ce système en développant une interface d'acquisition entièrement basée sur Linux qui permet une plus grande flexibilité opérationnelle, particulièrement pour la station de Resolute Bay.

Des cartes de température de surface de la mer (TSM), générées pour chaque passe d'un satellite NOAA, sont le principal produit du système de traitement d'images. Les données sont subdivisées en cartes régionales afin de faciliter l'accessibilité pour les utilisateurs locaux. Comme les nuages préviennent souvent l'observation de la surface de la mer, des images composites de moyennes hebdomadaires et semi-mensuelles sont aussi générées pour chaque zone (Fig. 2). Tous les produits numériques conservent la pleine résolution du capteur, i.e., environ 1 km. Des images JPG à résolution réduite sont aussi produites pour faciliter l'accès via le réseau internet. Les images à pleine résolution sont disponibles via un site FTP dans un format HDF.

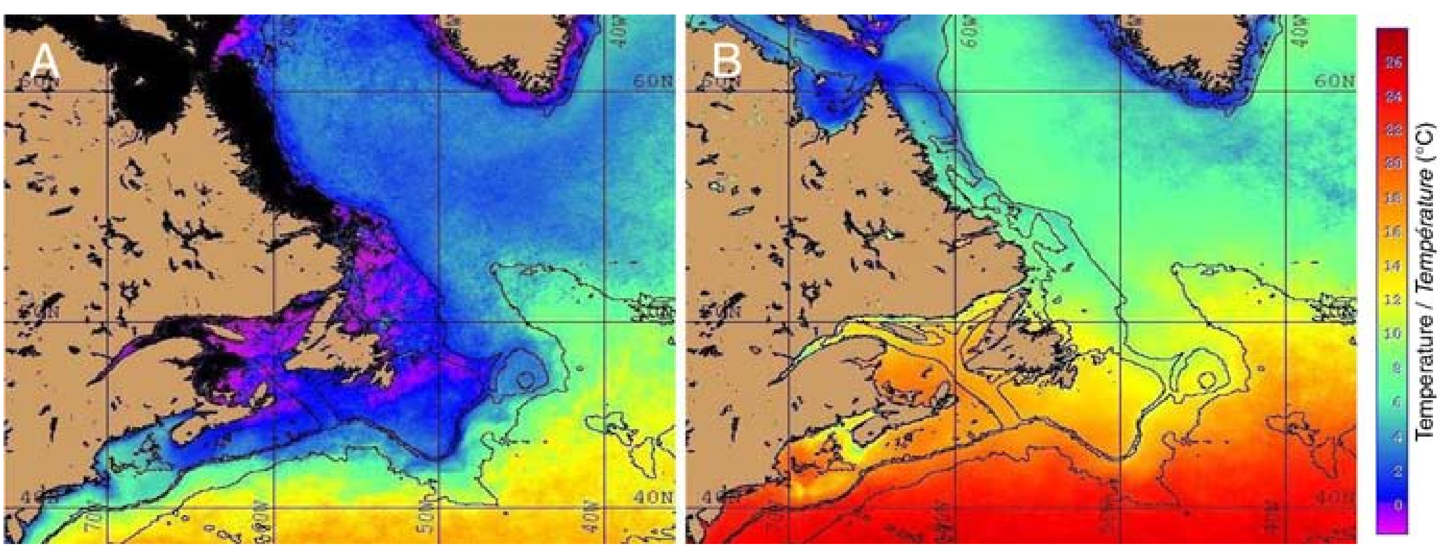

Fig. 3 Moyenne climatologique (1995-2004) de la température de surface pour la côte Atlantique montrant les deux extrêmes dans le cycle saisonnier annuel : A) 1 au 15 février et B) 1 au 15 août. Les pixels noirs représentent de la glace ou des nuages.

Climatological (1995-2004) mean sea-surface temperature for the Atlantic coast showing the two extremes in the yearly seasonal cycle: A) 1 to 15 February and B) 1 to 15 August. Black pixels represent either ice or clouds.

weekly and twice-monthly images are also generated for each zone (Fig. 2). All data products are available at the full sensor resolution, i.e., approximately 1 km. Lower resolution JPG images are also produced to allow easier access through the internet. The full resolution images are available through an FTP site in the HDF format.

Another important operational activity of the remote sensing laboratory was the participation in the international network of SeaWiFS data reception stations from September 1997 until December 2004, when free access to the high resolution data was terminated. The Resolute Bay station contributed significantly to the complete coverage of the Arctic Ocean by that satellite, providing more than 4000 images to the SeaWiFS project.

Operational projects of the remote sensing laboratory are not only limited to image processing. Over the years, the laboratory has also developed a system to validate the SST products for the Atlantic Zone. This system is based on a network of thermographs installed on navigational buoys and on fully instrumented oceanographic buoys that measure several atmospheric and oceanic variables, including radiance measurements (Larouche and Pettigrew 2003). The laboratory also produced a 10-year climatology (1995-2004) for the entire Atlantic Zone, resolving the annual cycle of sea-surface temperature at 7-day and twice-monthly intervals (Fig. 3). One specific project aims at using this climatology routinely to filter outliers from the remotely sensed data and at generating anomaly maps that will be made available through the St. Lawrence Observatory website. Another project aims at developing a 20-year database of full-resolution (1 km) satellite images using the data archives of the Canadian Centre for Remote Sensing (NRCan).

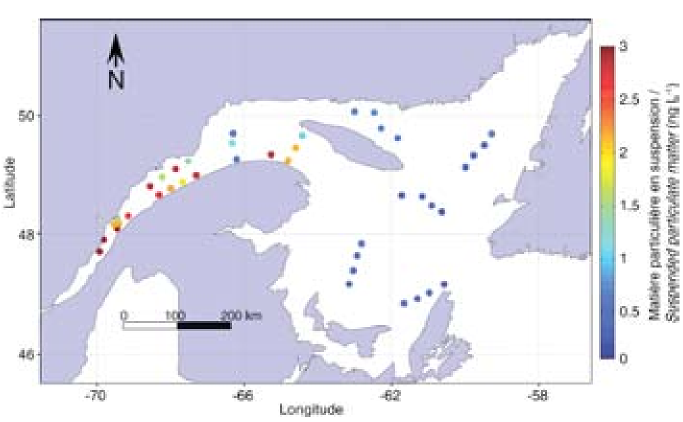

Fig. 4 Matière particulaire en suspension dans la couche de surface du golfe du Saint-Laurent en mai 2000.

Suspended particulate matter in the surface layer of the Gulf of St. Lawrence in May 2000.

Scientific Activities

The remote sensing laboratory has also been involved in several research programs and projects throughout the years. The most important program is certainly the study of the optical properties of the surface waters in the Gulf of St. Lawrence, with the objective of improving the algorithms that are used

Une autre activité opérationnelle importante du laboratoire de télédétection a été la participation au réseau international de stations de réception d'images du satellite SeaWiFS entre septembre 1997 et décembre 2004, date à laquelle l'accès gratuit aux données haute résolution de ce satellite s'est terminé. La station de Resolute Bay a ainsi contribué significativement à la couverture complète de l'océan Arctique par ce satellite en fournissant plus de 4000 images pour le projet SeaWiFS.

Les projets opérationnels du laboratoire de télédétection ne se limitent pas qu'au traitement d'images. Au fil des ans, le laboratoire a aussi développé un système permettant de valider les données de TSM pour la zone Atlantique. Ce système est basé sur un réseau de thermographes installés sur des bouées de navigation et sur des bouées océanographiques qui mesurent plusieurs variables océaniques et atmosphériques, incluant des mesures de luminances (Larouche et Pettigrew 2003). Le laboratoire a également calculé une climatologie portant sur une période de 10 années (1995-2004) pour l'ensemble de la zone atlantique qui permet de visualiser le cycle annuel de la température de surface aux échelles hebdomadaires et semi-mensuelles (Fig. 3). Un projet spécifique vise l'utilisation routinière de cette climatologie afin d'éliminer les données aberrantes parfois observées sur les images satellitaires et de générer des cartes d'anomalies qui seront aussi rendues disponibles via l'Observatoire du Saint-Laurent. Un autre projet vise l'extension à 20 ans de la base de données d'images à pleine résolution (1 km) en utilisant les données archivées du Centre Canadien de Télédétection (RNCan).

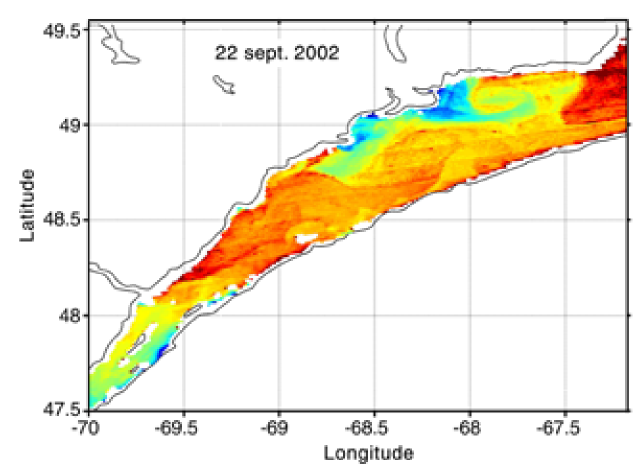

Fig. 5 Patron de salinité de la couche de surface de l'estuaire du Saint-Laurent générée à partir de la signature optique des matières organiques dissoutes. La couleur bleue représente les eaux plus douces.

Sea-surface salinity pattern in the St. Lawrence estuary generated using the coloured dissolved organic matter optical signature. Blue colour indicates fresher waters.

Activités scientifiques

Le laboratoire de télédétection a aussi été impliqué dans plusieurs programmes et projets de recherche au fil des ans. Le plus important est certainement l'étude des propriétés optiques des eaux de surface du golfe du Saint-Laurent, dans le but d'améliorer les algorithmes qui sont utilisés pour interpréter les images satellites de couleur de la mer dans les eaux côtières fortement influencées par les débits d'eau douce.

to interpret satellite ocean colour images in coastal waters strongly influenced by freshwater runoffs. These improved algorithms are needed to reveal the influence of various environmental factors on the reflectance signal seen by the satellite sensors and, therefore, to generate better estimations of phytoplankton biomass or production in coastal ecosystems. This research program was carried out jointly with three Canadian universities (UQAR, Sherbrooke and York) and has provided, for example, a better description of the distribution of suspended particulate matter in the Gulf of St. Lawrence (Fig. 4) and has allowed the mapping of the surface salinity of estuarine waters using the spectral signature of dissolved matter (Fig. 5).

IML's remote sensing laboratory was also involved in national research projects aimed at studying the optical properties of Canadian Arctic waters. Supported by DFO and the Canadian Space Agency, the remote sensing laboratory participated in the North Water Polynya Study (Bélanger 2000) and the Canadian Arctic Shelf Exchange Study (CASES) in the Beaufort Sea. IML's remote sensing laboratory is a partner of the ArcticNet program and is committed to participating in the International Polar Year program in the Hudson Bay complex. The first modern optical measurements of inherent and apparent optical properties in the surface waters of the Hudson Bay region were obtained during the last ArcticNet cruise in October 2005.

In future years, the IML remote sensing laboratory intends to put more emphasis on the study of hyperspectral properties of Canadian coastal waters (Silió-Calzada 2002) in preparation for data from the new satellite sensors (HERO, Canada; EnMap, Germany) that will soon become available. The laboratory is presently participating in the HYMEX National Defence program to determine the hyperspectral signatures of inorganic suspended matter. It also participates in international exchange projects with Chile (Barbieri et al. 2004) and the Ivory Coast (Djagoua 2004).

Over its 17 years of existence, IML's remote sensing laboratory has acquired the capacity and maturity that is needed to significantly increase the accessibility to better quality remote sensing data and data products for a continuously growing community of users.

Ces algorithmes améliorés sont nécessaires pour refléter l'influence de divers facteurs environnementaux sur le signal de réflectance capté par les satellites générant ainsi de meilleures estimations de la biomasse ou de la productivité du phytoplancton dans les écosystèmes côtiers. Ce programme réalisé avec la collaboration de trois universités canadiennes (UQAR, Sherbrooke et York) a fourni, par exemple, une meilleure description de la distribution de la matière particulaire en suspension dans le golfe du Saint-Laurent (Fig. 4) et a permis de cartographier la salinité des eaux estuariennes en utilisant la signature spectrale de la matière dissoute (Fig. 5).

Le laboratoire de télédétection de l'IML a aussi participé à des projets nationaux visant à mieux comprendre les propriétés optiques des eaux nordiques canadiennes. Supporté par le MPO et par l'Agence Spatiale Canadienne, le laboratoire a participé aux programmes d'étude de la polynie des Eaux du Nord (Northwater) (Bélanger 2000) et au programme Canadian Arctic Shelf Exchange Study (CASES) dans la mer de Beaufort. Le laboratoire de télédétection de l'IML est un partenaire actuel du programme ArcticNet et s'est engagé à participer à un programme de recherche dans la baie d'Hudson dans le cadre de l'Année Polaire Internationale. Les premières mesures modernes des propriétés optiques des eaux de surface dans la région de la baie d'Hudson ont été obtenues durant la mission ArcticNet d'octobre 2005.

Pour les années futures, le laboratoire de télédétection entend accentuer l'étude des propriétés hyperspectrales des eaux côtières canadiennes (Silió-Calzada 2002) en préparation pour les données de nouveaux senseurs (HERO, Canada; EnMap, Allemagne) qui seront bientôt disponibles. Le laboratoire participe actuellement au programme HYMEX de la défense nationale pour déterminer les signatures hyperspectrales de la matière inorganique en suspension. Il participe également à des programmes d'échange avec le Chili (Barbieri et al. 2004) et la Côte d'Ivoire (Djagoua 2004).

Pour conclure, le laboratoire de télédétection de l'IML a acquis au cours de ses 17 années d'existence la capacité et la maturité qui est nécessaire pour accroître significativement l'accessibilité à de meilleures données et produits de télédétection pour une communauté continuellement grandissante de clients.

References / Références

Barbieri, M.A., Silva, C., Larouche, P., Nieto, K., and Yáñez, E. 2004. Detection of mesoscale oceanic features using Radarsat-1, AVHRR and SeaWiFS images and the possible link with jack mackerel (*Trachurus murphyi*) distribution in central Chile. Gayana (Concepc.), 68 (suppl. l): 29-39.

Bélanger, S. 2000. Analyse spatio-temporelle des patrons de chlorophylle dans la polynie NOW par télédétection du capteur SeaWiFS. Thèse de maîtrise, Université de Sherbrooke, 153 pp.

Djagoua, E.V. 2004. Apports des images NOAA/AVHRR et d'un SIG à l'étude de la variabilité spatio-temporelle des phénomènes physiques de surface du Golfe de Guinée: cas de la Côte d'Ivoire. Thèse de doctorat, Université de Cocody, Côte d'Ivoire.

Hudier, E., and Larouche, P. 2005. A potential of polarimetric SAR data in mapping first year sea ice pressure ridges from the coherent and non-coherent components of HH and VV channels. EARSeL eProceedings, 4(1): 130-138.

Larouche, P. 1996. Observation of the Gaspé Current using ERS-1 SAR. J. can. télédétection, 22: 420-427.

Larouche, P., and Dubois, J.-M.M. 1990. Dynamical evaluation of the surface circulation using remote sensing of drifting ice floes. J. Geophys. Res. 95: 9755-9764.

Larouche, P., and Pettigrew, B. 2003. Oceanographic buoy network in the Gulf of St. Lawrence. AZMP Bulletin PMZA No. 3, pp. 42-45.

Silió-Calzada, A. 2002. Estimation of inherent optical properties of the St. Lawrence estuary using airborne hyperspectral data. Master's thesis, York University, 128 pp.